Annu. Rev. Astron. Astrophys. 2004. 42:211–73
doi: 10.1146/annurev.astro.41.011802.094859


# INTERSTELLAR TURBULENCE I: Observations and Processes

Bruce G. Elmegreen
*IBM Research Division, Yorktown Heights, New York 10598;*
*email: bge@watson.ibm.com*

John Scalo
*Department of Astronomy, University of Texas, Austin, Texas 78712;*
*email: parrot@astro.as.utexas.edu*

**Key Words** interstellar medium, energy sources, magnetohydrodynamics, turbulence simulations

■ **Abstract** Turbulence affects the structure and motions of nearly all temperature and density regimes in the interstellar gas. This two-part review summarizes the observations, theory, and simulations of interstellar turbulence and their implications for many fields of astrophysics. The first part begins with diagnostics for turbulence that have been applied to the cool interstellar medium and highlights their main results. The energy sources for interstellar turbulence are then summarized along with numerical estimates for their power input. Supernovae and superbubbles dominate the total power, but many other sources spanning a large range of scales, from swing-amplified gravitational instabilities to cosmic ray streaming, all contribute in some way. Turbulence theory is considered in detail, including the basic fluid equations, solenoidal and compressible modes, global inviscid quadratic invariants, scaling arguments for the power spectrum, phenomenological models for the scaling of higher-order structure functions, the direction and locality of energy transfer and cascade, velocity probability distributions, and turbulent pressure. We emphasize expected differences between incompressible and compressible turbulence. Theories of magnetic turbulence on scales smaller than the collision mean free path are included, as are theories of magnetohydrodynamic turbulence and their various proposals for power spectra. Numerical simulations of interstellar turbulence are reviewed. Models have reproduced the basic features of the observed scaling relations, predicted fast decay rates for supersonic MHD turbulence, and derived probability distribution functions for density. Thermal instabilities and thermal phases have a new interpretation in a supersonically turbulent medium. Large-scale models with various combinations of self-gravity, magnetic fields, supernovae, and star formation are beginning to resemble the observed interstellar medium in morphology and statistical properties. The role of self-gravity in turbulent gas evolution is clarified, leading to new paradigms for the formation of star clusters, the stellar mass function, the origin of stellar rotation and binary stars, and the effects of magnetic fields. The review ends with a reflection on the progress that has been made in our understanding of the interstellar medium and offers a list of outstanding problems.

## 1. INTRODUCTION

In 1951, von Weizsäcker (1951) outlined a theory for interstellar matter (ISM) that is similar to what we believe today: cloudy objects with a hierarchy of structures form in interacting shock waves by supersonic turbulence that is stirred on the largest scale by differential galactic rotation and dissipated on small scales by atomic viscosity. The "clouds" disperse quickly because of turbulent motions, and on the largest scales they produce the flocculent spiral structures observed in galaxies. In the same year, von Hoerner (1951) noticed that rms differences in emission-line velocities of the Orion nebula increased with projected separation as a power law with a power $\alpha$ between 0.25 and 0.5, leading him to suggest that the gas was turbulent with a Kolmogorov energy cascade (for which $\alpha$ would be 0.33; see Section 4.6). Wilson et al. (1959) later got a steeper function, $\alpha \sim 0.66$, using better data, and proposed it resulted from compressible turbulence. Correlated motions with a Kolmogorov structure function (Section 2) in optical absorption lines were observed by Kaplan (1958). One of the first statistical models of a continuous and correlated gas distribution was by Chandrasekhar & Münch (1952), who applied it to extinction fluctuations in the Milky Way surface brightness. Minkowski (1955) called the ISM "an entirely chaotic mass . . . of all possible shapes and sizes . . . broken up into numerous irregular details."

These early proposals regarding pervasive turbulence failed to catch on. Interstellar absorption and emission lines looked too smooth to come from an irregular network of structures—a problem that is still with us today (Section 2). The extinction globules studied by Bok & Reilly (1947) looked too uniform and round, suggesting force equilibrium. Oort & Spitzer (1955) did not believe von Weizsäcker's model because they thought galactic rotational energy could not cascade down to the scale of cloud linewidths without severe dissipation in individual cloud collisions. Similar concerns about dissipation continue to be discussed (Sections 3 and 5.3). Oort and Spitzer also noted that the ISM morphology appeared wrong for turbulence: "instead of more or less continuous vortices, we find concentrated clouds that are often separated by much larger spaces of negligible density." They expected turbulence to resemble the model of the time, with space-filling vortices in an incompressible fluid, rather than today's model with most of the mass compressed to a small fraction of the volume in shocks fronts. When a reddening survey by Scheffler (1967) used structure functions to infer power-law-correlated structures up to $5^\circ$ in the sky, the data were characterized by saying only that there were two basic cloud types, large (70 pc) and small (3 pc), the same categories popularized by Spitzer (1968) in his textbook.

Most of the interesting physical processes that could be studied theoretically at the time, such as the expansion of ionized nebulae and supernovae (SNe) and the collapse of gas into stars, could be modeled well enough with a uniform isothermal medium. Away from these sources, the ISM was viewed as mostly static, with discrete clouds moving ballistically. The discovery of broad emission lines and narrow absorption lines in *H I* at 21 cm reinforced this picture by suggesting a warm intercloud medium in thermal pressure balance with the cool clouds (Clark 1965).

ISM models with approximate force equilibrium allowed an ease of calculation and conceptualization that was not present with turbulence. Supernovae were supposed to account for the energy, but mostly by heating and ionizing the diffuse phases (McCray & Snow 1979). Even after the discoveries of the hot intercloud (Bunner et al. 1971, Jenkins & Meloy 1974) and cold molecular media (Wilson et al. 1970), the observation of a continuous distribution of neutral hydrogen temperature (Dickey, Salpeter, & Terzian 1977), and the attribution of gas motions to supernovae (e.g., McKee & Ostriker 1977), there was no compelling reason to dismiss the basic cloud-intercloud model in favor of widespread turbulence. Instead, the list of ISM equilibrium "phases" was simply enlarged. Supersonic linewidths, long known from *H I* (e.g., McGee, Milton, & Wolfe 1966, Heiles 1970) and optical (e.g., Hobbs 1974) studies and also discovered in molecular regions at this time (see Zuckerman & Palmer 1974), were thought to represent magnetic waves in a uniform cloud (Arons & Max 1975), even though turbulence was discussed as another possibility in spite of problems with the rapid decay rate (Goldreich & Kwan 1974, Zuckerman & Evans 1974). A lone study by Baker (1973) found large-scale correlations in *H I* emission and presented them in the context of ISM turbulence, deriving the number of "turbulent cells in the line of sight," instead of the number of "clouds." Mebold, Hachenberg & Laury-Micoulaut (1974) followed this with another statistical analysis of the *H I* emission. However, there was no theoretical context in which the Baker and Mebold et al. papers could flourish given the pervasive models about discrete clouds and two- or three-phase equilibrium.

The presence of turbulence was more widely accepted for very small scales. Observations of interstellar scintillation at radio wavelengths implied there were correlated structures (Rickett 1970), possibly related to turbulence (Little & Matheson 1973), in the ionized gas at scales down to $10^9$ cm or lower (Salpeter 1969; *Interstellar Turbulence II*, next chapter, this volume). This is the same scale at which cosmic rays (*Interstellar Turbulence II*) were supposed to excite magnetic turbulence by streaming instabilities (Wentzel 1968a). However, there was (and still is) little understanding of the physical connection between these small-scale fluctuations and the larger-scale motions in the cool neutral gas.

Dense structures on resolvable scales began to look more like turbulence after Larson (1981) found power-law correlations between molecular cloud sizes and linewidths that were reminiscent of the Kolmogorov scaling law. Larson's work was soon followed by more homogeneous observations that showed similar correlations (Myers 1983, Dame et al. 1986, Solomon et al. 1987). These motions were believed to be turbulent because of their power-law nature, despite continued concern with decay times, but there was little recognition that turbulence on larger scales could also form the same structures in which the linewidths were measured. Several reviews during this time reflect the pending transition (Dickey 1985, Dickman 1985, Scalo 1987, Dickey & Lockman 1990).

Perhaps the most widespread change in perception came when the Infrared Astronomical Satellite (IRAS) observed interstellar "cirrus" and other clouds in emission at 100 $\mu$ (Low et al. 1984). The cirrus clouds are mostly transparent at optical wavelengths, so they should be in the diffuse cloud category, but they were

seen to be filamentary and criss-crossed, with little resemblance to "standard" clouds. Equally complex structures were present even in IRAS maps of "dark clouds," like Taurus, and they were observed in maps of molecular clouds, such as the Orion region (Bally et al. 1987). The wide field of view and good dynamic range of these new surveys finally allowed the diffuse and molecular clouds to reveal their full structural complexity, just as the optical nebulae and dark clouds did two decades earlier. Contributing to this change in perception was the surprising discovery by Crovisier & Dickey (1983) of a power spectrum for widespread *H I* emission that was comparable to the Kolmogorov power spectrum for velocity in incompressible turbulence. CO velocities were found to be correlated over a range of scales, too (Scalo 1984, Stenholm 1984). By the late 1980s, compression from interstellar turbulence was considered to be one of the main cloud-formation mechanisms (see review in Elmegreen 1991).

Here we summarize observations and theory of interstellar turbulence. This first review discusses the dense cool phases of the ISM, energy sources, turbulence theory, and simulations. *Interstellar Turbulence II* considers the effects of turbulence on element mixing, chemistry, cosmic ray scattering, and radio scintillation.

There are many reviews and textbooks on turbulence. A comprehensive review of magnetohydrodynamical (MHD) turbulence is in the recent book by Biskamp (2003), and a review of laboratory turbulence is in Sreenivasan & Antonia (1997). A review of incompressible MHD turbulence is in Chandran (2003). For the ISM, a collection of papers covering a broad range of topics is in the book edited by Franco & Carraminana (1999). Recent reviews of ISM turbulence simulations are in Vázquez-Semadeni et al. (2000), Mac Low (2003), and Mac Low & Klessen (2004), and a review of observations is in Falgarone, Hily-Blant & Levrier (2003). A review of theory related to the ISM is given by Vázquez-Semadeni (1999). Earlier work is surveyed by Scalo (1987). General discussions of incompressible turbulence can be found in Tennekes & Lumley (1972), Hinze (1975), Lesieur (1990), McComb (1990), Frisch (1995), Mathieu & Scott (2000), Pope (2000), and Tsinober (2001). The comprehensive two volumes by Monin & Yaglom (1975) remain extremely useful. Work on compressibility effects in turbulence at fairly low Mach numbers is reviewed by Lele (1994). Generally the literature is so large that we can reference only a few specific results on each topic; the reader should consult the most recent papers for citations of earlier work.

We have included papers that were available to us as of December 2003. A complete bibliography including paper titles is available at http://www.as.utexas.edu/astronomy/people/scalo/research/ARAA/

## 2. DIAGNOSTICS OF TURBULENCE IN THE DENSE INTERSTELLAR MEDIUM

The interstellar medium presents a bewildering variety of intricate structures and complex motions that cannot be compressed entirely into a few numbers or functions (Figures 1 and 2). Any identification with physical processes or simulations

must involve a large set of diagnostic tools. Here we begin with analysis techniques involving correlation functions, structure functions, and other statistical descriptors of column density and brightness temperature. Then we discuss techniques that include velocities and emission-line profiles.

Interstellar turbulence has been characterized by structure functions, autocorrelations, power spectra, energy spectra, and delta variance, all of which are based on the same basic operation. The structure function of order $p$ for an observable $A$ is

$$S_p(\delta r) = \langle |A(r) - A(r + \delta r)|^p \rangle \tag{1}$$

for position $r$ and increment $\delta r$, and the power-law fit to this, $S_p(\delta r) \propto \delta r^{\zeta_p}$, gives the slope $\zeta_p$. The autocorrelation of $A$ is

$$C(\delta r) = \langle A(r) A(r + \delta r) \rangle, \tag{2}$$

and the power spectrum is

$$P(k) = \hat{A}(k) \hat{A}(k)^* \tag{3}$$

for Fourier transform $\hat{A} = \int e^{ikr} A(r) dr$ and complex conjugate $A^*$. The Delta variance (Stützki et al. 1998, Zielinsky & Stützki 1999) is a way to measure power on various scales using an unsharp mask:

$$\sigma_\Delta^2(L) = \left\langle \int_0^{3L/2} dx \, \{(A\,[r + x] - \langle A \rangle) \odot (x)\}^2 \right\rangle \tag{4}$$

for a two-step function

$$\odot(x) = \pi \, (L/2)^{-2} \times \{1 \;\text{ for }\; x < L/2, \quad \text{and} -0.125 \;\text{ for }\; L/2 < x < 3L/2\} \, . \tag{5}$$

In these equations, the average over the map, indicated by $\langle\rangle$, is used as an estimate of the ensemble average.

The power spectrum is the Fourier transform of the autocorrelation function, and for a statistically homogeneous and isotropic field, the structure function of order $p = 2$ is the mean-squared $A$ minus twice the autocorrelation: $S_2 = \langle A^2 \rangle - 2C$. The delta variance is related to the power spectrum: For an emission distribution with a power spectrum $\propto k^{-n}$ for wavenumber $k$, the delta variance is $\propto r^{n-2}$ for $r = 1/k$ (Bensch, Stützki & Ossenkopf 2001; Ossenkopf et al. 2001).

We use the convention where the energy spectrum $E(k)$ is one-dimensional (1D) and equals the average over all directions of the power spectrum, $E(k)dk = P(\mathbf{k})\, dk^D$ for number of dimensions $D$ (Section 4.6). For incompressible turbulence, the Kolmogorov power spectrum in three dimensions (3D) is $\propto k^{-11/3}$ and the energy spectrum is $E(k) \propto k^{-5/3}$; for a two-dimensional (2D) distribution of this fluctuating field, $P \propto k^{-8/3}$ and in 1D, $P \propto k^{-5/3}$ for the same $E(k)$. The term energy refers to any squared quantity, not necessarily velocity.

Power spectra of Milky Way *H I* emission (Green 1993, Dickey et al. 2001, Miville-Deschênes et al. 2003), *H I* absorption (Deshpande, Dwarakanath & Goss 2000), CO emission (Stützki et al. 1998, Plume et al. 2000, Bensch et al. 2001), and IRAS 100 $\mu$ emission (Gautier et al. 1992; Schlegel, Finkbeiner & Davis 1998) have power-law slopes of around $-2.8$ to $-3.2$ in 2D maps. The same power laws were found for 2D *H I* emission from the entire Small and Large Magellanic Clouds (SMC, LMC) (Stanimirovic et al. 1999; Elmegreen, Kim & Staveley-Smith 2001) and for dust emission from the SMC (Stanimirovic et al. 2000). These intensity power spectra are comparable to but steeper than the 2D (projected) power spectra of velocity in a turbulent incompressible medium, $-8/3$, although the connection between density and velocity spectra is not well understood (see discussion in Klessen 2000).

One-dimensional power spectra of azimuthal profiles in galaxies have the same type of power law, shallower by one because of the reduced dimension. This is shown by *H I* emission from the LMC (Elmegreen et al. 2001), star formation spirals in flocculent galaxies (Elmegreen et al. 2003), and dust spirals in galactic nuclei (Elmegreen et al. 2002). A transition in slope from $\sim -5/3$ on large scales to $\sim -8/3$ on small scales in the azimuthal profiles of *H I* emission from the LMC was shown to be consistent with a transition from 2D to 3D geometry, giving the line-of-sight thickness of the *H I* layer (Elmegreen et al. 2001).

Power spectra of optical starlight polarization over the whole sky have power-law structure too, with a slope of $-1.5$ for angles greater than $\sim$10 arcmin (Fosalba et al. 2002). A 3D model of field line irregularities with a Kolmogorov spectrum and random sources reproduces this result (Cho & Lazarian 2002a).

Models of the delta-variance for isothermal MHD turbulence were compared with observations of the Polaris Flare by Ossenkopf & Mac Low (2002). The models showed a flattening of the delta-variance above the driving scale and a steepening below the dissipation scale, leading Ossenkopf & Mac Low to conclude that turbulence is driven from the outside and probably dissipated below the resolution limit. Ossenkopf et al. (2001) compared delta-variance observations to models with and without gravity, finding that gravitating models produce relatively more power on small scales, in agreement with 3-mm continuum maps of Serpens. Zielinsky & Stützski (1999) examined the relation between wavelet transforms and the delta-variance, finding that the latter gives the variance of the wavelet coefficients. The delta-variance avoids problems with map boundaries, unlike power spectra (Bench et al. 2001), but it can be dominated by noise when applied to velocity centroid maps (Ossenkopf & Mac Low 2002).

Padoan, Cambrésy & Langer (2002) obtained a structure function for extinction in the Taurus region and found that $\zeta_p/\zeta_3$ varies for $p = 1$ to 20 in the same way as the velocity structure function in a model of supersonic turbulence proposed by Boldyrev (2002). Padoan et al. (2003a) got a similar result using $^{13}$CO emission from Perseus and Taurus. In Boldyrev's model, dissipation of supersonic turbulence is assumed to occur in sheets, giving $\zeta_p/\zeta_3 = p/9 + 1 - 3^{-p/3}$ for velocity (see Sections 4.7 and 4.13).

Other spatial information was derived from wavelet transforms, fractal dimensions, and multifractal analysis. Langer et al. (1993) studied hierarchical clump structure in the dark cloud B5 using unsharp masks, counting emission features as a function of size and mass for filter scales that spanned a factor of eight. Analogous structure was seen in galactic star-forming regions (Elmegreen & Elmegreen 2001), nuclear dust spirals (Elmegreen et al. 2002), and LMC *H I* emission (Elmegreen et al. 2001). Wavelet transforms were used on optical extinction data to provide high-resolution panoramic images of the intricate structures (Cambrésy 1999).

Perimeter-area scaling gives the fractal dimension of a contour map. Values of 1.2 to 1.5 were measured for extinction (Beech 1987, Hetem & Lepine 1993), *H I* emission in high velocity clouds (Wakker 1990), 100 micron dust intensity or column density (Bazell & Desert 1988, Dickman, Horvath & Margulis 1990, Scalo 1990, Vogelaar & Wakker 1994), CO emission (Falgarone, Phillips & Walker 1991), and *H I* emission from M81 group of galaxies (Westpfahl et al. 1999) and the LMC (Kim et al. 2003). This fractal dimension is similar to that for terrestrial clouds and rain areas and for slices of laboratory turbulence. If the perimeter-area dimension of a projected 3D structure is the same as the perimeter-area dimension of a slice, then the ISM value of $\sim$1.4 for projected contours is consistent with analogous measures in laboratory turbulence (Sreenivasan 1991).

Chappell & Scalo (2001) determined the multifractal spectrum, $f(\alpha)$, for column density maps of several regions constructed from IRAS 60 $\mu$ and 100 $\mu$ images. The parameter $\alpha$ is the slope of the increase of integrated intensity with scale, $F(L) \propto L^{\alpha}$. The fractal dimension $f$ of the column density surface as a function of $\alpha$ varies as the structure changes from point-like ($f \sim 2$) to filamentary ($f \sim 1$) to smooth ($f = 0$). Multifractal regions are hierarchical, forming by multiplicative spatial processes and having a dominant geometry for substructures. The region-to-region diversity found for $f(\alpha)$ contrasts with the uniform multifractal spectra in the energy dissipation fields and passive scalar fields of incompressible turbulence, and also with the uniformity of the perimeter-area dimension, giving an indication that compressible ISM turbulence differs qualitatively from incompressible turbulence.

Hierarchical structure was investigated in Taurus by Houlahan & Scalo (1992) using a structure tree. They found linear combinations of tree statistics that could distinguish between nested and nonnested structures in projection, and they also estimated tree parameters like the average number of clumps per parent. A tabulation of three levels of hierarchical structure in dark globular filaments was made by Schneider & Elmegreen (1979).

Correlation techniques have also included velocity information (see review in Lazarian 1999). The earliest studies used the velocity for $A$ in equations 1 to 4. Stenholm (1984) measured power spectra for CO intensity, peak velocity, and linewidth in B5, finding slopes of $-1.7 \pm 0.3$ over a factor of $\sim$10 in scale. Scalo (1984) looked at $S_2(\delta r)$ and $C(\delta r)$ for the velocity centroids of $^{18}$CO emission in $\rho$ Oph and found a weak correlation. He suggested that either the correlations are partially masked by errors in the velocity centroid or they occur on scales smaller

than the beam. In the former case the correlation scale was about 0.3–0.4 pc, roughly a quarter the size of the mapped region. Kleiner & Dickman (1985) did not see a correlation for velocity centroids of $^{13}$CO emission in Taurus, but later used higher-resolution data for Heiles Cloud 2 in Taurus and reported a correlation on scales less than 0.1 pc (Kleiner & Dickman 1987). Overall, the attempts to construct the correlation function or related functions for local cloud complexes have not yielded a consistent picture.

Pérault et al. (1986) determined $^{13}$CO autocorrelations for two clouds at different distances, noted their similarities, and suggested that the resolved structure in the nearby cloud was present but unresolved in the distant cloud. They also obtained a velocity-size relation with a power-law slope of $\sim$0.5. Hobson (1992) used clump-finding algorithms and various correlation techniques for $HCO^+$ and HCN in M17SW; he found correlations only on small scales ($<$1 pc) and got a power-spectrum slope for velocity centroid fluctuations that was slightly shallower than the Kolmogorov slope. Kitamura et al. (1993) considered clump algorithms and correlation functions for Taurus and found no power law but a concentration of energy on 0.03-pc scales; they noted severe edge effects, however. Miesch & Bally (1994) analyzed centroid velocities in several molecular clouds, cautioned about sporadic effects near the beam scale, and found a correlation length that increased with the map size. They concluded, as in Pérault et al. (1986), that the ISM was self-similar over a wide range of scales. Miesch & Bally also used a structure function to determine a slope of $0.43 \pm 0.15$ for the velocity-size relation. Gill & Henriksen (1990) introduced wavelet transforms for the analysis of $^{13}$CO centroid velocities in L1551 and measured a steep velocity-size slope, 0.7.

Correlation studies like these give the second-order moment of the two-point probability distribution functions (pdfs). One-point pdfs give no spatial information but contain all orders of moments. Miesch & Scalo (1995) and Miesch, Scalo & Bally (1999) found that pdfs for centroid velocities in molecular clouds are often non-Gaussian with exponential or power-law tails and suggested the physical processes involved differ from incompressible turbulence, which has nearly Gaussian centroid pdfs (but see Section 4.9). Centroid-velocity pdfs with fat tails have been found many times since the 1950s using optical interstellar lines, *H I* emission, and *H I* absorption (see Miesch et al. 1999). Miesch et al. (1999) also plotted the spatial distributions of the pixel-to-pixel differences in the centroid velocities for several molecular clouds and found complex structures. The velocity difference pdfs had enhanced tails on small scales, which is characteristic of intermittency (Section 4.7). The velocity difference pdf in the Ophiuchus cloud has the same enhanced tail, but a map of this difference contains filaments reminiscent of vortices (Lis et al. 1996, 1998). Velocity centroid distributions observed in atomic and molecular clouds were compared with hydrodynamic and MHD simulations by Padoan et al. (1999), Klessen (2000), and Ossenkopf & Mac Low (2002). Lazarian & Esquivel (2003) considered a modified velocity centroid, designed to give statistical properties for both the supersonic and subsonic regimes and the power spectrum of solenoidal motions in the subsonic regime.

The most recent techniques for studying structure use all the spectral line data, rather than the centroids alone. These techniques include the spectral correlation function, principal component analysis, and velocity channel analysis.

The spectral correlation function $S(x, y)$ (Rosolowsky et al. 1999) is the average over all neighboring spectra of the normalized rms difference between brightness temperatures. A histogram of $S$ reveals the autocorrelation properties of a cloud: If $S$ is close to unity the spectra do not vary much. Rosolowsky et al. found that simulations of star-forming regions need self-gravity and magnetic fields to account for the large-scale integrity of the cloud. Ballesteros-Paredes, Vázquez-Semadeni & Goodman (2002) found that self-gravitating MHD simulations of the atomic ISM need realistic energy sources, while Padoan, Goodman & Juvela (2003) got the best fit to molecular clouds when the turbulent speed exceeded the Alfvén speed. Padoan et al. (2001c) measured the line-of-sight thickness of the LMC using the transition length where the slope of the spectral correlation function versus separation goes from steep on small scales to shallow on large scales.

Principle component analysis (Heyer & Schloerb 1997) cross correlates all pairs of velocity channels, $(v_i, v_j)$, by multiplying and summing the brightness temperatures at corresponding positions:

$$S_{i,j} \equiv S(v_i, v_j) = \frac{1}{n} \sum_{a=1}^{n} T([x, y]_a, v_i) T([x, y]_a, v_j); \tag{6}$$

$n$ is the number of positions in the map. The matrix $S_{i,j}$ contains information about the distribution of all emitting velocities, but averages out spatial information. The analysis uses $S_{i,j}$ to find an orthogonal normalized basis set of eigenvectors that describes the velocity distribution. A typical cloud may need only a few eigenvectors; a field of CO emission in NGC 7538 needed only seven components before the level of variation was comparable to the noise (Brunt & Heyer 2002). Brunt & Heyer (2002) used this technique to determine the average scaling between correlations in velocity and position, obtaining a power law with a slope of $\sim$0.6 for several CO sources. Their fractal Brownian motion models of clouds then suggested the intrinsic slope was $\sim$0.5. More recent studies comparing observations to simulations suggest the slope is 0.5 to 0.8, which implies a steep energy spectrum, $E(k) \propto k^{-2}$ to $k^{-2.6}$, although there are some ambiguities in the method (Brunt et al. 2003).

Velocity channel analysis was developed by Lazarian & Pogosyan (2000) to make use of the fact that the power spectrum of emission from a turbulent gas has a shallower slope in narrow velocity channels than in wide channels. This is a general property of correlated velocity fields. The shallow slope is the result of an excess of small features from unrelated physical structures that blend by velocity crowding on the line of sight. This blending effect has been studied and substantially confirmed in a number of observations (Dickey et al. 2001, Stanimirovic & Lazarian 2001) and simulations (Ballesteros-Paredes, Vázquez-Semadeni & Scalo 1999; Pichardo et al. 2000; Lazarian et al. 2001; Esquivel et al. 2003).

Miville-Deschênes, Levrier & Falgarone (2003) noted that the method would not give the correct intrinsic power spectrum if the velocity channels were not narrow enough. If there are no velocity fluctuations, then the power spectrum of projected emission from a slab that is thinner than the inverse wavenumber is shallower than the 3D density spectrum by one (Goldman 2000, Lazarian et al. 2001).

Emission-line profiles also contain information about interstellar turbulence. Molecular cloud observations suggest that profile width varies with size of the region to a power between 0.3 and 0.6 (e.g., Falgarone, Puget & Perault 1992; Jijina, Myers & Adams 1999). Similar scaling was found for *H I* clouds by Heithausen (1996). However other surveys using a variety of tracers and scales yield little correlation (e.g., Plume et al. 1997, Kawamura et al. 1998, Peng et al. 1998, Brand et al. 2001, Simon et al. 2001, Tachihara et al. 2002), or yield correlations dominated by scatter (Heyer et al. 2001). An example of extreme departure from this scaling is the high-resolution CO observation of clumps on the outskirts of Heiles Cloud 2 in Taurus, with sizes of $\sim$0.1 pc and unusually large linewidths of $\sim$2 km s$^{-1}$ (Sakamoto & Sunada 2003). Overall, no definitive characterization of the linewidth-size relation has emerged.

Most clouds with massive star formation have non-Gaussian and irregular line profiles, as do some quiescent clouds [MBM12 (Park et al. 1996) and Ursa Majoris (Falgarone et al. 1994, figure 2b,c)], whereas most quiescent clouds and even clouds with moderate low-mass star formation appear to have fairly smooth profiles (e.g., Padoan et al. 1999, figure 4 for L1448). Broad faint wings are common (Falgarone & Phillips 1990). The ratios of line-wing intensities for different isotopes of the same molecule typically vary more than the line-core ratios across the face of a cloud. However, the ratio of intensities for transitions from different levels in the same isotope is approximately constant for both the cores and the wings (Falgarone et al. 1998; Ingalls et al. 2000; Falgarone, Pety & Phillips 2001).

Models have difficulty reproducing all these features. If the turbulence correlation length is small compared with the photon mean free path (microturbulence), then the profiles appear flat-topped or self-absorbed because of non-LTE effects (e.g., Liszt et al. 1974; Piehler & Kegel 1995 and references therein). If the correlation length is large (macroturbulence), then the profiles can be Gaussian, but they are also jagged if the number of correlation lengths is small. Synthetic velocity fields with steep power spectra give non-Gaussian shapes (Dubinski, Narayan & Phillips 1995).

Falgarone et al. (1994) analyzed profiles from a decaying $512^3$ hydrodynamic simulation of transonic turbulence and found line skewness and wings in good agreement with the Ursa Majoris cloud. Padoan et al. (1998, 1999) got realistic line profiles from Mach 5–8 3D MHD simulations having super-Alfvénic motions with no gravity, stellar radiation, or outflows. Both groups presented simulated profiles that were too jagged when the Mach numbers were high. For example, L1448 in Padoan et al. (1999, figures 3 and 4) has smoother $^{13}$CO profiles than the simulations even though this is a region with star formation. Large-scale forcing in these simulations also favors jagged profiles by producing a small number of strong shocks.

Ossenkopf (2002) found jagged structure in CO line profiles modelled with $128^3$–$256^3$ hydrodynamic and MHD turbulence simulations. He suggested that subgrid velocity structure is needed to smooth them, but noted that the subgrid dispersion has to be nearly as large as the total dispersion. The sonic Mach numbers were very large in these simulations (10–15), and the forcing was again applied on the largest scales. Ossenkopf noted that the jaggedness of the profiles could be reduced if the forcing was applied at smaller scales (producing more shock compressions along each line of sight), but found that these models did not match the observed delta-variance scaling. Ossenkopf also found that subthermal excitation gave line profiles broad wings without requiring intermittency (Falgarone & Phillips 1990) or vorticity (Ballesteros-Paredes, Hartmann & Vázquez-Semandini 1999), although the observed line wings seem thermally excited (Falgarone, Pety & Phillips 2001).

The importance of unresolved structure in line profiles is unknown. Falgarone et al. (1998) suggested that profile smoothness in several local clouds implies emission cells smaller than $10^{-3}$ pc, and that velocity gradients as large as 16 km s$^{-1}$ pc$^{-1}$ appear in channel maps. Such gradients were also inferred by Miesch et al. (1999) based on the large Taylor-scale Reynolds number for interstellar clouds (this number measures the ratio of the rms size of the velocity gradients to the viscous scale, $L_K$; see Section 4.2). Tauber et al. (1991) suggested that CO profiles in parts of Orion were so smooth that the emission in each beam had to originate in an extremely large number, $10^6$, of very small clumps, AU-size, if each clump has a thermal linewidth. They required $10^4$ clumps if the internal dispersions are larger, $\sim$1 km s$^{-1}$. Fragments of $\sim 10^{-2}$ pc size were inferred directly from CCS observations of ragged line profiles in Taurus (Langer et al. 1995).

Recently, Pety & Falgarone (2003) found small (<0.02 pc) regions with very large velocity gradients in centroid difference maps of molecular cloud cores. These gradient structures were not obviously correlated with column density or density, in which case they would not be shocks. They could be shear flows, as in the dissipative regions of subsonic turbulence. Highly supersonic simulations have apparently not produced such sheared regions yet. Perhaps supersonic turbulence has this shear in the form of tiny oblique shocks that simulations cannot yet reproduce with their high numerical viscosity at the resolution limit. Alternatively, ISM turbulence could be mostly decaying, in which case it could be dominated by low Mach number shocks (Smith, Mac Low & Heitsch 2000; Smith, Mac Low & Zuev 2000).

## 3. POWER SOURCES FOR INTERSTELLAR TURBULENCE

The physical processes by which kinetic energy gets converted into turbulence are not well understood for the ISM. The main sources for large-scale motions are: (*a*) stars, whose energy input is in the form of protostellar winds, expanding *H II* regions, O star and Wolf-Rayet winds, supernovae, and combinations of these producing superbubbles; (*b*) galactic rotation in the shocks of spiral arms or bars, in the Balbus-Hawley (1991) instability, and in the gravitational scattering

of cloud complexes at different epicyclic phases; (*c*) gaseous self-gravity through swing-amplified instabilities and cloud collapse; (*d*) Kelvin-Helmholtz and other fluid instabilities; and (*e*) galactic gravity during disk-halo circulation, the Parker instability, and galaxy interactions.

Sources for the small-scale turbulence observed by radio scintillation (*Interstellar Turbulence II*) include sonic reflections of shock waves hitting clouds (Ikeuchi & Spitzer 1984, Ferriere et al. 1988), cosmic ray streaming and other instabilities (Wentzel 1969b, Hall 1980), field star motions (Deiss, Just & Kegel 1990) and winds, and energy cascades from larger scales (Lazarian, Vishniac & Cho 2004). We concentrate on the large-scale sources here.

Van Buren (1985) estimated that winds from massive main-sequence stars and Wolf-Rayet stars contribute comparable amounts, $1 \times 10^{-25}$ erg cm$^{-3}$ s$^{-1}$, supernovae release about twice this, and winds from low-mass stars and planetary nebulae are negligible. Van Buren did not estimate the rate at which this energy goes into turbulence, which requires multiplication by an efficiency factor of ~0.01–0.1, depending on the source. Mac Low & Klessen (2004) found that main-sequence winds are negligible except for the highest-mass stars, in which case supernovae dominate all the stellar sources, giving $3 \times 10^{-26}$ erg cm$^{-3}$ s$^{-1}$ for the energy input, after multiplying by an efficiency factor of 0.1. Mac Low & Klessen (2004) also derived an average injection rate from protostellar winds equal to $2 \times 10^{-28}$ erg cm$^{-3}$ s$^{-1}$ including an efficiency factor of ~0.05. *H II* regions are much less important as a general source of motions because most of the stellar Lyman continuum energy goes into ionization and heat (Mac Low & Klessen 2004). Kritsuk & Norman (2002a) suggested that moderate turbulence can be maintained by variations in the background nonionizing UV radiation (Parravano et al. 2003).

These estimates agree well with the more detailed "grand source function" estimated by Norman & Ferrara (1996), who also considered the spatial range for each source. They recognized that most Type II SNe contribute to cluster winds and superbubbles, which dominate the energy input on scales of 100–500 pc (Oey & Clarke 1997). Superbubbles are also the most frequent pressure disturbance for any random disk position (Kornreich & Scalo 2000).

Power rates for turbulence inside molecular clouds may exceed these global averages. For example, Stone, Ostriker & Gammie (1998) suggested that the turbulent heating rate inside a giant molecular cloud (GMC) is $\sim 1\text{–}6 \times 10^{-27} n_H \Delta v^3 / R$ erg cm$^{-3}$ s$^{-1}$ for velocity dispersion $\Delta v$ in km s$^{-1}$ and size $R$ in pc. For typical $n_H \sim 10^2\text{–}10^3$ cm$^{-3}$, $\Delta v \sim 2$ and $R \sim 10$, this exceeds the global average for the ISM by a factor of ~10, even before internal star formation begins (see also Basu & Murali 2001). This suggests that power density is not independent of scale as it is in a simple Kolmogorov cascade. An alternative view was expressed by Falgarone, Hily-Blant & Levrier (2003) who suggested that the power density is about the same for the cool and warm phases, GMCs, and dense cores. In either case, self-gravity contributes to the power density locally, and even without self-gravity, dissipation is intermittent and often concentrated in small regions.

Galactic rotation has a virtually unlimited supply of energy if it can be tapped for turbulence (Fleck 1981). Several mechanisms have been proposed. Magneto-rotational instabilities (Sellwood & Balbus 1999, Kim et al. 2003) pump energy into gas motion at a rate comparable to the magnetic energy density times the angular rotation rate. This was evaluated by Mac Low & Klessen (2004) to be $3 \times 10^{-29}$ erg cm$^{-3}$ s$^{-1}$ for $B = 3$ $\mu$G. This is smaller than the estimated stellar input rate by a factor of $\sim$1000, but it might be important in the galactic outer regions where stars form slowly (Sellwood & Balbus 1999) and in low-surface brightness galaxies. Piontek & Ostriker (2004) considered how reduced dissipation can enhance the power input to turbulence from magnetorotational instabilities.

Rotational energy also goes into the gas in spiral shocks where the fast-moving interspiral medium hits the slower moving dense gas in a density wave arm (Roberts 1969). Additional input comes from the gravitational potential energy of the arm as the gas accelerates toward it. Some of this energy input will be stored in magnetic compressional energy, some will be converted into gravitational potential energy above the midplane as the gas deflects upward (Martos & Cox 1998), and some will be lost to heat. The fraction that goes into turbulence is not known, but the total power available is $0.5\rho_{ism}v_{sdw}^3/(2H) \sim 5 \times 10^{-27}$ erg cm$^{-3}$ s$^{-1}$ for interspiral density $\rho_{ism} \sim 0.1$ m$_{\rm H}$ cm$^{-3}$, shock speed $v_{sdw} \sim 30$ km s$^{-1}$, and half disk thickness $H = 100$ pc. Zhang et al. (2001) suggest that a spiral wave has driven turbulence in the Carina molecular clouds because the linewidth-size relation is not correlated with distance from the obvious sources of stellar energy input.

Fukunaga & Tosa (1989) proposed that rotational energy goes to clouds that gravitationally scatter off each other during random phases in their epicycles. Gammie et al. (1991) estimated that the cloud velocity dispersion can reach the observed value of $\sim$5 km s$^{-1}$ in this way. Vollmer & Beckert (2002) considered the same mechanism with shorter cloud lifetimes and produced a steady state model of disk accretion. A second paper (Vollmer & Beckert 2003) included supernovae.

The gravitational binding energy in a galaxy disk heats the stellar population during swing-amplified shear instabilities that make flocculent spiral arms (e.g., Fuchs & von Linden 1998). It can also heat the gas (Thomasson, Donner & Elmegreen 1991; Bertin & Lodato 2001; Gammie 2001) and feed turbulence (Huber & Pfenniger 2001; Wada, Meurer & Norman 2002). Continued collapse of the gas may feed more turbulence on smaller scales (Semelin et al. 1999, Chavanis 2002, Huber & Pfenniger 2002). A gravitational source of turbulence is consistent with the observed power spectra of flocculent spiral arms (Elmegreen et al. 2003). The energy input rate for the first e-folding time of the instability is approximately the ISM energy density, $1.5\,\rho\Delta v^2$, times the growth rate $2\pi G\rho H/\Delta v$ for velocity dispersion $\Delta v$. This is $\sim 10^{-27}$ erg cm$^{-3}$ s$^{-1}$ in the Solar neighborhood—less than supernovae by an order of magnitude. However, continued energy input during cloud collapse would increase the power available for turbulence in proportion to $\rho^{4/3}$. The efficiency for the conversion of gravitational binding energy into turbulence is unknown, but because gravitational forces act on all the matter and,

unlike stellar explosions, do not require a hot phase of evolution during which energy can radiate, the efficiency might be high.

Conventional fluid instabilities provide other sources of turbulence on the scales over which they act. For example, a cloud hit by a shock front will shed its outer layers and become turbulent downstream (Xu & Stone 1995), and the interior of the cloud can be energized as well (Miesch & Zweibel 1994, Kornreich & Scalo 2000). Cold decelerating shells have a kinematic instability (Vishniac 1994) that can generate turbulence inside the swept-up gas (Blondin & Marks 1996, Walder & Folini 1998). Bending mode and other instabilities in cloud collisions generate a complex filamentary structure (Klein & Woods 1998). It is also possible that the kinetic energy of a shock can be directly converted into turbulent energy behind the shock (Rotman 1991; Andreopoulos, Agui & Briassulis 2000). Kritsuk & Norman (2002a,b) discuss how thermal instabilities can drive turbulence, in which case the underlying power source is stellar radiation rather than kinetic energy. There are many individual sources for turbulence, but the energy usually comes from one of the main categories of sources listed above.

Sources of interstellar turbulence span such a wide range of scales that it is often difficult to identify any particular source for a given cloud or region. Little is known about the behavior of turbulence that is driven like this. The direction and degree of energy transfer and the morphology of the resulting flow could be greatly affected by the type and scale of energy input (see Biferale et al. 2004). However, it appears that for average disk conditions the power input is dominated by cluster winds or superbubbles with an injection scale of $\sim$50–500 pc.

## 4. THEORY OF INTERSTELLAR TURBULENCE

### 4.1. What Is Turbulence and Why Is It So Complicated?

Turbulence is nonlinear fluid motion resulting in the excitation of an extreme range of correlated spatial and temporal scales. There is no clear scale separation for perturbation approximations, and the number of degrees of freedom is too large to treat as chaotic and too small to treat in a statistical mechanical sense. Turbulence is deterministic and unpredictable, but it is not reducible to a low-dimensional system and so does not exhibit the properties of classical chaotic dynamical systems. The strong correlations and lack of scale separation preclude the truncation of statistical equations at any order. This means that the moments of the fluctuating fields evaluated at high order cannot be interpreted as analogous to moments of the microscopic particle distribution, i.e., the rms velocity cannot be used as a pressure.

Hydrodynamic turbulence arises because the nonlinear advection operator, $(\mathbf{u}\cdot\nabla)\,\mathbf{u}$, generates severe distortions of the velocity field by stretching, folding, and dilating fluid elements. The effect can be viewed as a continuous set of topological deformations of the velocity field (Ottino 1989), but in a much higher dimensional space than chaotic systems so that the velocity field is, in effect, a stochastic field

of nonlinear straining. These distortions self-interact to generate large amplitude structure covering the available range of scales. For incompressible turbulence driven at large scales, this range is called the inertial range because the advection term corresponds to inertia in the equation of motion. For a purely hydrodynamic incompressible system, this range is measured by the ratio of the advection term to the viscous term, which is the Reynolds number $Re = UL/\nu \sim 3 \times 10^3 M_a L_{pc} n$, where $U$ and $L$ are the characteristic large-scale velocity and length, $L_{pc}$ is the length in parsecs, $M_a$ is the Mach number, $n$ is the density, and $\nu$ is the kinematic viscosity. In the cool ISM, $Re \sim 10^5$ to $10^7$ if viscosity is the damping mechanism (less if ambipolar diffusion dominates; Section 5). Another physically important range is the Taylor scale Reynolds number, which is $Re_\lambda = U_{rms} L_T/\nu$ for $L_T =$ the ratio of the rms velocity to the rms velocity gradient (see Miesch et al. 1999).

With compressibility, magnetic fields, or self-gravity, all the associated fields are distorted by the velocity field and exert feedback on it. Hence, one can have MHD turbulence, gravitational turbulence, or thermally driven turbulence, but they are all fundamentally tied to the advection operator. These additional effects introduce new globally conserved quadratic quantities and eliminate others (e.g., kinetic energy is not an inviscid conserved quantity in compressible turbulence), leading to fundamental changes in the behavior. This may affect the way energy is distributed among scales, which is often referred to as the cascade.

Wave turbulence occurs in systems dominated by nonlinear wave interactions, including plasma waves (Tsytovich 1972), inertial waves in rotating fluids (Galtier 2003), acoustic turbulence (L'vov, L'vov & Pomyalov 2000), and internal gravity waves (Lelong & Riley 1991). A standard procedure for treating these weakly nonlinear systems is with a kinetic equation that describes the energy transfer attributable to interactions of three (in some cases four) waves with conservation of energy and momentum (see Zakharov, L'vov & Falkovich 1992). Wave turbulence is usually propagating, long-lived, coherent, weakly nonlinear, and weakly dissipative, whereas fully developed fluid turbulence is diffusive, short-lived, incoherent, strongly nonlinear, and strongly dissipative (Dewan 1985). In both wave and fluid turbulence, energy is transferred among scales, and when it is fed at the largest scales with dissipation at the smallest scales, a Kolmogorov or other power-law power spectrum often results. Court (1965) suggested that wave turbulence be called undulence to distinguish it from the different physical processes involved in fully developed fluid turbulence.

## 4.2. Basic Equations

The equations of mass and momentum conservation are

$$\partial\rho/\partial t + \nabla \cdot (\rho \mathbf{u}) = 0, \tag{7}$$

$$\partial \mathbf{u}/\partial t + (\mathbf{u} \cdot \nabla)\,\mathbf{u} = -\frac{1}{\rho}\nabla P + \mathbf{F} + \frac{1}{\rho}\nabla \cdot \sigma, \tag{8}$$

where $\rho$, $\mathbf{u}$, $P$ are the mass density, velocity, and pressure, respectively, and $\sigma$ is the shear stress tensor. The last term is often written as $\nu(\nabla^2\mathbf{u} + \nabla[\nabla \cdot \mathbf{u}]/3)$, where $\nu \sim 10^{20} c_5/n$ is the kinematic viscosity (in cm$^2$ s$^{-1}$) for thermal speed $c_5$ in units of $10^5$ cm s$^{-1}$ and density $n$ in cm$^{-3}$. This form of $\sigma$ is valid only in an incompressible fluid because the viscosity depends on density (and temperature). The scale $L_K$ at which the dissipation rate equals the advection rate is called the Kolmogorov microscale and is approximately $L_K = 10^{15}/(nM_a)$ cm.

In the compressible case, the scale at which dissipation dominates advection will vary with position because of the large density variations. This could spread out the region in wavenumber space at which any power-law cascade steepens into the dissipation range. Usually the viscosity is assumed to be constant for ISM turbulence. The force per unit mass $\mathbf{F}$ may include self-gravity and magnetism, which introduce other equations to be solved, such as the Poisson and induction equations. The pressure $P$ is related to the other variables through the internal energy equation. For this discussion, we assume an isentropic (or barotropic) equation of state, $P \sim \rho^\gamma$, with $\gamma$ a parameter (=1 for an isothermal gas). The inclusion of an energy equation is crucial for ISM turbulence; otherwise the energy transfer between kinetic and thermal modes may be incorrect. An important dimensionless number is the sonic Mach number $M_a = u/a$, where $a$ is the sound speed. For most ISM turbulence, $M_a \sim 0.1$–10, so it is rarely incompressible and often supersonic, producing shocks.

## 4.3. Statistical Closure Theories

In turbulent flows, all the variables in the hydrodynamic equations are strongly fluctuating and can be described only statistically. The traditional practice in incompressible turbulence is to derive equations for the two- and three-point correlations as well as various other ensemble averages. An equation for the three-point correlations generates terms involving four-point correlations, and so on. The existence of unknown high-order correlations is a classical closure problem, and there are a large number of attempts to close the equations, i.e., to express the high-order correlations in terms of the low-order correlations. Examples range from simple gradient closures for mean flow quantities to mathematically complex approaches such as the Lagrangian history Direct Interaction Approximation (DIA, see Leslie 1973), the Eddy-Damped Quasi-Normal Markovian (EDQNM) closure (see Lesieur 1990), diagrammatic perturbation closures, renormalization group closures, and others (see general references given in Section 1).

The huge number of additional unclosed terms that are generated by compressible modes and thermal modes using an energy equation (see Lele 1994) render conventional closure techniques ineffective for much of the ISM, except perhaps for extremely small Mach numbers (e.g., Bertoglio, Bataille & Marion 2001). Besides their intractability, closure techniques only give information about the correlation function or power spectrum, which yields an incomplete description because all phase information is lost and higher-order moments are not treated. An

exact equation for the infinite-point correlation functional can be derived (Beran 1968) but not solved. For these reasons we do not discuss closure models here. Other theories involving scaling arguments (e.g., She & Leveque 1994), statistical mechanical formulations (e.g., Shivamoggi 1997), shell models (see Biferale 2003 for a review), and dynamical phenomenology (e.g., Leorat et al. 1990) may be more useful, along with closure techniques for the one-point pdfs, such as the mapping closure (Chen, Chen & Kraichnan 1989).

## 4.4. Solenoidal and Compressible Modes

For compressible flows relevant to the ISM, the Helmholtz decomposition theorem splits the velocity field into compressible (dilatational, longitudinal) and solenoidal (rotational, vortical) modes $u_c$ and $u_s$, defined by $\nabla \times \mathbf{u}_c = 0$ and $\nabla \cdot \mathbf{u}_s = 0$. In strong 3D turbulence these components have different effects, leading to shocks and rarefactions for $\mathbf{u}_c$ and to vortex structures for $\mathbf{u}_s$. Only the compressible mode is directly coupled to the gravitational field. The two modes are themselves coupled and exchange energy. The coupled evolution equations for the vorticity $\omega = \nabla \times \mathbf{u}$ and dilatation $\nabla \cdot \mathbf{u}$ contain one asymmetry that favors transfer from solenoidal to compressible components in the absence of viscous and pressure terms (Vázquez-Semadeni, Passot & Pouquet 1996; Kornreich & Scalo 2000) and another asymmetry that transfers from compressible to solenoidal when pressure and density gradients are not aligned, as in an oblique shock. This term in the vorticity equation, proportional to $\nabla P \times \nabla(1/\rho)$, causes baroclinic vorticity generation. If turbulence is modeled as barotropic or isothermal, vorticity generation is suppressed. One or the other of these asymmetries can dominate in different parts of the ISM (Section 5).

Only the solenoidal mode exists in incompressible turbulence, so vortex models can capture much of the dynamics (Pullin & Saffman 1998). Compressible supersonic turbulence has no such conceptual simplification, because even at moderate Mach numbers there will be strong interactions with the solenoidal modes, and with the thermal modes if isothermality is not assumed.

## 4.5. Global Inviscid Quadratic Invariants Are Fundamental Constraints on the Nature of Turbulent Flows

Quadratic-conserved quantities constrain the evolution of classical systems. A review of continuum systems with dual quadratic invariants is given by Hasegawa (1985). For turbulence, the important quadratic invariants are those conserved by the inviscid momentum equation. The conservation properties of turbulence differ for incompressible versus compressible, 2D versus 3D, and hydrodynamic versus MHD (see also Biskamp 2003). For incompressible flows, the momentum equation neglecting viscosity and external forces is, from Equation 8 above,

$$\partial \mathbf{u}/\partial t + (\mathbf{u} \cdot \nabla)\,\mathbf{u} = -\nabla P/\rho. \tag{9}$$

Taking the scalar product of this equation with **u**, integrating over all space, using Gauss' theorem, and assuming that the velocity and pressure terms vanish at infinity gives

$$\partial/\partial t \int \left(\frac{1}{2}u^2\right) \mathbf{dr} = 0 \tag{10}$$

demonstrating that kinetic energy per unit mass is globally conserved by the advection operator. In Fourier space this equation leads to a "detailed" conservation condition in which only triads of wavevectors participate in energy transfer. It is this property that makes closure descriptions in Fourier space so valuable. Virtually all the phenomenology associated with incompressible turbulence traces back to the inviscid global conservation of kinetic energy; unfortunately, compressible turbulence does not share this property. Another quadratic conserved quantity for incompressible turbulence is kinetic helicity $\langle \mathbf{u} \cdot \omega \rangle$, which measures the asymmetry between vorticity and velocity fields. This is not positive definite so its role in constraining turbulent flows is uncertain (see Chen, Chen & Eyink 2003). Kurien, Taylor & Matsumoto (2003) found that helicity conservation controls the inertial range cascade at large wavenumbers for incompressible turbulence.

For 2D turbulence, there is an additional positive-definite quadratic invariant, the enstrophy or mean square vorticity $\langle (\nabla \times \mathbf{u})^2 \rangle$. The derivative in the enstrophy implies that it selectively decays to smaller scales faster than the energy, with the result that the kinetic energy undergoes an inverse cascade to smaller wavenumbers. This result was first pointed out by Kraichnan (1967) and has been verified in numerous experiments and simulations (see Tabeling 2002 for a comprehensive review of 2D turbulence). Because of the absence of the vorticity stretching term $\omega \cdot \nabla u$ in the 2D vorticity equation, which produces the complex system of vortex worms seen in 3D turbulence, 2D turbulence evolves into a system of vortices that grow with time through their merging.

In 2D-compressible turbulence the square of the potential vorticity $(\omega/\rho)$ is also conserved (Passot, Pouquet & Woodward 1988), unlike the case in 3D-compressible turbulence. This means that results obtained from 2D simulations may not apply to 3D. However, if energy is fed into galactic turbulence at very large scales, e.g., by galactic rotation, then the ISM may possess quasi-2D structure on these scales.

Compressibility alters the conservation properties of the flow. Momentum density $\rho \mathbf{u}$ is the only quadratic-conserved quantity but it is not positive definite. Momentum conservation controls the properties of shocks in isothermal supersonic nonmagnetic turbulence. Interacting oblique shocks generate flows that create shocks on smaller scales (Mac Low & Norman 1993), possibly leading to a shock cascade controlled by momentum conservation. Kinetic energy conservation is lost because it can be exchanged with the thermal energy mode: compression and shocks heat the gas. The absence of kinetic energy conservation means that in Fourier space the property of detailed conservation by triads is lost, and so is the basis for many varieties of statistical closures. Energy can also be transferred

between solenoidal and compressional modes, and even when expanded to only second order in fluctuation amplitude, combinations of any two of the vorticity, acoustic, and entropy modes, or their self-interactions, generate other modes.

The assumption of isothermal or isentropic flow forces a helicity conservation that is unphysical in general compressible flows; it suppresses baroclinic vorticity creation, and affects the exchange between compressible kinetic and thermal modes. Isothermality is likely to be valid in the ISM only over a narrow range of densities, from $10^3$ to $10^4$ cm$^{-3}$ in molecular clouds for example (Scalo et al. 1998), and this is much smaller than the density variation found in simulations. Isothermality also suppresses the ability of sound waves to steepen into shocks.

Magnetic fields further complicate the situation. Energy can be transferred between kinetic and magnetic energy so only the total, $\frac{1}{2}\rho u^2 + B^2/8\pi$, is conserved. Kolmogorov-type scaling may still result in the cross-field direction (Goldreich & Sridhar 1995). The magnetic helicity $\mathbf{A} \cdot \mathbf{B}$ ($\mathbf{A}$ = magnetic vector potential) and cross helicity $\mathbf{u} \cdot \mathbf{B}$ are conserved but their role in the dynamics is uncertain. Pouquet et al. (1976) addressed the MHD energy cascade using EDQNM closure and predicted an inverse cascade for large magnetic helicities. Ayyer & Verma (2003) assumed a Kolmogorov power spectrum and found that the cascade direction depends on whether kinetic and magnetic helicities are nonzero. Without helicity, all the self- and cross-energy transfer between kinetic and magnetic energies are direct, meaning to larger wavenumbers, whereas the magnetic and kinetic helical contributions give an inverse cascade for the four sets of possible magnetic and kinetic energy exchanges, confirming the result of Pouquet et al. (1976). With or without helicity, the net energy transfer within a given wavenumber band is from magnetic to kinetic on average. It is seen that while kinetic helicity cannot reverse the direct cascade in hydrodynamic turbulence, magnetic helicity in MHD turbulence can. The effects of kinetic and magnetic helicity on supersonic hydrodynamic or MHD turbulence are unexplored.

These considerations suggest that the type of cascade expected for highly compressible MHD turbulence in the ISM cannot be predicted yet. Numerical simulations may result in an incorrect picture of the cascade if restricted assumptions like isothermality and constant kinematic viscosity are imposed.

## 4.6. Scale-Invariant Kinetic Energy Flux and Scaling Arguments for the Power Spectrum

In the Kolmogorov (1941) model of turbulence, energy injected at large scales "cascades" to smaller scales by kinetic-energy-conserving interactions that are local in Fourier space at a rate independent of scale, and then dissipates by viscosity at a much smaller scale. At a given scale $\ell$ having velocity $u_\ell$, the rate of change of kinetic energy per unit mass from exchanges with other scales is $u_\ell^2$ divided by the characteristic timescale, taken to be $\ell/u_\ell$. The constant energy rate with scale gives $u_\ell \sim \ell^{1/3}$. If one considers $u_\ell$ to represent the ensemble average velocity difference over separation $\ell$, this result gives the second-order structure function

$S_2(\ell) \sim \ell^{2/3}$. In terms of wavenumber, $u_k^2 \sim k^{-2/3}$, so the kinetic energy per unit mass per unit wavenumber, which is the energy spectrum $E(k)$ (equal to $4\pi k^2 P(k)$ where $P(k)$ is the 3D power spectrum), is given by

$$E(k) \sim u_k^2/k \propto k^{-5/3}. \tag{11}$$

This 5/3 law was first confirmed experimentally 20 years after Kolmogorov's proposal using tidal channel data to obtain a large inertial range (Grant, Stewart & Moillet 1962). More recent confirmations of this relation and the associated second-order structure function have used wind tunnels, jets, and counter-rotating cylinders (see Frisch 1995). The largest 3D incompressible simulations (Kaneda et al. 2003) indicate that the power-law slope of the energy spectrum might be steeper by approximately 0.1. Similar considerations applied to the helicity cascade (Kurien et al. 2003) predict a transition to $E(k) \sim k^{-4/3}$ at large $k$, perhaps explaining the flattening of the spectrum, or "bottleneck effect" seen in many simulations. Leorat, Passot & Pouquet (1990) generalized the energy cascade phenomenology to the compressible case assuming locality of energy transfer (no shocks), but allowing for the fact that the kinetic energy transfer rate will not be constant. It is commonly supposed that highly supersonic turbulence should have the spectrum of a field of uncorrelated shocks, $k^{-2}$ (Saffman 1971), although this result has never been derived in more than 1D, and shocks in most turbulence should be correlated.

These scaling arguments make only a weak connection with the hydrodynamical equations, either through a conservation property or an assumed geometry (see also Section 4.1). The only derivation of the $-5/3$ spectrum for incompressible turbulence that is based on an approximate solution of the Navier-Stokes equation is Lundgren's (1982) analysis of an unsteady stretched-spiral vortex model for the fine-scale structure (see Pullin & Saffman 1998). No such derivation exists for compressible turbulence.

Kolmogorov's (1941) most general result is the "four-fifths law." For statistical homogeneity, isotropy, and a stationary state driven at large scales, the energy flux through a given wavenumber band $k$ should be independent of $k$ for incompressible turbulence (Frisch 1995, Section 6.2.4). Combined with a rigorous relation between energy flux and the third-order structure function, this gives (Frisch 1995) an exact result in the limit of small $\delta r$:

$$S_3(\delta r) = \langle (\delta v(r, \delta r)^3 \rangle = -(4/5)\epsilon \delta r; \tag{12}$$

$\epsilon$ is the rate of dissipation due to viscosity, $\delta v\,(r, \delta r)$ is the velocity difference over spatial lag $\delta r$ at position $r$, and the ensemble average is over all positions. Kolmogorov (1941) obtained this result for decaying turbulence using simpler arguments. Notice that self-similarity is not assumed. A more general version of this relation has been experimentally tested by Moisy, Tabeling, & Willaime (1999) and found to agree to within a few percent over a range of scales up to three decades.

For compressible ISM turbulence, kinetic energy is not conserved between scales; for this reason, the term "inertial range" is meaningless. As a result, there is no guarantee of scale-free or self-similar power-law behavior. The driving agents span a wide range of scales (Section 3) and the ISM is larger than all of them. Excitations may spread to both large and small scales, independent of the direction of net energy transfer. In the main disks of galaxies where the Toomre parameter $Q$ is less than $\sim$2, vortices larger than the disk thickness may result from quasi-2D turbulence; recall that $Q$ equals the ratio of the scale height to the epicyclic length. Large-scale vortical motions in a compressible, self-gravitating ISM may amplify to look like flocculent spirals.

## 4.7. Intermittency and Structure Function Scaling

Kolmogorov's (1941) theory did not recognize that dissipation in turbulence is "intermittent" at small scales, with intense regions of small filling factor, giving fat, nearly exponential tails in the velocity difference or other probability distribution functions (pdfs). Intermittency can refer to either the time, space, or probability structures that arise. The best-studied manifestation is "anomalous scaling" of the high-order velocity structure functions (Equation 1), $S(\delta r) = (v[r] - v[r + \delta r])^p \sim \delta r^{\zeta_p}$. For Kolmogorov turbulence with the four-fifths law and an additional assumption of self-similarity ($\delta v(\lambda \delta r) = \lambda^h \delta v(\delta r)$ for small $\delta r$ with $h = 1/3$) $\zeta_p = p/3$. In real incompressible turbulence, $\zeta_p$ rises more slowly with $p$ (compare Section 4.13; e.g., Anselmet et al. 1984).

Interstellar turbulence is probably intermittent, as indicated by the small filling fraction of clouds and their relatively high energy dissipation rates (Section 3). Velocity pdfs and velocity difference pdfs also have fat tails (Section 2), as may elemental abundance distributions (*Interstellar Turbulence II*). Other evidence for intermittency in the dissipation field is the $10^3$ K collisionally excited gas required to explain $CH^+$, $HCO^+$, OH, and excited $H_2$ rotational lines (Falgarone et al. 2004) (*Interstellar Turbulence II*). Although it is difficult to distinguish between the possible dissipation mechanisms (Pety & Falgarone 2000), the dissipation regions occupy only $\sim$1% of the line of sight and they seem to be ubiquitous (Falgarone et al. 2004). If they are viscous shear layers, then their sizes ($10^{15}$ cm) cannot be resolved with present-day simulations.

A geometrical model for $\zeta_p$ in incompressible nonmagnetic turbulence was proposed by She & Leveque (1994, see also Liu & She 2003). The model considers a box of turbulent fluid hierarchically divided into sub-boxes in which the energy dissipation is either large or small. The mean energy flux is conserved at all levels with Kolmogorov scaling, and the dissipation regions are assumed to be 1D vortex tubes or worms, known from earlier experiments and simulations. Then $\zeta_p$ was derived to be $p/9 + 2(1 - [2/3]^{p/3})$ and shown to match the experiments up to at least $p = 10$ (see Dubrulle 1994 and Boldyrev 2002 for derivations). Porter, Pouquet & Woodward (2002) found a flow dominated by vortex tubes in simulations of decaying transonic turbulence at fairly small Mach numbers (Figure 3)

and got good agreement with the She-Leveque formula. A possible problem with the She-Leveque approach is that the dimension of the most intense vorticity structures does not have a single value, and the average value is larger than unity for incompressible turbulence (Vainshtein 2003). A derivation of $\zeta_p$ based on a dynamical vortex model has been given by Hatakeyama & Kambe (1997).

Politano & Pouquet (1995) proposed a generalization for the MHD case (also see Section 4.13). It depends on the scaling relations for the velocity and cascade rate and on the dimensionality of the dissipative structures. They noted solar wind observations that suggested the most dissipative structures are 2D current sheets. Müller & Biskamp (2000) confirmed that dissipation in incompressible MHD turbulence occurs in 2D structures, in which case $\zeta_p = p/9 + 1 - (1/3)^{p/3}$. However, Cho, Lazarian & Vishniac (2002a) found that for anisotropic incompressible MHD turbulence measured with respect to the local field, She-Leveque scaling with 1D intermittent structures occurs for the velocity and a slightly different scaling occurs for the field. Boldyrev (2002) assumed that turbulence is mostly solenoidal with Kolmogorov scaling, while the most dissipative structures are shocks, again getting $\zeta_p = p/9 + 1 - (1/3)^{p/3}$ because of the planar geometry; the predicted energy spectrum was $E(k) \sim k^{-1-\zeta_2} \sim k^{-1.74}$. Boldyrev noted that the spectrum will be steeper if the shocks have a dimension equal to the fractal dimension of the density.

The uncertainties in measuring ISM velocities preclude a test of these relations, although they can be compared with numerical simulations. Boldyrev, Nordlund & Padoan (2002b) found good agreement in 3D super-Alfvénic isothermal simulations for both the structure functions to high order and the power spectrum. The simulations were forced solenoidally at large scales and have mostly solenoidal energy, so they satisfy the assumptions in Boldyrev (2002). Padoan et al. (2004) showed that the dimension of the most dissipative structures varies with Mach number from one for lines at subsonic turbulence to two for sheets at Mach 10. The low Mach number result is consistent with the nonmagnetic transonic simulation in Porter et al. (2002) (see Figure 3). Kritsuk & Norman (2003) showed how nonisothermality leads to more complex folded structures with dimensions larger than two.

## 4.8. Details of the Energy Cascade: Isotropy and Independence of Large and Small Scales

Kolmogorov's model implies an independence between large and small scales and a resulting isotropy on the smallest scales. Various types of evidence for and against this prediction were summarized by Yeung & Brasseur (1991). One clue comes from the incompressible Navier-Stokes equation written in terms of the Fourier-transformed velocity. Global kinetic energy conservation is then seen to occur only for interactions between triads of wavevectors (e.g., Section 4.12). The trace of the equation for the energy spectrum tensor gives the rate of change of energy per unit wavenumber in Fourier modes $E(k)$ owing to the exchange of energy with all other

modes $T(k)$ and the loss from viscous dissipation: $\partial E(k)/\partial t = T(k) - 2\nu k^2 E(k)$. The details of the energy transfer can be studied by decomposing the transfer function T(k) into a sum of contributions $T(k|p, q)$ defined as the energy transfer to $k$ resulting from interactions between wavenumbers $p$ and $q$.

Domaradzki & Rogallo (1990) and Yeung & Brasseur (1991) analyzed $T(k|p, q)$ from simulations to show that, whereas there is a net local transfer to higher wavenumbers, at smaller and smaller scales the cascade becomes progressively dominated by nonlocal triads in which one leg is in the energy-containing (low-$k$) range. This means that small scales are not decoupled from large scales. Waleffe (1992) pointed out that highly nonlocal triad groups tend to cancel each other in the net energy transfer for isotropic turbulence; the greatest contribution is from triads with a scale disparity of about an order of magnitude (Zhou 1993). Yeung & Brasseur (1991) and Zhou, Yeung & Brasseur (1996) demonstrated that long-range couplings are important in causing small-scale anisotropy in response to large-scale anisotropic forcing, and that this effect increases with Reynolds number.

The kinetic energy transfer between scales can be much more complex in the highly compressible case where the utility of triad interactions is lost. Fluctuations with any number of wavevector combinations can contribute to the energy transfer. Momentum density is still conserved in triads, but the consequences of this are unknown. Even in the case of very weakly compressible turbulence, Bataille & Zhou (1999) found 17 separate contributions to the total compressible transfer function $T(k)$. Nevertheless, the EDQNM closure theory applied to very weakly compressible turbulence by Bataille & Zhou (1999) and Bertoglio, Bataille & Marion (2001), assuming only triadic interactions, yields interesting results that may be relevant to warm *H I*, the hot ionized ISM, or dense molecular cores where the turbulent Mach number might be small. Then the dominant compressible energy transfer is not a cascade-type but a cross-transfer involving local (in spectral space) transfer from solenoidal to compressible energy. At Mach numbers approaching unity (for which the theory is not really valid) the transfer changes to cascade-type, with a net flux to higher wavenumbers.

Pouquet et al. (1976) were among the first to address the locality and direction of the MHD energy cascade using a closure method. For more discussions see Ayyer & Verma (2003), Biferale (2003) and Biskamp (2003).

## 4.9. Velocity Probability Distribution

A large number of papers have demonstrated non-Gaussian behavior in the pdfs of vorticity, energy dissipation, passive scalars, and fluctuations in the pressure and nonlinear advection, all for incompressible turbulence. Often the pdfs have excess tails that tend toward exponentials at small scale (see Chen et al. 1989; Castaing, Gagne & Hopfinger 1990 for early references). Velocity fluctuation differences and derivatives exhibit tails of the form $\exp(-v^\alpha)$ with $1 < \alpha < 2$ and $\alpha \sim 1$ at small scale (e.g., Anselmet et al. 1984, She et al. 1993). Physically

this is a manifestation of intermittency, with the most intense turbulence becoming less space-filling at smaller scales. The behavior may result from the stretching properties of the advection operator (see She 1991 for a review).

This same kind of behavior has been observed for the ISM in the form of excess CO line wings (Falgarone & Phillips 1990) and in the pdfs of CO (Padoan et al. 1997, Lis et al. 1998, Miesch et al. 1999) and *H I* (Miville-Deschênes, Joncas & Falgarone 1999) centroid velocities. The regions include quiescent and active star formation, diffuse *H I*, and self-gravitating molecular clouds. Lis et al. (1996, 1998) compared the observations with simulations of mildly supersonic decaying turbulence and associated the velocity-difference pdf tails with filamentary structures and regions of large vorticity.

The first comparison of observations with simulations for velocity difference pdfs was given by Falgarone et al. (1994), who used optically thin line profile shapes from a simulation of decaying transonic hydrodynamic turbulence. They found that the excess wings could be identified in some cases with localized regions of intense vorticity. Klessen (2000) compared observations with the centroid-velocity-difference distributions from isothermal hydrodynamic simulations and found fair agreement with an approach to exponential tails on the smallest scales. Smith, Mac Low & Zuev (2000) found an exponential distribution of velocity differences across shocks in simulations of hypersonic decaying turbulence and were able to derive this result using an extension of the mapping closure technique (e.g., Gotoh & Kraichnan 1993). Ossenkopf & Mac Low (2002) gave a detailed comparison between observations of the Polaris flare and MHD simulation velocity and velocity centroid-difference pdfs, along with other descriptors of the velocity field. Cosmological-scale galaxy velocity-difference pdfs (Seto & Yokoyama 1998) also exhibit exponential forms at small separations.

The pdf of the velocity is not yet understood. The argument that the velocity pdf should be Gaussian based on the central-limit theorem applied to independent Fourier coefficients of an expansion of the velocity field, or to sums of independent velocity changes (e.g., Tennekes & Lumley 1972), neglects correlations and only applies to velocities within a few standard deviations of the mean. Perhaps this is why the early work found Gaussian velocity pdfs (e.g., Monin & Yaglom 1975, Kida & Murakami 1989, figure 6; Jayesh & Warhaft 1991, figure 1; Chen et al. 1993, figure 3). The velocity pdf must possess nonzero skewness (unlike a Gaussian) to have energy transfer among scales (e.g., Lesieur 1990).

Recent evidence for non-Gaussian velocity pdfs have been found for incompressible turbulence from experimental atmospheric data (Sreenivasan & Dhruva 1998), turbulent jets (Noullez et al. 1997), boundary layers (Mouri et al. 2003), and quasi-2D turbulence (Bracco et al. 2000). The sub-Gaussian results (with pdf flatness factor $F = \langle u^4 \rangle / \langle u^2 \rangle$ less than 3) are probably from the dominance of a small number of large-scale modes, while the hyper-Gaussian results ($F > 3$) may be the result of correlations between Fourier modes (Mouri et al. 2003), an alignment of vortex tubes (Takaoka 1995), or intermittency (Schlichting & Gersten 2000). The results are unexplained quantitatively.

For the ISM, exponential or $1/v$ centroid-velocity distributions were discovered and rediscovered several times over the past few decades (see Miesch, Scalo & Bally 1999). Miesch & Scalo (1995) and Miesch et al. (1999) found near-exponential tails in the $^{13}$CO centroid-velocity pdfs of several molecular regions. The pdf of the *H I* gas centroid-velocity component perpendicular to the disk of the LMC is also an exponential (Kim et al. 1998).

Rigorous derivations of the equation for the velocity pdf of incompressible hydrodynamic turbulence are presented in chapter 12 and appendix H of Pope (2000). Dopazo, Valino & Fueyo (1997) showed how to derive evolution equations for the moments of the velocity distribution from the kinetic equation. Closure methods for pdf equations are discussed in Chen & Kollman (1994), Dopazo (1994), Dopazo et al. (1997), and Pope (2000). Results generally predict Gaussian pdfs, although this depends somewhat on the closure method and assumptions.

Simulations have not generally examined the velocity pdf in detail, and when they have, the centroid-velocity pdf or optically thin line profile is usually given. An important exception is the 3D incompressible simulation of homogeneous shear flows by Pumir (1996), who found nearly exponential velocity fluctuation pdfs for velocity components perpendicular to the streamwise component. However, for conditions more applicable to the compressible ISM, the results are mixed. Smith, Mac Low & Zuev (2000) found a Gaussian distribution of shock speeds in 3D simulations of hypersonic decaying turbulence, but did not relate this to the pdf of the total velocity field. Lis et al. (1996) found the pdf of centroid velocities to be Gaussian or sub-Gaussian in hydrodynamic simulations of transonic compressible turbulence. The centroid velocity pdf for a 3D-forced MHD simulation given by Padoan et al. (1999) looks Gaussian at velocities above the mean but has a fat tail at small velocities. A detailed simulation study of the centroid-velocity pdf was presented by Klessen (2000), who examined driven and decaying hydrodynamic simulations with and without self-gravity at various Mach numbers. The centroid pdfs are nearly Gaussian, but the 3D pdfs were not discussed. The only 3D (not centroid) velocity pdf for an ISM-like simulation we know of, a decaying MHD simulation with initial Mach number of 5 displayed by Ossenkopf & Mac Low (2002, figure 11a), is distinctly exponential deep into the pdf core at their highest resolution run; nevertheless they remark in the text that all the pdfs are Gaussian.

Chappell & Scalo (2001) found nearly exponential tails in 2D simulations of wind-driven pressureless (Burgers) turbulence, and showed that the tail excesses persisted even in the absence of forcing. They proposed that these excesses could be understood in terms of the extreme inelasticity of the shell interactions in the Burgers model, and speculated that the result could be more general for systems in which interactions are inelastic, so that kinetic energy is not a globally conserved quantity. For example, a Gibbs ensemble for particles that conserve mass and momentum, but not energy, gives an exponential velocity distribution. Ricotti & Ferrara (2002) studied simulated systems of inelastically colliding clouds driven by supernovae and showed how the velocity pdf of the clouds approaches an exponential as the assumed inelasticity becomes large. Hyper-Gaussian velocity

distributions with exponential and even algebraic tails have also been observed in laboratory and simulated inelastic granular fluids (Barrat & Trizac 2002, Ben-Naim & Krapivsky 2002, Radjai & Roux 2002). All these systems dissipate energy on all scales.

The reason for the fat tails may be the positive velocity fluctuation correlations introduced by the inelasticity. This can be seen by noting that successive velocities are positively correlated for inelastic point particles conserving mass and momentum but not energy. Then the velocity changes are not independent and the central limit theorem does not apply (see Mouri et al. 2003). Such correlations, resulting entirely from the large range of dissipation scales, would be a fundamental difference between incompressible and supersonic turbulence. If true, then hyper-Gaussian pdfs need not be a signature of intermittency (Klessen 2000).

## 4.10. Turbulent "Pressure"

The idea of turbulent "pressure" is difficult to avoid because of its convenience. It has been used to generalize the gravitational instability (e.g., Bonazzola et al. 1987, Vázquez-Semadeni & Gazol 1995), to confine molecular clouds (e.g., McKee & Zweibel 1992, Zweibel & McKee 1995), and to approximate an equation of state (e.g., Vázquez-Semadeni, Canto & Lizano 1998). Rigorous analysis (Bonazzola et al. 1992) shows that turbulence can be represented as a pressure only if the dominant scale is much smaller than the size of the region under consideration ("microturbulence"). In fact this is not the case. The turbulent energy spectrum places most of the energy on the largest scale, and because the spectrum is continuous, the scale separation required for the definition of pressure (Bonazzola et al. 1992) does not exist. Ballesteros-Paredes, Vázquez-Semadeni & Scalo (1999) evaluated the volume and surface terms in the virial theorem and showed that the kinetic energy surface term is so large that the main effect of turbulence is to distort, form, and dissolve clouds rather than maintain them as quasi-permanent entities. Supersonic turbulence is also likely to be dominated by highly intermittent shocks whose effect is difficult to model as a pressure even with an ensemble average.

Simulations of turbulent fragmentation in self-gravitating clouds showed that turbulence suppresses global collapse while local collapse occurs in cores produced by the turbulence (Sections 5.10 and 5.11). This process does not resemble pressure, however. Global collapse is avoided because the gravitational and turbulent energies are transferred to separate pieces that have smaller and smaller scales.

## 4.11. Below the Collision Mean Free Path

Scintillation observations suggest interstellar electron density irregularities extend at a weak level down to tens or hundreds of kilometers (*Interstellar Turbulence II*), which is slightly larger than the ion gyroradius ($m_i c v_{th}/eB \sim 10^8/B(\mu G)$ cm) in the warm ionized medium and much smaller than the ion-neutral ($10^{15}/n$ cm) and Coulomb ($10^{14}/n_i$ cm) mean free paths at unit density, $n$, and $n_i$. Collisionless

plasma processes involving magnetic irregularities on small scales are probably involved.

Collisionless plasmas behave like a fluid on scales larger than the ion cyclotron radius. The equation of motion includes the coupling between charged particles and the magnetic field. There are also equations for mass and magnetic flux continuity and for the heat flux. The parallel and perpendicular components of the pressure tensor that account for their gyromotions were included by Chew, Goldberger & Low (1956). A general review is in Kulsrud (1983). Dissipation on very small scales is by cyclotron resonance, which is not considered in these equations. Dissipation on scales larger than the cyclotron radius is by Landau damping and other processes, such as Ohmic and ambipolar diffusion. Landau damping arises from a resonance between particle thermal speeds and wave speeds in various directions. Proper treatment of Landau damping in ISM turbulence is essential for understanding fast mode waves that may scatter cosmic rays (*Interstellar Turbulence II*). Landau damping could also modify the energy cascade because it covers a wide range of scales.

Landau damping was included in the MHD equations by Snyder, Hammett & Dorland (1997). Passot & Sulem (2003a) added dispersive effects that are important on scales close to the ion inertial length, $v_A/\Omega_i$, for Alfvén speed $v_A = B/(4\pi\rho)^{1/2}$ and cyclotron frequency $\Omega_i = eB/mc$. They used the equations of continuity and motion plus Ohm's law for the time derivative of the perturbed field **b**:

$$\frac{\partial \mathbf{b}}{\partial t} - \nabla \times (\mathbf{u} \times \mathbf{b}) = -\frac{1}{\hat{\Omega}_i} \nabla \times \left( \frac{1}{\rho} (\nabla \times \mathbf{b}) \times \mathbf{b} \right), \tag{13}$$

where the quantities are normalized to the ambient field and Alfvén speed, and $\hat{\Omega}_i = \Omega_i L/v_A$ is the normalized ion cyclotron frequency for system scale $L$. The last term is the Hall term, which comes from the inertia of the ions as the magnetic field follows the electrons. Pressure and density can be related by an equation for the heat flux (Passot & Sulem 2003a) or an adiabatic power law on scales larger than the mean free path (Laveder, Passot & Sulem 2001). The result is a system of equations for Hall-MHD. An interesting instability appears in this regime resulting in a collapse of gas and field into thin helical filaments (Laveder, Passot & Sulem 2001, 2002). Because the instability still operates in the collisionless regime (Passot & Sulem 2003b), such filaments may account for some of the elongated structure seen by ISM scintillation on scales smaller than the collision mean free path.

## 4.12. MHD Turbulence Theory: Power Spectra

The hydrodynamic turbulent cascades and intermittency effects discussed in Sections 4.6 and 4.7 have analogs in the magnetohydrodynamic case. An important difference between MHD and hydrodynamic turbulence arises because the magnetic field gives a preferred direction for forces. Turbulence in the solar wind (Matthaeus, Bieber & Zank 1995) and on the scale of interstellar scintillations is anisotropic with larger gradients of density perpendicular to the field. Shebalin

et al. (1983) showed from incompressible numerical simulations with a background magnetic field that the energy spectrum of velocity fluctuations parallel to the field is steeper than perpendicular, which suggests a diminished cascade in the parallel direction and increasing anisotropy on small scales. The suppression of the parallel cascade depends on the strength of the mean field, increasing for stronger fields (Müller, Biskamp & Grappin 2003). In the extreme case, there is no cascade at all in the parallel direction, leading to purely 2D or quasi-2D turbulence (Zank & Matthaeus 1993, Chen & Kraichnan 1997, Matthaeus et al. 1998). Parallel structures at high spatial frequencies passively follow the longer wavelengths in incompressible MHD without cascading to the dissipation range (Kinney & McWilliams 1998).

Incompressible MHD turbulence can be characterized in terms of interactions between three shear-Alfvén wave packets (Montgomery & Matthaeus 1995, Ng & Bhattacharjee 1996, Galtier et al. 2000), which satisfy the wavenumber and frequency sum conditions, $\mathbf{k}_1 + \mathbf{k}_2 = \mathbf{k}_3$ and $\omega_1 + \omega_2 = \omega_3$, to conserve momentum and energy. When the interacting waves are Alfvén waves, $\omega = k_\parallel v_A$, and when they are oppositely directed, $\mathbf{k}_1$ and $\mathbf{k}_2$ have opposite signs. Then solutions exist only when the parallel Fourier modes have energy at $k_{1\parallel} = 0$ or $k_{2\parallel} = 0$, which correspond to long-wavelength field-line wandering. Also, when $k_\parallel = 0$, there is no cascade in the parallel direction (e.g., Bhattacharjee & Ng 2001, Galtier et al. 2002). In this limit of incompressible or weakly compressible MHD with a strong mean field, the transverse velocity scales with wavenumber as $v_\perp \propto k^{-1/2}$ and the 1D transverse energy scales as $E_\perp(k) \propto k^{-2}$ (Ng & Bhattacharjee 1997, Goldreich & Sridhar 1997, Galtier et al. 2000).

Velocity and energy scalings with wavenumber may be obtained from heuristic arguments that give physical insight to turbulence theory (Connaughton, Nazarenko & Newell 2003). There are two important rates: the eddy interaction rate, $\omega_{int}$, and the cascade rate, $\omega_{cas}$. These rates are related by the number $N$ of interactions the fluid has to experience before the energy at a certain wavenumber cascades, $\omega_{cas} = \omega_{int}/N$. For weak interactions, the velocity change per interaction, $\delta v$, is small and the number required is determined by a random walk: $N \sim (v/\delta v)^2$. For strong interactions, each one is significant, so $\delta v \sim v$ and $N \sim 1$. The velocity change comes from the integral over the equation of motion for an interaction time: $\delta v = (dv/dt)\,\omega_{int}^{-1}$. The most important acceleration is the inertial term, $\mathbf{v} \cdot \nabla \mathbf{v}$, giving $dv/dt \sim kv^2$ for wavenumber $k$ and velocity $v$ in the cascading direction.

When $\delta v$ has this form, the interaction may be viewed as consisting of three waves; three-wave systems have a constant flux of energy, which is the cascade over wavenumber (Zakharov, L'vov & Falkovich 1992). Some systems such as gravity waves in deep water (Pushkarev, Resio, Zakharov 2003) have stronger four-wave interactions, and these conserve both energy and wave-action. Their velocity change is given by $\delta v = (d^2v/dt^2)\omega_{int}^{-2}$.

The last step in the derivation of the energy spectrum for weak turbulence is to assume a constant energy flux in wavenumber space, where energy is the square of the perturbed velocity or the summed squares of the velocity and the perturbed

field: $\epsilon = v^2\omega_{cas}$. Combining terms for three-wave interactions, we get,

$$\epsilon = \frac{v^4k^2}{\omega_{int}} = \text{constant}. \tag{14}$$

For weak nearly incompressible turbulence the interaction consists of oppositely directed "waves" or Fourier components moving at the Alfvén speed. The interaction rate is $\omega_{int} = k_\parallel v_A$ for parallel wavenumber $k_\parallel$ and Alfvén speed $v_A$. When the field is strong, $k_\parallel \sim$ constant so $\omega_{int} \sim$ constant, giving a transverse velocity scaling $v_\perp \propto k_\perp^{-1/2}$ from Equation 14. The energy spectrum follows from the relation $\int E(k)dk = v^2$, so that $E(k) \propto v^2/k \propto k^{-2}$. This is the result obtained by Ng & Bhattacharjee (1997) and others.

The Kolmogorov spectrum follows from an isotropic picture in which the wavenumber and velocity of the incoming perturbations are the same as those leaving the interaction as part of the cascade. Then $\omega_{int} = kv$ and $v^3k =$ constant, giving $E(k) \propto k^{-5/3}$.

Goldreich & Sridhar (1997) proposed that weak MHD turbulence is irrelevant in the ISM because it quickly strengthens in the cascade. They suggested that ISM turbulence is usually strong, and in this case there is a simplification that can be made from a critical balance condition, $\omega_{cas} = \omega_{int}$ (Goldreich & Sridhar 1995). This condition gives a parallel cascade and Kolmogorov scaling for transverse motions because if $\epsilon = v_\perp^4 k_\perp^2/\omega_{cas}$ from Equation 14 and $\omega_{cas} = k_\perp v_\perp$, then the energy flux is $\epsilon = v_\perp^3 k_\perp$. Goldreich & Sridhar reasoned that inequalities between $\omega_{cas}$ and $\omega_{int}$ would lead to changes in the interaction process that would restore equality. If $\omega_{cas} > \omega_{int}$, for example, then local field line curvature would decrease in time as the transverse energy leaked away without adequate replacement from the parallel direction. The field lines would then be more easily bent by the next incoming packet. An important assumption for their model is that the wave interactions that dominate the energy transfer are local in wavenumber space (see Lithwick & Goldreich 2003).

For isotropic turbulence with a fixed incoming velocity, such as an Alfvén speed, $\omega_{int} = kv_A$. Then one of the $k$'s cancels from the numerator in Equation 14, but a velocity does not cancel, giving $v^4k =$ constant and $E(k) \propto k^{-3/2}$. This is the scaling suggested by Iroshnikov (1964) and Kraichnan (1965) for magnetic turbulence, before the anisotropy of this turbulence was appreciated. Recent studies of 2D MHD turbulence also showed Iroshnikov-Kraichnan scaling (Politano, Pouquet & Carbone 1998; Biskamp & Schwarz 2001; Lee et al. 2003). Politano et al. actually got $\zeta_4 \sim 1$, which corresponds to $\langle v^4 \rangle \propto k^{-1}$, but they got $\zeta_2 \sim 0.7$, which gives about the Kolmogorov 1D energy spectrum, $k^{-1.7}$. The nonlinear dependence of $\zeta_p$ on $p$ is the result of intermittency.

Iroshnikov-Kraichnan scaling and a suppressed parallel cascade occurs in incompressible MHD turbulence if the energy transfer among modes is dominated by interactions between waves with very different sizes (Nakayama 2002). It may also apply in 2D MHD turbulence with such nonlocal interactions (Pouquet, Frisch &

Léorat 1976). The issue of locality in wavenumber space is not understood even in hydrodynamic turbulence (Yeung, Brasseur & Wang 1995) although local transfer is commonly assumed. A study of the degree of cancellation of long-range three-wave interactions in incompressible hydrodynamic turbulence by Zhou, Yeung & Brasseur (1996) shows that nonlocal interactions cause anisotropy at small scales, and the effect may increase with the scale separation. This suggests that long-range dynamics persist at large Reynolds numbers, in which case current MHD simulations may not have the resolution to capture the effect.

Kolmogorov $k^{-5/3}$ scaling changes over to Iroshnikov-Kraichnan $k^{-3/2}$ scaling as the mean field gets stronger, all else being equal. Müller, Biskamp & Grappin (2003) found this from simulations of incompressible turbulence using a spectral code of size $512^3$. As the transition to $k^{-3/2}$ occurred, the inertial range parallel to the mean field became shorter indicating an inability to cascade in this direction, as mentioned above. Dmitruk, Gómez & Matthaeus (2003) also found a spectral slope that depends sensitively on conditions. They considered incompressible turbulence driven at speed $v_d$ at two opposing boundaries of an elongated box measuring $L_\perp \times L_\perp \times L_\parallel$. When the ratio of the Alfvén propagation time along the field, $L_\parallel / v_A$, to the stirring time perpendicular to the field, $L_\perp / v_d$, was large, the relatively rapid stirring produced more small-scale structure and a shallow energy spectrum. When the ratio was small, the spectrum was steep.

The energy spectrum of weak nonmagnetic turbulence driven in a rapidly rotating medium also shows Iroshnikov-Kraichnan scaling in a direction perpendicular to the spin axis (Galtier 2003).

Scintillation observations (*Interstellar Turbulence II*) suggest the energy spectrum of density fluctuations is close to Kolmogorov. This limits the range of possible models in these applications. Also, the relevance of scaling laws derived under the assumption of weak turbulence ($N = (v/\delta v)^2 \gg 1$) is questionable. For these reasons, there is continued interest in the critical balance model of strong turbulence discussed by Goldreich and collaborators. We review their proposals and the related numerical simulations next.

## 4.13. The Anisotropic Kolmogorov Model

Goldreich & Sridhar (1995) proposed that interstellar turbulence on small scales results from nonlinear interactions between shear Alfvén waves in an incompressible, ionized medium. The energy spectrum was determined from a critical balance condition that the wave interaction rate in the parallel direction, $\omega_{int} \sim k_\parallel v_A$, is comparable to the cascade rate in the perpendicular direction, $\omega_{cas} \sim k_\perp v_\perp$. This condition gives a cascading energy flux $\epsilon \sim v_\perp^2 \omega_{cas} \sim v_\perp^3 k_\perp$, which leads to a scaling relation for perpendicular motions, $v_\perp / v_A \sim (\lambda_\perp / L)^{1/3}$, and a cascade in the parallel direction, making $k_\parallel L \sim (k_\perp L)^{2/3}$. Here $L$ is the scale at which extrapolated turbulent motions would be isotropic and comparable to the Alfvén speed, $v_A$.

The energy spectrum is related to the velocity scaling law as $v^2 = \int E(k) dk$. Cho, Lazarian & Vishniac (2002a) found from 3D MHD simulations that the

energy spectrum for parallel motions is $E(k_\parallel) \sim k_\parallel^{-2}$. They also obtained $k_\parallel \propto k_\perp^{2/3}$ as above and fit the 3D power spectrum to

$$P(k_\perp, k_\parallel) = \left(B_0^2/L^{1/3}\right) k_\perp^{-10/3} \exp\left(-L^{1/3} k_\parallel / k_\perp^{2/3}\right) \tag{15}$$

for unperturbed field strength $B_0$.

In this model, perturbations get stronger as they cascade to smaller scales, and they get more elongated with $\lambda_\parallel/\lambda_\perp \sim (2\pi L/\lambda_\perp)^{1/3}$ increasing for smaller $\lambda_\perp$ ($\lambda_\parallel/\lambda_\perp \sim 1000$ on the smallest scales). These local relations also follow if the local anisotropy, $k_\parallel/k_\perp$, is proportional to the ratio of the local perturbed field to the total field (Matthaeus et al. 1998; Cho, Lazarian & Vishniac 2003a). The global relation between $\lambda_\parallel$ and $\lambda_\perp$, averaged over a large scale, can actually be more isotropic, $\lambda_\perp \sim \lambda_\parallel$, if the local field lines bend significantly on the small scale (Cho, Lazarian & Vishniac 2002a).

A schematic diagram of a turbulent cascade is shown in Figure 4 (from Maron & Goldreich 2001). Wave packets travel along the field and become distorted as the lines of force interchange with other lines containing different waves. A density pattern gets distorted by this motion too.

Electron density fluctuations in the theory of Goldreich & Sridhar (1995) are a combination of entropy fluctuations, i.e., temperature changes with approximate

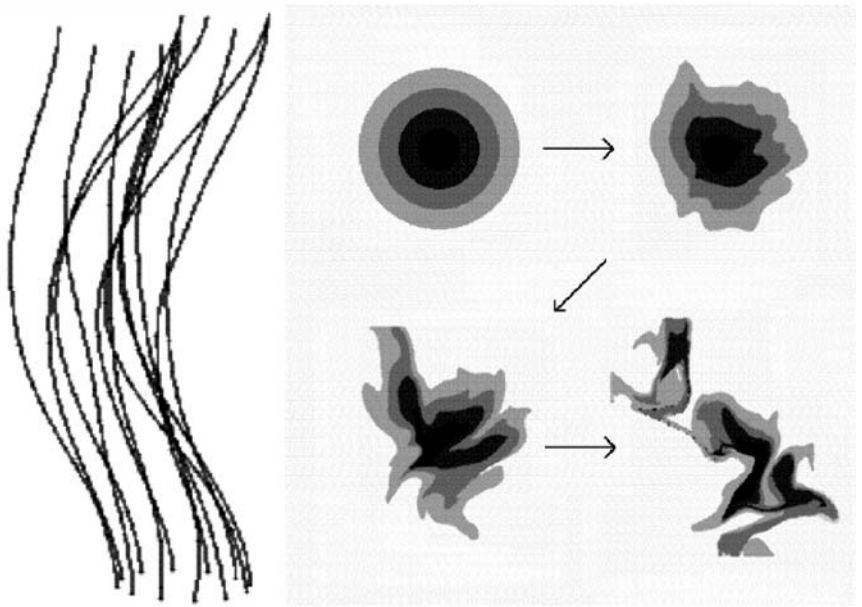

**Figure 4** Distorted field lines with a downward propagating wave (*left*) and distortion of a bullseye pattern moving upward along these lines (*right*). From Maron & Goldreich (2001) reproduced by permission of the AAS.

pressure equilibrium (Higdon 1986), and slow-mode wave compressions (Lithwick & Goldreich 2001). Turbulence distorts and divides the large-scale density structures into smaller structures, giving them the same power spectrum as the velocity. This is "passive mixing" if the density irregularities are weak and have little back reaction on the velocity field.

Passive mixing is a key component of the model by Goldreich et al. for which essentially all the dynamics comes from incompressible waves. Numerical simulations confirm the small degree of coupling between these Alfvén shear modes and the compressional modes, which are the fast and slow magnetosonic modes (section 4.1 in *Interstellar Turbulence II*). Cho & Lazarian (2002b) considered the low $\beta = P_{thermal}/P_{mag}$ case and separated the shear, fast, and slow modes in a compressible MHD simulation. The relative energy in the compressible part grew from zero to only 5%–10% after three crossing times, which implies the slow mode is weakly coupled to the shear mode. For purely solenoidal driving, the Alfvén and slow modes had $k^{-5/3}$ energy scaling for velocity and field, and the slow mode had $k^{-5/3}$ scaling for the density; the fast modes had all three variables scale like $k^{-3/2}$. Cho & Lazarian (2003) conducted similar calculations for the high $\beta$ case and got the same results for mode coupling and energy spectra. Most of the density structure was from slow modes at low $\beta$, but at high $\beta$, it came from a nearly equal combination of slow and fast modes. Cho & Lazarian (2003) showed that even for highly compressible supersonic turbulence, the Alfvén mode, which barely couples to the compression, cascades like an incompressible fluid with an energy spectrum $\propto k^{-5/3}$.

These scalings are consistent with the isotropies measured for the three modes (Cho & Lazarian 2002b). Alfvén modes and their passive slow counterparts have velocities that depend on the propagation direction relative to the field (at low $\beta$). This makes them anisotropic with $k_\parallel \propto k_\perp^{2/3}$, as discussed above. Fast modes have equal velocities in all directions at low $\beta$, and the resulting isotropy makes $k_\parallel \propto k_\perp$, as proposed by Kraichnan (1965). Cho & Lazarian (2002b) further reasoned that slow modes are passive at low $\beta$ because they move very slowly relative to the Alfvén waves ($a \cos\theta \ll v_A$ for thermal speed $a$), so the Alfvén waves can distort them easily.

Cho, Lazarian & Vishniac (2002b) proposed that magnetic irregularities should persist without corresponding velocity irregularities below the viscous damping length ($L_K$; see Section 4.2), down to the scale at which magnetic diffusion becomes important. Damping in the equation of motion comes from a term $\nu\nabla^2 v$, and magnetic diffusion comes from a term like $\eta\nabla^2 B$; the ratio $\nu/\eta$ is the Prandtl number. Cho et al. considered large Prandtl numbers and found that the kinetic energy between the viscous and the diffusion lengths cascaded more steeply than the magnetic energy: $E_v(k_\perp) \propto k_\perp^{-4.5}$ and $E_B(k_\perp) \propto k_\perp^{-1}$. The latter relation implies that the perturbed field, $B_\perp$, is independent of scale (using $kE_b(k) \sim b_\perp^2$), presumably because the cascade time into the pure-magnetic regime is equal to the cascade time at its outer scale, which is the viscous scale (Cho, Lazarian & Vishniac 2003b). In their compressible MHD simulations, Cho, Lazarian &

Vishniac (2003b) and Cho & Lazarian (2003) found density fluctuations below the viscous length with the same power spectrum as the field, $E_\rho(k_\perp) \sim k_\perp^{-1}$. More recently, Lazarian, Vishniac & Cho (2004) suggested that velocity fluctuations below the viscous length can be driven by magnetic fluctuations. Schekochihin et al. (2002) found a folded field line structure on small scales in incompressible MHD simulations at high Prandtl number, with the most sharply curved fields being the weakest. They also found comparable magnetic and kinetic energy densities and explained this result in terms of a back-reaction of the field on the motions.

Maron & Goldreich (2001) and Cho, Lazarian & Vishniac (2002a) studied the velocity structure functions in strong incompressible MHD turbulence. Recall that in a power-law approximation, these functions can be written

$$S_p(\delta r) = \langle [\mathbf{v}(\mathbf{r} + \delta\mathbf{r}) - \mathbf{v}(\mathbf{r})]^p \rangle \sim \delta r^{\zeta_p} \tag{16}$$

for two points separated by distance $\delta\mathbf{r}$. For Kolmogorov turbulence without intermittency, $\zeta_p = p/3$; with intermittency, $\zeta_p(p)$ is nonlinear. Politano & Pouquet (1995) derived $\zeta_p(p)$ as

$$\zeta_p = \frac{p}{g}(1-x) + C\left[1 - \left(1 - \frac{x}{C}\right)^{p/g}\right] \tag{17}$$

where $g$ is the exponent in the velocity relation $v_\perp \propto k_\perp^{-1/g}$, $x$ is the exponent in the cascade rate, $\omega_{cas} \propto k_\perp^x$, and $C$ is the codimension of the dissipation region: $C = 2$ for lines and $C = 1$ for sheets (the codimension is equal to the number of spatial dimensions minus the fractal dimension of the structure). For nonmagnetic Kolmogorov turbulence with intermittency, $g = 3$, $x = 2/3$, and $C = 2$, giving the expression for $\zeta_p(p)$ originally found by She & Leveque (1994).

Cho, Lazarian & Vishniac (2002a) determined that strong turbulent motions perpendicular to the local field have the same $\zeta_p(p)$ dependence as nonmagnetic turbulence. Relative to the global magnetic field, the scaling of the perpendicular velocity structure function was different (Cho, Lazarian & Vishniac 2003b), following instead a form with $C = 1$ (sheet-like) as suggested by Müller & Biskamp (2000). In both cases, the magnetic structure function had an index $\zeta_p$ that was lower than the velocity structure function, suggesting that $B_\perp$ is more intermittent than $v_\perp$. The structure function of velocity parallel to the mean local field had $\zeta_p$ larger than for $v_\perp$ by a factor of 1.5, which is consistent with the elongated geometry of the turbulence, for which $\lambda_\parallel^{3/2} \propto \lambda_\perp$ (Cho, Lazarian & Vishniac 2002a).

Haugen et al. (2003) did $1024^3$ simulations of forced, weakly compressible, nonhelical MHD turbulence and found a codimension of $C \sim 1.8$ (nearly line-like). The total energy spectrum integrated over 3D shells in $k$-space is $\sim k^{-5/3}$ at small $k$ and $\sim k^{-1.5}$ at intermediate $k$ just before the dissipation range. This flattening to $k^{-1.5}$ was attributed to a bottleneck in the cascade and not an Iroshnikov-Kraichnan inertial spectrum. In the saturated state, 70% of the energy was kinetic but 70% of the dissipation occurred by magnetic resistivity. Such Ohmic

dissipation can increase the temperature in a turbulent medium by an order of magnitude (Brandenburg et al. 1996).

Simulations of compressible MHD turbulence with zero mean field (Cho, Lazarian & Vishniac 2003b) had $\zeta_p$ for velocity the same as for incompressible turbulence, giving $C = 2$, and they had $\zeta_p$ for the field in global coordinates satisfying the above expression with $C = 1$. Maps of the high-$k$ field structure in planes perpendicular to the mean field clearly showed this sheet-like field geometry for both compressible and incompressible cases. There was a transition from somewhat uniform magnetic waves on large scales to highly intermittent sheet-like regions on small scales.

## 5. SIMULATIONS OF INTERSTELLAR TURBULENCE

### 5.1. Introduction

Numerical simulations of the hydrodynamical or MHD equations provide the only means by which we can actually "observe" interstellar turbulence in action, although what we see depends on the physical processes included, whether and how external forcing is applied, the dimensionality of the simulations, the imposed initial and boundary conditions, the discretization technique, and the spatial resolution. The first simulations of what can now be seen as ISM turbulence go back more than 20 years (Bania & Lyon 1980), but it is only within the past 5 to 10 years that the field has matured enough to concentrate on the inherently turbulent aspects of the problem.

The first simulations of nonmagnetic and nonself-gravitating supersonic turbulence at relatively high resolution were by Passot, Pouquet & Woodward (1988). Higher resolution studies of such transonic turbulence are given by Porter et al. (1999) and Porter, Pouquet & Woodward (2002). Their models are dominated by filaments in both vorticity (Figure 3) and divergence of the velocity field, and the filaments cluster into larger filaments and sheet-like structures in the compressible part of the flow, forming sheets and spirals in the vorticity field (Porter et al. 2002). Transonic nonself-gravitating models like this may illustrate the morphology of diffuse clouds and small molecular clouds when magnetic and gravitational forces are not important. They are also able to isolate the effects of moderate compressibility from other phenomena.

The first nonmagnetic simulations to include gravity were by Leorat et al. (1990) on a $128^2$ grid, and the first nongravitating compressible simulations to include magnetic fields in an ISM context were by Yue et al. (1993) on a $20^2$ grid. Over the next decade, these works were greatly expanded to include many aspects of the ISM, such as magnetic and gravitational forces, realistic heating and cooling, stellar energy injection and galactic shear. The first efforts in this direction were by Chiang & Prendergast (1985) and Chiang & Bregman (1988), who modeled star-formation feedback in a 2D ISM, and by Passot, Vázquez-Semadeni & Pouquet (1995), Vázquez-Semadeni, Passot & Pouquet (1995), and

Vázquez-Semadeni, Passot & Pouquet (1996), who emphasized the importance of cooling and the nature of turbulent forcing, and explored the relation between magnetism and the star-formation rate. These were the first simulations to include magnetic fields, self-gravity, heating and cooling, and Coriolis forces, and they were meant to represent the relatively large-scale (∼1 kpc) diffuse neutral ISM. By the late 1990s, 3D MHD simulations of isothermal molecular clouds without self-gravity were performed by several groups (e.g., Mac Low et al. 1998; Stone, Ostriker & Gammie 1998; Mac Low 1999; Padoan & Nordlund 1999), and detailed comparisons with observations were made by Padoan, Jones & Nordlund (1997) and Padoan et al. (1998, 1999). Some problems with isothermal simulations are summarized in Section 4.5.

These models and others mentioned below are important steps toward understanding the complex interactions that occur in the ISM, and they provide useful statistical comparisons with observations. However, like all turbulence simulations, they have a fundamental limitation from the lack of dynamic range over the full ISM Reynolds number, $Re$. The number of degrees of freedom for 3D incompressible turbulence scales like $Re^{9/4}$, meaning that a simulation at $Re = 10^6$ would require a resolution of $10^5$ zones per dimension, far beyond the reach of present-day approaches (but see the lattice Boltzmann method of Chen et al. 2003). Generalizing to compressible self-gravitating MHD with physically consistent driving agents and an equation of state makes the proposition even more implausible. One possibility for molecular clouds with low ionization fraction is that the energy dissipation scale is set by ambipolar diffusion and not viscosity (Klessen, Heitsch & Mac Low 2000). Then the effective Reynolds number might be (Balsara 1996, Zweibel & Brandenburg 1997)

$$R_{AD} \approx (L/0.04 \text{ pc})\, M_A (x/10^{-6})(n/10^3 \text{ cm}^{-3})^{3/2}\, (B/10\ \mu\text{G})^{-1} \qquad (18)$$

where $L$ is the large scale of interest, $M_A$ the Alfvén Mach number, $x$ the ionization fraction, $n$ the particle density, and $B$ the magnetic field strength. In this case the available resolution of numerical simulations would be adequate for dense molecular clouds. However this argument neglects the possibility that ambipolar diffusion acts on small scales to produce even finer structure (Brandenburg & Zweibel 1994; Tagger, Falgarone & Shukurov 1995; Balsara, Crutcher & Pouquet 2001), and it only applies in well-shielded molecular clouds, not in the general ISM.

An example of the importance of resolution for turbulence studies is the test of whether the energy flux through the inertial range is constant. This is the basis for Kolmogorov's model of incompressible turbulence, and it has only recently been verified in $2048^3$ simulations on the Earth Simulator (Kaneda et al. 2003). Higher resolution ($4096^3$) simulations also find a constant energy flux but suggest there may be a significant small departure from Kolmogorov's predicted energy spectrum (Kaneda et al. 2003). Another example is the emergence of new phenomena at very large $Re$, such as the transition in the power-law scaling of the flatness factor, or kurtosis, of the velocity derivative pdf observed for incompressible turbulence by

Tabeling & Willaime (2002) at Taylor scale Reynolds numbers $Re_\lambda$ larger than that attainable by current simulations. For compressible turbulence in the cold ISM, Adaptive Mesh Refinement simulations with effective resolution as large as $10^3 \times 10^3 \times 10^4$ have not converged yet either: a twofold increase in resolution yielded an increase in maximum density and a decrease in minimum temperature by factors greater than five (de Avillez & Breitschwerdt 2003).

Simulations at imperfect resolution can still reveal much of the underlying physics as long as the range of scales resolved is large enough that the intricate spatial fluid distortions resulting from nonlinear interactions are expressed. Resolving the inertial range for incompressible turbulence requires a resolution equivalent to more than ~500 zones in each direction (perhaps significantly more; Pouquet, Rosenberg, & Clyne 2003)—something that is now commonly available in 3D and easily obtained for smaller dimensions. With adequate resolution, simulations reveal geometrical and topological properties, whereas theories using statistical closure assumptions wash out the phase information. Simulations also allow many more opportunities for comparison with observations than do phenomenological or statistical models.

Here we give a brief summary of what seem to be the most important accomplishments of ISM turbulence simulations and the questions that remain unanswered. Details of numerical techniques and their associated problems are not discussed here. For example, the use of periodic boundary conditions in solving the Poisson equation introduces artificial tidal forces that can be important away from the density maxima (Gammie et al. 2003). The use of hyperviscosity, sensitivity to assumed initial conditions, differences between simulations using different numerical techniques, the violation of the Jeans condition found by Bate & Burkert (1997) and Truelove et al. (1997) in some self-gravitating simulations, and the assumption of isothermality in some simulations are also not addressed. Systematic effects resulting from varying the parameters (especially the mean magnetic field) are also omitted (see Ostriker et al. 2001, Lee et al. 2003). Readers are referred to reviews of some of these problems and more detailed discussions of statistical properties in Vázquez-Semadeni et al. (2000), Ballesteros-Paredes (2003), Mac Low (2003), Nordlund & Padoan (2003), Ostriker (2003), and Mac Low & Klessen (2004).

## 5.2. Scaling Relations

Probably no result has generated more research on ISM turbulence than Larson's (1981) finding that the density and velocity dispersion of molecular clouds scale with the size of the the region as power laws, suggestive of scaling relations that are found in incompressible turbulence. Simulations have examined these relations in detail. The density-size relation found by Larson (1981), which implies a constant column density, may be a selection effect because a wide range of densities is present for each scale in the simulations, whereas observations tend to pick the strongest emission regions and select for a restricted range of column density

(Kegel 1989; Scalo 1990; Vázquez-Semadeni, Ballesteros-Paredes & Rodriguez 1997; Ballesteros-Paredes & Mac Low 2002). However, Ostriker et al. (2001) reproduced Larson's squared dependence of the mass on size.

The linewidth-size relation is also problematic. Some studies show little correlation, whereas others have a correlation dominated by scatter; power-law fits also vary depending on tracer and type of cloud (see references in Section 2). Even if there is a power-law with an exponent 0.4–0.6, the interpretation is ambiguous. It was attributed to a field of shock discontinuities by Vázquez-Semadeni et al. (1997), considering that the associated velocity discontinuities should give an energy spectrum $E(k) \propto k^{-2}$ (Saffman 1971) and so $v^2 \propto k^{-1}$, which gives $v \propto L^{1/2}$. The problem with the shock model is that energy spectra found for supersonic simulations are not necessarily $k^{-2}$ (Boldyrev, Nordlund & Padoan 2002a; Wada et al. 2002; Vestuto et al. 2003). Also, the Kolmogorov spectrum for incompressible turbulence, $E(k) \propto k^{-1.67}$, is not much different. Further, the proposed shocks themselves have not been observed directly in real clouds. Nevertheless, the linewidth-size relations in Ballesteros-Paredes & Mac Low (2002) and Kim et al. (2001) were not just virialized motions as these simulations did not include self-gravity; it is not clear whether self-gravity is required to get the observed absolute scale. Kudoh & Basu (2003) obtained the Larson relations in numerical simulations of self-gravitating clouds with internal energy from magnetic waves. Other simulation studies of this relation are in Ostriker et al. (2001) and Ballesteros-Paredes & Mac Low (2002).

One problem with the linewidth-size observations is that it is impossible to identify physically coherent condensations using only radial velocities and sky coordinates of position. This was first pointed out by Burton (1971) and Adler & Roberts (1992) in connection with velocity crowding along galactic spiral arms, and then recognized for interstellar turbulence by Lazarian & Pogosyan (2000), Pichardo et al. (2000), and Ostriker et al. (2001). Another aspect of the problem is that the physically relevant correlation may be between linewidth and density (Xie 1997, Padoan et al. 2001b), which gives $v \propto n^{-0.4}$ to $n^{-0.3}$ for Larson-like scaling. For supersonic turbulence, a relation like this makes sense because the densest regions have been decelerated behind shock fronts, although shocks propagating in a turbulent medium can increase the velocity dispersion behind them (Rotman 1991, Andreopoulos et al. 2000), which gives the opposite effect.

Another scaling relation is between magnetic field strength and density, which appears flat at densities $<100$ cm$^{-3}$ and then has an upper limit that rises as $B \sim n^{0.5}$ above that (Troland & Heiles 1986, Crutcher 1999; Bourke et al. 2001). Pre-simulation work concentrated on cloud contraction, but MHD simulations account for the power index and scatter without monotonic contraction. Examples include 2D models for the diffuse ISM with self-gravity, cooling, and *H II* region expansion (Passot et al. 1995), isothermal 3D models with and without gravity forced with Fourier modes (Padoan & Nordlund 1999, Ostriker et al. 2001, Li et al. 2004), and 3D simulations with supernovae (Kim et al. 2001). Turbulent ambipolar diffusion could significantly affect the relation and its scatter (Heitsch

et al. 2004). Passot & Vázquez-Semadeni (2003) present a detailed analysis of the problem. Other considerations are discussed in Section 5.13.

## 5.3. Decay of Supersonic MHD Turbulence

A major discovery as a result of simulations is that supersonic MHD turbulence decays in roughly a crossing time (based on the rms turbulent velocity) regardless of magnetic effects and the discreteness of energy injection (Mac Low et al. 1998; Stone, Ostriker & Gammie 1998; Mac Low 1999; Padoan & Nordlund 1999; Avila-Reese & Vázquez-Semadeni 2001; Ostriker et al. 2001). Decay is faster with cooling (Kritsuk & Norman 2002b, Pavlovski et al. 2002) because the average Mach number is larger. Pavlovski et al. fit the energy to $E(t) = E_0\,(1 + t/t_1)^{\eta}$, for $t_1 = L_{inj}/v_{rms}$ equal to the initial ratio of the mean energy injection scale to the rms velocity, and $\eta \sim -1.3$. For isothermal compressible MHD turbulence that is either super- or sub-Alfvénic, $\eta \sim -1$ (e.g., Mac Low et al. 1998). This type of decay may be dominated by the pure Alfvénic (shear) modes that have this time dependence if the compressional modes are barely coupled to the shear (see Figure 1a in Cho & Lazarian 2002b). Thus, damping is not just through the compressional modes as originally thought. Alfvén wave propagation may actually delay the energy decay (Cho & Lazarian 2003). In addition, compressible modes can propagate and diffuse freely along the magnetic field lines.

Incompressible nonmagnetic turbulence is also believed to decay as a power law with time, with an exponent between approximately $-1.2$ and $-1.4$. Several approaches using various assumptions about the preservation of the spectrum or the nature of the low wavenumber part of the initial spectrum (e.g., Saffman's invariant, Loitsianskii's invariant, closures whose results depend on the initial spectrum) give results in this same range (see summaries in Hinze 1975, Lesieur 1990, Frisch 1995, Biskamp 2003). Biskamp & Müller (1999, 2000) showed that for incompressible isotropic MHD turbulence the total and kinetic energies vary as $t^{-1}$ when there is no magnetic helicity but the total energy varies as $t^{-1/2}$ with the same $t^{-1}$ kinetic energy decay when helicity is present and nearly conserved. The physical reason for the similar time dependencies in the incompressible, compressible, and MHD cases is unknown.

A closely related result, that clouds are transient entities not confined by thermal or intercloud pressure, was found by Ballesteros-Paredes, Vázquez-Semadeni & Scalo (1999) and Elmegreen (1999). These results, along with observations of short star-formation times (Ballesteros-Paredes, Hartmann & Vázquez-Semadeni 1999; Elmegreen 2000; Hartmann et al. 2001), eliminate the old problem of how clouds could be supported for long times in the presence of supersonic turbulence (Zuckerman & Evans 1974).

The details of shock energy dissipation in 3D supersonic turbulence have been studied by Smith, Mac Low & Heitsch (2000) and Smith, Mac Low & Zuev (2000) for decaying and uniformly (Fourier) forced motions; the latter paper includes models with self-gravity. Besides the frequency distribution of shock velocities

whose form is explained with a phenomenological theory, Smith et al. found that in the decaying runs the dissipation rate peaks at small Mach numbers. For example, at rms Mach number of 5, the power loss peaks around Mach 1 to 2, whereas at rms Mach 50, the peak is from Mach 1 to 4, decreasing with time in both cases. Most of the dissipation is from a large number of weak shocks. In uniformly forced simulations, however, the dissipation occurs in a small range of high Mach number shocks, peaking at greater than the rms value. This result emphasizes the crucial role of the driving process in controlling interstellar turbulence and line profiles. For example, the smoothness of line profiles (see Section 2) may imply that cool clouds spend most of their time in the decaying mode, with only sporadic and/or spatially discrete forcing. It is notable that in both cases the magnetic field had little effect on the distribution of shock strengths or their dissipation rate. As stated by Smith, Mac Low & Heitsch (2000), magnetic pressure is not damping the shocks but helps maintain them by transferring energy from the strong magnetic waves to the shock waves.

## 5.4. The Density Probability Distribution

Vázquez-Semadeni (1994) suggested that the probability distribution of densities (the density pdf) is lognormal as a result of the central limit theorem applied to a multiplicative hierarchical density field. Several groups subsequently found that the pdf should exhibit an approximately lognormal distribution if the gas is isothermal (Ostriker, Gammie & Stone 1999; Klessen 2000; Ostriker et al. 2001; Li et al. 2004), with quasi-power-law tails if nonisothermal (Passot & Vázquez-Semadeni 1998; Scalo et al. 1998; Nordlund & Padoan 1999). Recent simulations of dense cluster formation (Li, Klessen & Mac Low 2003) confirmed the approximately lognormal behavior for isothermal turbulence and the increasingly prominent high-density tail that appears when the equation of state is softer. Li et al. (2004) found density pdfs with negative skewness from shocks that evacuate large regions, and positive skewness from self-gravity that makes clumps. The large-scale central disk galaxy simulations by Wada & Norman (2001) found a surprisingly robust and invariant lognormal form of the density pdf (above the average density) when the density field is generated by turbulence that includes a variety of physical processes. At densities below the peak, the pdf found by Wada and Norman departs significantly from a lognormal.

This important theoretical result is difficult to verify from observations of column densities alone. Gaustad & VanBuren (1993) sampled the 3D density distribution for fairly low densities, $\sim$1 cm$^{-3}$, using 1800 OB stars as probes of the local dust density. Their pdf resembles a lognormal, but it can also be fit by a power law above the mean. Berkhuijsen (1999) measured the volume filling factor as a function of density for ionized and neutral gas and obtained a power law.

The probability distribution function for column density was studied theoretically by Padoan et al. (2000), Ostriker et al. (2001), and Vázquez-Semadeni & García (2001) using numerical simulations of isothermal MHD turbulence. For the

isothermal case the spatial density distribution is log-normal, so the column density distribution is similar except for blending, which depends on the ratio of cloud depth to autocorrelation length. For a large ratio, the central limit theorem gives a Gaussian distribution of column densities and for a very large ratio the column density becomes nearly constant over the face of the cloud (Vázquez-Semadeni & García 2001).

## 5.5. Energy Cascades

One of the oldest ideas in turbulence theory is that energy cascades in wavenumber space. Molecular cloud simulations often inject energy at large scales, and this energy cascades to smaller scales where dissipation occurs. In analytical work, the transfer is usually assumed to occur locally in wavenumber space, i.e., between similar-sized regions (compare Section 4.12). In fact, it is not well understood why turbulence cascades in a given direction or how important nonlocal energy transfer is (see Zhou, Yeung & Brasseur 1996). Good examples of nonlocal transfers are in shocks, where large-scale flows abruptly convert kinetic energy into atomic random motions at the front, and superbubbles, where localized energy gets transferred in a single step to much larger scales. In 2D incompressible turbulence, the energy cascades to large scales regardless of where it is injected; only the mean squared vorticity (enstrophy) cascades down to the viscous scale. Recent work (Kurien, Taylor & Matsumoto 2003) even indicates that the inertial range of incompressible turbulence is a dual cascade of energy and helicity that generates a $k^{-5/3}$ energy spectrum at intermediate wavenumbers but $k^{-4/3}$ at large wavenumbers.

How should interstellar turbulence cascade? Energy could be fed in from rotation on the largest scales, self-gravity on intermediate scales, and individual stars or clusters on intermediate to small scales. The key concept behind a direct cascade to smaller scales is absent, i.e., that an inertial range exists in which advection alone distorts the fluid elements while conserving kinetic energy. In addition, ISM turbulence is highly compressible, so there is no quadratic invariant conserved by the advection operator; energy can transfer directly between kinetic and thermal modes.

Energy may cascade in either direction or in both simultaneously. Most simulations that observe a cascade to small scales force the turbulence over the whole computational domain and often use purely solenoidal fluctuations, which favor the direct cascade. Recently, Wada et al. (2002) showed that for 2D inner galaxy models, the energy injected by self-gravity on $\sim$10 pc scales cascades to larger regions; this is probably not an artifact of the 2D geometry because the system is strongly compressible and does not have the conservation properties that give incompressible 2D turbulence an inverse cascade. Vestuto, Ostriker & Stone (2003) found an inverse cascade in MHD simulations where the forcing was not at the largest scales. Christensson, Hindmarsh & Brandenburg (2001) found inverse cascade in decaying 3D MHD turbulence with helical fields. Because the range of wavenumber space over which forcing by *H II* regions, supernovae, and

superbubbles occurs is extremely broad and the energy input rate is relatively uniform, the energy flow between scales in ISM turbulence remains essentially unknown. Strong forcing over a wide range of scales could even remove intermittency effects (Biferale, Lanotte & Toschi 2004).

## 5.6. Compressible Versus Solenoidal Motions

Any turbulent velocity field can be decomposed into a solenoidal (rotational) mode and a compressible (potential or irrotational) mode and each mode can feed the other (Sasao 1973). It is of great interest to know the relative energy in each. Intuitively it might seem that the result should scale with Mach number because at zero Mach number the flow is purely incompressible and at infinite Mach number it should be mostly compressible. Some discussion of the flow of energy between the two modes, based on the coupling of the evolution equations for the vorticity and dilatation, is given by Vázquez-Semadeni et al. (1996) and Kornreich & Scalo (2000). Bataille & Zhou (1999) and Bertoglio, Bataille & Marion (2001) used a closure method with simulations to predict that the compressible to solenoidal energy ratio should increase with the square of the rms Mach number for very small Mach numbers. However, Shivamoggi (1997) used a statistical mechanical approach and found that the advection operator should evolve toward an equipartition between compressible and vortical modes.

What do simulations have to say about this ratio? A major problem with simulations, especially at the molecular cloud level, is the use of large-scale forcing in Fourier space. This has the effect of stirring the gas in the entire computational domain simultaneously. The situation in the ISM, at least at intermediate and small scales, is likely to be different. Artificial forcing is usually solenoidal also, whereas stellar energy sources will mostly generate compressible fluctuations. Generally, in the magnetic case, the solenoidal component is maintained at finite levels by magnetic torsions but in the nonmagnetic case it can become very small (Vázquez-Semadeni, Passot & Pouquet 1996).

Nordlund & Padoan (2003) explain their solenoidal/compressional ratio of 2/1 geometrically: Interacting flows generate shear in 2D but compression is only normal to the intersection plane. Other simulations have solenoidal/compressional ratios ranging from less than unity (Vázquez-Semadeni et al. 1996) to 5–10, depending on Mach number (Boldyrev, Nordlund & Padoan 2002b, Porter et al. 2002—the quantity quoted in the text of Porter et al. 2002 is $E_{Com}/E_{tot}$, whereas the quantity plotted in their figure 2 is $E_{Com}/E_{Vor}$). Most results are controlled by the degree to which the forcing is solenoidal or compressible, the initial value of their ratio (Porter et al. 2002), the rms Mach number, the magnetic field strength, and the importance of cooling (Vázquez-Semadeni et al. 1996). Vestuto, Ostriker & Stone (2003) found that the solenoidal/compressional ratio increases with higher magnetic field strength, verifying an effect present in simulations by Passot et al. (1995) and Vázquez-Semadeni et al. (1996). The unforced simulations of Kritsuk & Norman (2003) have an initially high fraction of turbulent energy in the

compressible form following thermal instabilities and pancake formation, and then the energy converts into mostly solenoidal form as the turbulence decays owing to baroclinic vorticity generation from shell instabilities. The value of this ratio was unfortunately not given in papers whose simulations included supernova energy input; those should be the most realistic for the ISM.

## 5.7. Filamentary Structure

The prevalence of filaments in the ISM has never been adequately explained by turbulence theory, although they are obviously present in the majority of simulations. Some ISM filaments are not from turbulence but are the edges of expanding shells, cometary tails of shocked clouds, or shocked regions in spiral density waves. However, filamentary structure appears elsewhere too, even in regions without obvious pressure sources (Kulkarni & Heiles 1988, Jackson et al. 2003), and it occurs with similar morphologies in turbulence simulations. Prominent suggestions for the origin of these turbulence filaments include oblique shocks or shock intersections, expanding gas along magnetic field lines, confinement by helical magnetic fields, cooling instabilities in a flattened large-scale structure, vorticity tubes from solenoidal motions, and ambipolar diffusion.

Filamentary structure is often the result of shock interactions (Heitsch et al. 2001). Even in the simulations by Balsara, Ward-Thompson & Crutcher (2001), who emphasized the role of magnetic field alignments, filaments were still found in the converging flows. However, filamentary structures are also prevalent in low Mach number, nonmagnetic simulations (Porter, Pouquet & Woodward 2002), where solenoidal forcing keeps the compressible energy low and the shocks rare; they dominate the vorticity field of incompressible turbulence (Figure 3).

## 5.8. Thermal Instability and Thermal Phases

The idea that thermal instability drives ISM condensation to distinct phases (Field, Goldsmith & Habing 1969) has lost much of its appeal as a result of simulations that explicitly allow the instability to operate. Vázquez-Semadeni, Gazol & Scalo (2000) and Sánchez-Salcedo, Vázquez-Semadeni & Gazol (2002) showed how turbulence smears the bimodal density distribution expected in an ISM whose structure forms solely by thermal instability. The nonlinear development of a thermal instability in an initially quiescent medium generates turbulence that reduces the initial signature of the instability (Kritsuk & Norman 2002b). These results do not arise because of strong departures from thermal equilibrium (which is usually a good approximation away from shocks), but simply because there is so much more kinetic than thermal energy in supersonic turbulence.

Thermal pressure equilibrium of clouds is of minor importance in a turbulent ISM (Ballesteros-Paredes, Vázquez-Semadeni & Scalo 1999). A high fraction of the gas mass can be in the thermally unstable regime. In the instability model, the underheated regions in the unstable regime are slightly denser and at lower pressure than the overheated regions so they contract at the sound speed to become

denser and more underheated. In a turbulent medium, however, the underheated regions are not necessarily at low pressure because they are pushed around by the surrounding flow (Gazol et al. 2001). Large unstable fractions have also been found in high-resolution simulations of supernova-driven turbulence (de Avillez & Breitschwerdt 2004).

These results explain the observed large fraction of interstellar gas in the supposedly unstable regime (Dickey, Salpeter & Terzian 1977; Heiles 2001; Kanekar et al. 2003) and they explain the much broader range of observed pressures than expected in the thermal instability model (Jenkins 2004), as shown by Kim, Balsara & Mac Low (2001). Neither of these features can be explained by nonturbulent thermal instability models with pressure equilibrium.

## 5.9. Supernova-Driven Turbulence

Numerical simulations that have sufficient dynamic range to include supernovae (Gazol-Patiño & Passot 1999; Korpi et al. 1999a,b; de Avillez 2000; de Avillez & Berry 2001; Kim, Balsara & Mac Low 2001; Wada & Norman 2001; Shukurov et al. 2004) produce a continuous distribution of physical quantities, unlike the previously prevailing paradigm of discrete ISM phases (Section 5.8). Temperatures weighted by volume segregate into quasidiscrete ranges because the time spent in each temperature range is proportional to the inverse of the derivative of the cooling function (Gerola et al. 1974). The density distribution is not bi- or multimodal, however, as in a true multiphase ISM. Thus, filling fractions of gas with various temperatures may be approximately stable over long times in a statistical sense, but these should not be interpreted as phases because no phase transition is involved. Shukurov et al. (2004) and Sarson et al. (2003) found that the filling factor of hot gas is dependent on the presence, strength, and topology of the magnetic field, since a strongly ordered field confines the expanding gas produced by supernovae. In the models by Wada & Norman (1999), the hot gas is heated primarily by turbulence.

Comparisons between these studies are difficult because some include self-gravity (Wada & Norman 2001) and magnetic fields (Gazol-Patiño & Passot 1999) but are 2D, whereas others are 3D and either include the magnetic field with no self-gravity (Korpi et al. 1999a, Kim et al. 2001, Shukurov et al. 2004) or include neither field nor gravity (de Avillez 2000, de Avillez & Berry 2001). There are also significant differences in the adopted spatial distribution of the supernova explosions. For example, Gazol-Patiño & Passot (1999), Wada & Norman (2001), and Shukurov et al. (2004) allowed the supernovae to explode only at sites where the turbulence produces local conditions conducive to star formation, whereas Kim et al. (2001) exploded supernovae randomly. There are additional differences concerning how this energy is distributed in time (e.g., whether a wind is allowed before the explosion). Many of these studies concentrate on the resulting distribution of warm and hot gas, so it is difficult to see from the published results how the phenomenology of the dense gas is affected; in Shukurov et al. (2004), the cold gas is explicitly omitted.

Nevertheless, the wealth of structure found in these simulations is impressive. de Avillez (2000), de Avillez & Berry (2001), and de Avillez & Breitschwerdt (2004) modeled the 3D vertical structure in a galaxy disk at high resolution and found an amazing array of structure over 400 Myr, including a thin cold disk extruding vertical "worms" and a thick frothy disk of warm neutral gas, thin sheets representing superbubble interactions connected by tunnel-like structures, small clouds resulting from the interaction and breakup of worms and sheets, networks of hot gas, and "chimneys" rising high above the plane (see also Rosen, Bregman & Norman 1993).

The evolution of supernova remnants and superbubbles in a 3D MHD turbulent medium is substantially different than in a uniform external medium. Balsara, Benjamin & Cox (2001) showed how the induced time variations of synchrotron emission in young remnants might serve as a diagnostic for the ambient medium, and they pointed out how shock amplification of turbulent motions might be important for cosmic rays. Korpi et al. (1999b) showed that superbubble breakout from galactic disks is easier in a turbulent medium because of deformation of the expansion.

## 5.10. The Role of Self-Gravity in the ISM

Elmegreen (1993) suggested that dense clouds or cloud cores could form in colliding turbulent gas streams and that gravitational instabilities in the shocked regions would lead to collapse and star formation. The formation of self-gravitating condensations in converging streams was suggested before this (Hunter et al. 1986), but it was uncertain whether the compressed regions in a turbulent flow would be large enough and live long enough to collapse gravitationally before they dispersed. Ballesteros-Paredes, Vázquez-Semadeni & Scalo (1999) confirmed that density maxima in turbulent flows coincide with abrupt velocity jumps, indicating shock formation. Other simulations showed that dense regions generally form by oblique stream collisions and intersecting shocks, and that the most strongly self-gravitating of these regions have enough time to collapse significantly (see Nordlund & Padoan 2003). Accretion and core-core collisions often follow with more and more of the gas entering this gravitating state. This process may terminate in a real cloud when the resulting star formation becomes intense enough to push the remaining gas away, or when the Mach number drops below one (Section 5.11).

The ability of nongravitating turbulence to fragment the ISM or the interior of a GMC down to stellar masses and below leads to a new concept for the role of gravity in forming interstellar structure and stars (see Mac Low & Klessen 2004 for a comprehensive review). Clouds and clumps are no longer seen as the result of gravitational instabilities in a region containing a large number of Jeans masses, but simply the result of supersonic turbulence, whatever the source. On kiloparsec scales, this turbulence may be driven by interstellar gravity through swing-amplified spiral arms, so gravity is important, but much of the cloudy structure on smaller scales, including whole GMCs and their cores and clumps, could result entirely from "turbulent fragmentation," a term that dates back to Kolesnik &

Ogul′Chanskii (1990). Cloud structure also results from pressurized shell formation, spiral arm shocks, and other processes, but even in these cases, the hierarchical clumpiness inside the clouds probably arises from supersonic turbulence.

The role of gravity in determining gas structure is small when the motions are faster than the virial speed. This is the case for the diffuse ISM and the smaller *H I* and molecular clouds (Heyer et al. 2001), and it applies to most of the small clumps inside clouds (Loren 1989, Bertoldi & McKee 1992, Falgarone et al. 1992). Self-gravitating nonmagnetic simulations by Klessen (2001) confirmed that the fraction of clumps with significant self-gravity increases with mass. Many cloud properties can be matched by MHD simulations without gravity, including the statistical properties of extinction and intensity, the magnetic field strength–density correlation, the size-linewidth relation, and the absolute value and size independence of core rotation (Padoan & Nordlund 1999; Kim, Balsara & Mac Low 2001; Ostriker et al. 2001; Ballesteros-Paredes & Mac Low 2002; Nordlund & Padoan 2003). The appearance of Bonner-Ebert density profiles does not imply self-gravity either because turbulent condensations can have this property even when they are not in equilibrium (Ballesteros-Paredes, Klessen & Vázquez-Semadeni 2003). Quasi-hydrostatic structures are actually difficult to produce by turbulent fragmentation (Ballesteros-Paredes, Vázquez-Semadeni & Scalo 1999). Moreover, the mass functions of dense cores resemble the stellar initial mass function (IMF) in both nongravitating (see Nordlund & Padoan 2003) and gravitating (Li, Klessen & Mac Low 2003) simulations because the dense local regions that can collapse were generated by turbulent interactions, not gravitational instabilities. Self-gravity is mainly important for the dense cores of turbulent regions, whereas the large-scale structure is decoupled from these cores (Ossenkopf et al. 2001).

If turbulence is viewed as preventing global collapse, then it is not because of some "turbulent pressure." In fact the conditions required for turbulence to be represented as a pressure are quite severe (Bonazzola et al. 1992), requiring a scale separation for turbulent fluctuations (Section 4.10). Structures generated by turbulence, even if bound, can be immune to global collapse because the gravitational and turbulent energy is transferred quickly to motions of substructures on smaller and smaller scales, and the densest of these small structures does the collapsing instead of the whole cloud. Collapse of turbulence-compressed cores requires a low effective ratio of specific heats $d \log P / d \log \rho = \gamma < 2\,(1 - 1/n)$, where $n = 3, 2$, or 1 for spherical, planar, or filamentary compressions, so the gravitational energy change exceeds the compressional energy change (Vázquez-Semadeni, Passot & Pouquet 1996).

## 5.11. Formation of Star Clusters and the IMF

One of the holy grails of ISM simulations has been to follow the collapse and fragmentation of a cloud to form a stellar cluster and to calculate the resulting initial mass function of stars, a goal that has been thwarted until recently by severe resolution requirements. The first studies of this type did not include self-gravity but

showed that the resulting cores would collapse if self-gravity were present, given their masses and densities (see Nordlund & Padoan 2003 and references therein). Self-gravitating models illustrate the process in detail (Bonnell et al. 1997, 2003; Bate, Bonnell & Bromm 2003; Klessen, Burkert & Bate 1998; Klessen & Burkert 2000; Klessen, Heitsch & Mac Low 2000), including magnetic fields (Heitsch, Mac Low & Klessen 2001; Li et al. 2004). Figure 5 shows a simulation result from Bonnell et al. (2003). The time sequence illustrates the collapse of nonmagnetic gas into sink-particles ("stars"), competition among these particles for gas, and the formation of disks, binaries, and complex turbulent structures.

A major result of these studies is the demonstration that turbulence can suppress global collapse, whereas local collapse still occurs in the cores that it forms. This result was found even for magnetic simulations, where local collapse could be suppressed only if the field was so strong that it supported the whole cloud (Heitsch et al. 2001, Ostriker et al. 2001).

Klessen (2001) examined the mass spectrum of collapsing cores in nonmagnetic, self-gravitating turbulence simulations and found good agreement with the overall form of the stellar IMF (see observations in Chabrier 2003). It is interesting that roughly similar clump mass spectra have been found in simulations including self-gravity but neglecting magnetic fields (see also Klessen & Burkert 2001), simulations that include magnetic fields but not self-gravity (Ballesteros-Paredes & Mac Low 2002), and simulations that include both (Gammie et al. 2003). Differences do appear, but it is difficult to disentangle them from variations resulting from numerical techniques and core definitions.

Gammie et al. (2003) presented a detailed discussion of the mass spectra of gravitating and nonself-gravitating clumps in 3D self-gravitating, decaying MHD simulations. They found that the slope of the high-mass part of the spectrum becomes shallower with time, that the magnetic field strength does not affect the spectrum significantly, and that the spectrum depends on how the clumps are defined (Ballesteros-Paredes & Mac Low 2002). The dependence of the clump mass spectrum and the IMF on the equation of state was studied by Li, Klessen & Mac Low (2003). A dependence of the substellar mass function on the power spectrum of turbulence was found by Delgado-Donate, Clarke & Bate (2004).

## 5.12. Rotation and Binary Star Formation

The rotational properties of molecular clouds and cores have been investigated by several groups (e.g., Goldsmith & Arquilla 1985, Goodman et al. 1993, Caselli et al. 2002). Detectable gradients range mostly from 0.3 to 3 km $s^{-2}$ $pc^{-1}$. Although the average ratio of rotational to gravitational energy is small ($\sim$0.03), the nature of these gradients has been obscure.

Burkert & Bodenheimer (2000) used synthetic velocity fields with an assumed linewidth-size relation to show that even if turbulent motions are random, the dominance of large-scale modes can lead to velocity gradients that look like ordered rotation. The resulting core rotational properties as functions of size and the spread in the ratio of rotational to gravitational energies were in good agreement

with observations, including the spread in binary periods, although the median angular momentum in the models was about an order of magnitude larger than in the observations. Gammie et al. (2003) studied properties of cores in 3D MHD simulations of molecular clouds and also found angular momenta larger than observed; they suggested higher resolution would eventually allow simulations to probe turbulence-produced angular momentum on the scale of binary star orbits. Fisher (2004) used a semianalytic approach to show that the distribution of binary periods was consistent with turbulence.

These results apply only to cores that are mildly subsonic. Whether the small velocity gradients detected in some larger dark clouds can be accounted for by turbulence alone remains to be seen (but see Kim, Ostriker & Stone 2003). Some gradients are probably from pressurized motions. In any case, the angular momentum problem that played a central role in most early discussions of star formation (e.g., Mouschovias 1991) is beginning to disappear. Angular momentum is still conserved in a turbulent ISM, but it gets channeled mostly into vorticity structures as turbulence distributes its energy among scales. It is unknown whether turbulence can also explain the low levels of rotation in prestellar cores (Jessop & Ward-Thompson 2001).

Turbulence simulations are approaching the scales on which binary star angular momenta are determined (Bate, Bonnell & Bromm 2002; Gammie et al. 2003). Even mild levels of turbulence during a collapse can induce multiple star formation (Klein et al. 2003; Goodwin, Whitworth & Ward-Thompson 2004).

## 5.13. Effects of Magnetic Fields on Interstellar Turbulence

Most MHD simulations suggest that magnetic fields have a smaller role in the ISM than previously expected. For example, they seem unable to postpone the energy dissipation in a supersonically turbulent medium (Section 5.3) and unable to prevent local gravitational collapse unless they are strong (Heitsch et al. 2001; Ostriker et al. 2001; however, see Kudoh & Basu 2003). Passot & Vázquez-Semadeni (2003) and Cho & Lazarian (2003) demonstrated that magnetic fluctuations do not act as an effective pressure at high Mach numbers because of their lack of one-to-one correspondence with density: The field acts more like a random forcing of the turbulence. What magnetic fields appear to do is reduce the core density contrast (Balsara, Crutcher & Pouquet 2001) and slow down the local collapse rate (Heitsch et al. 2001). This may not affect the overall star-formation rate much because the timescale for core formation is much longer than the core collapse. For turbulent fragmentation, star-formation rates should be regulated on the largest scale where the dynamical time is longest. The marginal effects of magnetic fields on the clump or core mass spectra and presumably the stellar IMF were discussed in Section 5.11. Padoan & Nordlund (1999) suggested that magnetic fields are relatively weak in molecular clouds, having energy densities less than turbulent so the motions are super-Alfvénic (see review in Nordlund & Padoan 2003).

Polarization observations show smooth magnetic fields, but this does not mean turbulence is absent (see review by Ostriker 2003). As discussed by

Vázquez-Semadeni et al. (1998), cloud formation by turbulence can compress the field perpendicular to the compression direction, making it elongated in the same direction as the cloud; turbulent magnetic field energy spectra are peaked at small wavenumbers in simulations, so the field should be dominated by the largest scales, and the observed field orientations are an average on the line of sight (Heiles et al. 1993, Goodman et al. 1990). Visual polarization also probes only a small range of extinction.

Ambipolar diffusion is relatively unimportant in the overall dynamics of molecular cloud turbulence at high Mach numbers (Balsara, Crutcher & Pouquet 2001). Indeed, observations now suggest that ion-neutral drift is rapid at $\sim 10^6$ cm$^{-3}$, based on comparisons of $HCO^+$ and HCN linewidths (Houde et al. 2002). The old idea that protostellar cores form on timescales controlled by ambipolar diffusion may not apply.

Ion-neutral drift is not without consequences, however. The ambipolar diffusion heating rate in molecular cloud turbulence simulations (Padoan, Zweibel & Nordlund 2000) can be orders of magnitude larger on small scales than the background heating rate by cosmic rays, and even the volume-averaged drift heating rate can exceed the cosmic ray heating rate (Scalo 1977). Heating can be important if dynamical effects are not because there is much less thermal energy than kinetic energy in a supersonic flow. Drift heating is also more important locally because it depends on a high-order derivative of the magnetic field. Thus, turbulence can enhance ambipolar diffusion by driving structures to smaller scales (Zweibel 2002, Heitsch et al. 2004) and compressing the field (Fatuzzo & Adams 2002). Ambipolar diffusion also leads to sharp filamentary structures (Brandenburg & Zweibel 1994; Mac Low et al. 1995; Tagger, Falgarone & Shukurov 1995), rather than diffusive smoothing as once thought.

Turbulent cloud simulations (Gammie et al. 2003) also illustrate why the observed clumps and cores in molecular clouds tend to be prolate (Myers et al. 1991, Ryden 1996) with no preferred orientation relative to the field (Goodman et al. 1990). Quasistatic models with a slow contraction along field lines predicted oblate and aligned cores.

Another interesting result concerning magnetic fields is the possibility that they could control the accretion rate onto protostellar cores or larger structures. Balsara, Ward-Thompson & Crutcher (2001) found with $256^3$ self-gravitating MHD simulations that molecular cloud cores tend to accrete matter nonuniformly along interconnecting magnetic filaments. They cite evidence for this process in the S106 molecular cloud using $^{13}$CO channel maps, submillimeter maps, and polarimetry. Falgarone, Pety & Phillips (2001) found six dense filaments pointing toward the starless core L1512 extending out to about 1 pc, with evidence for the filamentary matter moving toward the core. In this case the final masses of prestellar cores could be controlled in part by the topology of the magnetic field.

Another magnetic effect is angular momentum braking, which has been discussed for decades using idealized models of clouds and fields. In a turbulent medium the magnetic field structure and its connection to density condensations is complex, and there is no guarantee that braking will occur. Vázquez-Semadeni,

Passot & Pouquet (1996) and Vestuto, Ostriker & Stone (2003) showed relatively more power in rotational and shear energy than compressional energy as the field strength increases, contrary to naive models of magnetic braking.

That magnetic braking does occur in a turbulent fluid with complex fields has been shown in simulations of the magnetorotational instability on a galactic scale (Kim, Ostriker & Stone 2003). The degree of braking of their largest coherent condensations may explain the low specific angular momenta inferred for molecular clouds. This is a much larger scale than star-forming cores, but the basic effect of angular momentum transfer along field lines is analogous to the cases considered in idealized collapse models by Mouschovias & Paleologou (1979) and others.

A different approach was introduced by Cho and coworkers (see Cho & Lazarian 2002a,b; Cho, Lazarian & Vishniac 2002a,b), Maron & Goldreich (2001), and Müller & Biskamp (2003) using a combination of theoretical calculations and simulations to address the properties of anisotropic Kolmogorov turbulence. They emphasized regimes that are more appropriate to the diffuse ionized ISM than dense cold regions. Several interesting and fundamental results have come from this, as reviewed in Section 4.13 and *Interstellar Turbulence II*.

## 5.14. Turbulent Rotating Galaxy Disk Simulations

Simulation codes are finally becoming sophisticated enough to model at least the central regions of differentially rotating galaxies, with simulations of 2 kpc $\times$ 2 kpc up to $4096^2$ (Wada & Norman 2001, Wada et al. 2002). Various models include self-gravity, cooling and background heating, and dynamical heating from cluster winds and supernovae coupled to star formation. The resulting density and temperature structures span seven and five orders of magnitude, respectively. The Wada et al. (2002) models are not yet 3D, and they neglect magnetic fields, but a lot of realistic structure is present anyway. For example, filaments form in oblique converging flows and strong local shear (Wada et al. 2002), statistically stable temperature regimes appear on large scales, the supernova rate fluctuates in recurrent bursts from propagating-star formation, and the density pdf is lognormal over four orders of magnitude above the mean. The models also find that the energy spectrum and direction of the energy flow in wavenumber space depends on the presence of star formation feedback, the wavelength dependence of the disk gravitational instability, and the assumed rotation curve for the galaxy (compare figure 18 in Wada & Norman 2001 and figures 4 and 5 in Wada et al. 2002). Wada, Spaans & Kim (2000) also suggested that turbulence alone could account for the kiloparsec-sized holes seen in other galaxies, independent of star formation.

# 6. SUMMARY AND REFLECTIONS

Interstellar turbulence has been studied using power spectra and structure functions of the distributions of radial velocity, emission, and absorption. Studies have also considered statistical properties of line profiles, unsharp masks, and wavelet transforms; one-point probability distribution functions of column densities and velocity

centroids; fractal dimensions and multifractal spectra; and various other techniques including the Spectral Correlation Function and Principal Component Analysis, which are applied to spectral-line data cubes.

The results are often ambiguous and difficult to interpret. The density of the neutral medium seems to possess spatial correlations over a wide range of scales, possibly from the subparsec limit of resolution to hundreds of parsecs. Such correlations probably reflect the hierarchical nature of turbulence in a medium with a very large Reynolds number. The power spectrum of the associated intensity fluctuations is a robust power law with a slope between $-1.8$ and $-2.3$ for the Milky Way, LMC, and SMC. A steeper slope has been obtained for Galactic CO using Principle Component Analysis. However, no clear power spectrum or autocorrelation function has been found yet for centroid velocities as a function of spatial lag inside individual clouds, even though they might be expected if the clouds are turbulent.

Statistical properties of the ISM are difficult to recover with only line-of-sight motions in projected cloud maps that have limited spatial extent and substantial noise. Linewidths often seem correlated with region size in an average sense, but there are large variations between different regions and surveys. At the moment, this relation seems to be dominated by scatter. Because the linewidth-size correlation is analogous to a second-order structure function, which is well defined for incompressible turbulence, the regional variations are difficult to understand in the context of conventional turbulence theory. Certainly a case could be made that ISM turbulence is not conventional: It is not statistically homogeneous, stationary, or isotropic.

Given the difficulty of observing 3D structure and motion in space, the value of statistical descriptors lies primarily in their ability to make detailed comparisons between observations and simulations. Many such comparisons have been made, but a comprehensive simulation of a particular region including many of the descriptors listed above is not yet available.

Among the many differences between interstellar turbulence and classical incompressible turbulence is the broad spatial scale for energy input in space. In spite of the wide-ranging spatial correlations in emission and absorption maps, there is no analogy with classical turbulence in which energy is injected on the largest scale and then cascades in a self-similar fashion to the very small scale of dissipation. In the ISM, energy is injected over a wide range of scales, from kiloparsec disturbances in spiral density waves, shear instabilities, and superbubbles, to parsec-sized explosions in supernovae, massive-star winds, and *H II* regions, to subparsec motions in low-mass stellar winds and stellar gravitational wakes, to astronomical unit–sized motions powered by cosmic ray streaming instabilities. Estimates of power input indicate that stellar explosions are the largest contributor numerically, but this does not mean that other sources are unimportant on other scales.

Energy is also dissipated over a wide range of scales. Shock fronts, ambipolar and Ohmic diffusion, Landau wave damping, and viscosity in vortex tubes should

all play a role. The geometrical structures of the dissipating regions are not well constrained by observations. Energy is also dissipated in regions with little density substructure, as in the ionized gas that produces scintillation or along perturbed magnetic field lines that scatter some cosmic rays. Viscosity and Landau damping can produce heat from the tiny wave-like motions that occur in these regions (see *Interstellar Turbulence II*), although the nature of this dissipation below the collision mean-free path is not understood yet.

Self-gravity makes interstellar turbulence more difficult to understand than terrestrial turbulence. The contribution to ISM motions from self-gravity appears to increase with cloud mass until it dominates above $10^4$–$10^5$ $M_\odot$. Many selection effects may contribute to this correlation, however. Self-gravity is also important in the smaller clumps that form stars. What happens between these scales remains a mystery. We would like to know how the distribution function of the ratio of virial mass to luminous mass for ISM clouds and clumps varies with the spatial scales of these structures. What fraction of clouds or clumps are self-gravitating for each mass range? Does the apparent trend toward diminished self-gravity on small scales turn around on the scale of individual protostars?

The balance between solenoidal and compressible energy density in the ISM varies with time. Compressibility transfers energy between kinetic and thermal modes, short-circuiting the cascade of energy in wavenumber space that occurs in a self-similar fashion for incompressible turbulence. Consequently, the ISM turbulent power spectra for kinetic and magnetic energy are not known from terrestrial analogies, and there is not even a theoretical or heuristic justification for expecting self-similar or power-law behavior. Numerical simulations make predictions of these quantities, but these simulations are usually idealized and they are always limited by resolution and other numerical effects.

A considerable effort has been put into modeling compressible MHD turbulence under idealized conditions, i.e., without self-gravity and without dispersed and realistic energy sources (e.g., explosions). Some models predict analytically and confirm numerically a Kolmogorov energy spectrum transverse to the mean field when the magnetic energy density is not much larger than the kinetic energy density. These models also predict intermittency properties identical to hydrodynamic turbulence in this trans-field direction. However, other models find steeper power spectra. One has mostly solenoidal motions on large scales and sheet-like dissipation regions on small scales. Another has more realistic heating and cooling. At very strong fields, the turbulence becomes more restricted to the two transverse dimensions and then the energy spectrum seems to become flatter, as in the Iroshnikov-Kraichnan model. Overall, the situation regarding the energy spectrum of MHD ISM turbulence is unsettled.

Our understanding of the ISM has benefited greatly from numerical simulations. In the 10 or so years since the first simulations of ISM turbulence, numerical models have reproduced most of the observed correlations and scaling relations. They have demonstrated that supersonic turbulence always decays quickly and concluded

that star formation is equally fast, forcing a link between cold clouds and their energy-rich environments. They have also predicted a somewhat universal probability function for density in an isothermal gas, implying that only a small fraction of the gas mass can ever be in a dense enough state to collapse gravitationally—thereby explaining the low efficiency of star formation.

Simulations have demonstrated that magnetism does not support clouds, prevent collapse, systematically align small clumps, or act like an effective pressure. Magnetism can slow collapsing cores and remove angular momentum on large and small scales, and it may contribute to filamentary structures that control the accretion rate of gas onto protostars. Simulations have also shown that thermal instabilities do not lead to bimodal density distributions as previously believed, although they probably enhance the compressibility of the ISM and might contribute to the turbulent motions. The high abundance of atomic gas in what would be the thermally unstable regime of static models is easily explained in a turbulent medium.

However, simulations have a long way to go before solving some of the most important problems. Models that include realistic cooling, ionization balance, chemistry, radiative transfer, ambipolar diffusion, magnetic reconnection, and, especially, realistic forcing are needed because it is not clear that any of these effects are negligible. Detailed models should be able to form star clusters in a realistic fashion, continuing the progress that has already been made with restricted resolution and input physics. Complete models need to include energy sources from young stellar winds, ionization, and heating. They should also be able to follow the orbital dynamics of binaries. Successful models should eventually explain the stellar initial mass function, mass segregation, the binary fraction and distribution of binary orbital periods, the mean magnetic flux in a star, and the overall star-formation efficiency at the time of cloud disruption.

Realistic simulations of galactic-scale processes are also challenging because they should include a large range of scales and fundamentally different physical processes in the radial and vertical directions. Background galactic dynamics and the possibility of energy and mass exchange with a 3D halo are also important.

The turbulent model of the ISM also raises substantial new questions. Why is the power spectrum of ISM density structure a power law when direct observation shows the ISM to be a collection of shells, bubbles, comets, spiral wave shocks, and other pressurized structures spanning a wide range of scales? Do directed pressures and turbulence combine to produce the observed power spectrum or does one dominate the other? Does the input of energy on one scale prevent the turbulent cascade of energy that is put in on a larger scale? In this respect, is ISM turbulence more similar to turbulent combustion than incompressible turbulence because of the way in which energy is injected?

Our current embrace of turbulence as an explanation for ISM structures and motions may be partly based on an over-simplification of available models and a limitation of observational techniques. This state of the field guarantees more surprises in the coming decade.

## ACKNOWLEDGMENTS

We are grateful to J. Ballesteros-Paredes, J. Dickey, N. Evans, E. Falgarone, A. Goodman, A. Lazarian, P. Padoan, and E. Vázquez-Semadeni for helpful comments on Section 2; to C. Norman for a careful reading of Section 3; to A. Brandenberg, A. Lazarian, P. Padoan, T. Passot, E. Vázquez-Semadeni, and E. Vishniac for helpful comments on Section 4; and to A.G. Kritsuk, M-M. Mac Low, E. Ostriker, P. Padoan, and E. Vázquez-Semadeni for helpful comments on Section 5. We also thank J. Kormendy for helpful comments on the manuscript.



## LITERATURE CITED

Adler DS, Roberts WW Jr. 1992. *Ap. J.* 384:95–104

Andreopoulos Y, Agui JH, Briassulis G. 2000. *Annu. Rev. Fluid Mech.* 32:309–45

Anselmet F, Gagne Y, Jopfinger EJ, Antonia RA. 1984. *J. Fluid Mech.* 140:63–89

Arons J, Max CE. 1975. *Ap. J.* 196:L77–81

Avila-Reese V, Vázquez-Semadeni E. 2001. *Ap. J.* 553:645–60

Ayyer A, Verma MK. 2003. Energy transfer and locality in magnetohydrodynamic turbulence. (ArXiv:nlin.CD/0308005)

Baker PL. 1973. *Astron. Astrophys.* 23:81–92

Balbus SA, Hawley JF. 1991. *Ap. J.* 376:214–22

Ballesteros-Paredes J. 2003. Turbulent fragmentation and star formation. (astro-ph/0311319)

Ballesteros-Paredes J, Hartmann L, Vázquez-Semadeni E. 1999. *Ap. J.* 527:285–97

Ballesteros-Paredes J, Klessen RS, Vázquez-Semadeni E. 2003. *Ap. J.* 592:188–202

Ballesteros-Paredes J, Mac Low M-M. 2002. *Ap. J.* 570:734–48

Ballesteros-Paredes J, Vázquez-Semadeni E, Goodman AA. 2002. *Ap. J.* 571:334–55

Ballesteros-Paredes J, Vázquez-Semadeni E, Scalo J. 1999. *Ap. J.* 515:286–303

Bally J, Langer WD, Stark AA, Wilson RW. 1987. *Ap. J.* 312:L45–49

Balsara DS. 1996. *Ap. J.* 465:775–94

Balsara D, Benjamin RA, Cox DP. 2001. *Ap. J.* 563:800–5

Balsara D, Ward-Thompson D, Crutcher RM. 2001. *MNRAS* 327:715–20

Balsara DS, Crutcher RM, Pouquet A. 2001. *Ap. J.* 557:451–63

Bania TM, Lyon JG. 1980. *Ap. J.* 239:173–92

Barrat A, Trizac E. 2002. *Phys. Rev. E* 66: 051303

Basu S, Murali C. 2001. *Ap. J.* 551:743–46

Bataille F, Zhou Y. 1999. *Phys. Rev. E* 59:5417–26

Bate MR, Bonnell IA, Bromm V. 2002. *MNRAS* 336:705–13

Bate MR, Bonnell IA, Bromm V. 2003. *MNRAS* 339:577–99

Bate MR, Burkert A. 1997. *MNRAS* 288:1060–72

Bazell D, Desert FX. 1988. *Ap. J.* 333:353–58

Beech M. 1987. *Astrophys. Space Sci.* 133:193–95

Ben-Naim E, Krapivsky PL. 2002. *Phys. Rev. E* 66:011309

Bensch F, Stützki J, Ossenkopf V. 2001. *Astron. Astrophys.* 366:636–50

Beran MJ. 1968. *Statistical Continuum Theories.* New York: Interscience. 424 pp.

Berkhuijsen EM. 1999. See Ostrowski & Schlickeiser 1999, pp. 61–65

Bertin G, Lodato G. 2001. *Astron. Astrophys.* 370:342–50

Bertoglio JP, Bataille F, Marion JD. 2001. *Phys. Fluids* 13:290–310

Bertoldi F, McKee CF. 1992. *Ap. J.* 395:140–57

Bhattacharjee A, Ng CS. 2001. *Ap. J.* 548:318–22

Biferale L. 2003. *Annu. Rev. Fluid Mech.* 35: 441–68

Biferale L, Lanotte A, Toschi F. 2004. *Phys. Rev. Lett.* 92:094503

Biferale L, Boffetta G, Celani A, Lanotte A, Toschi F, Vergassola M. 2004. *Phys. Fluids* 15:2105–12

Biskamp D. 2003. *Magnetohydrodynamic Turbulence.* Cambridge: Cambridge Univ. Press. 310 pp.

Biskamp D, Müller W-C. 1999. *Phys. Rev. Lett.* 83:2195–98

Biskamp D, Müller W-C. 2000. *Phys. Plasmas* 7:4889–900

Biskamp D, Schwarz E. 2001. *Phys. Plasmas* 8:3282–92

Black DC, Matthews MS, eds. 1985. *Protostars and Planets II*. Tucson: Univ. Ariz. Press

Blondin JM, Marks BS. 1996. *NewA* 1:235–44

Bok BJ, Reilly EF. 1947. *Ap. J.* 105:255–57

Boldyrev S. 2002. *Ap. J.* 569:841–45

Boldyrev S, Nordlund A, Padoan P. 2002a. *Ap. J.* 573:678–84

Boldyrev S, Nordlund A, Padoan P. 2002b. *Phys. Rev. Lett.* 89:031102

Bonazzola S, Heyvaerts J, Falgarone E, Perault M, Puget JL. 1987. *Astron. Astrophys.* 172:293–98

Bonazzola S, Perault M, Puget JL, Heyvaerts J, Falgarone E, Panis JF. 1992. *J. Fluid Mech.* 245:1–28

Bonnell IA, Bate MR, Clarke CJ, Pringle JE. 1997. *MNRAS* 285:201–8

Bonnell IA, Bate MR, Vine SG. 2003. *MNRAS* 343:413–18

Bourke TL, Myers PC, Robinson G, Hyland AR. 2001. *Ap. J.* 554:916–32

Bracco A, LaCasce J, Pasquero C, Provenzale A. 2000. *Phys. Fluids* 12:2478–88

Brand J, Wouterloot JGA, Rudolph AL, deGeus EJ. 2001. *Astron. Astrophys.* 377:644–71

Brandenburg A, Nordlund A, Stein RF, Torkelsson U. 1996. *Ap. J.* 458:L45–48

Brandenburg A, Zweibel EG. 1994. *Ap. J.* 427:L91–94

Brunt CM, Heyer MH. 2002. *Ap. J.* 566:289–301

Brunt CM, Heyer MH, Vázquez-Semadeni E, Pichardo B. 2003. *Ap. J.* 595:824–41

Bunner AN, Coleman PL, Kraushaar WL, McCammon D. 1971. *Ap. J.* 167:L3–8

Burkert A, Bodenheimer P. 2000. *Ap. J.* 543: 822–30

Burton WB. 1971. *Astron. Astrophys.* 10:76–96

Cambrésy L. 1999. *Astron. Astrophys.* 345: 965–76

Caselli P, Walmsley CM, Zucconi A, Tafalla M, Dore L, Myers PC. 2002. *Ap. J.* 565:331–43

Castaing B, Gagne Y, Hopfinger EJ. 1990. *Physica D* 46:177–200

Chabrier G. 2003. *PASP* 115:763–95

Chandran BDG. 2003. In *International Workshop on Magnetic Fields and Star Formation: Theory versus Observations.* Dordrecht: Kluwer

Chandrasekhar S, Münch G. 1952. *Ap. J.* 115:103–23

Chappell D, Scalo J. 2001. *Ap. J.* 551:712–29

Chavanis PH. 2002. *Astron. Astrophys.* 381: 340–56

Chen H, Chen S, Kraichnan RH. 1989. *Phys. Rev. Lett.* 63:2657–60

Chen H, Herring JR, Kerr RM, Kraichnan RH. 1989. *Phys. Fluids A* 1:1844–54

Chen J-Y, Kollman W. 1994. In *Turbulent Reacting Flows*, ed. PA Libby, FA Williams, pp. 211–308. New York: Springer-Verlag. 474 pp.

Chen Q, Chen S, Eyink GL. 2003. *Phys. Fluids* 15:361–74

Chen S, Kraichnan RH. 1997. *J. Plasma Phys.* 57:187–93

Chen SY, Doolen G, Herring JR, Kraichnan RH, Orszag SA, She ZS. 1993. *Phys. Rev. Lett.* 70:3051–54

Chen SY, Ecke RE, Eyink GL, Wang X, Xiao ZL. 2003. *Phys. Rev. Lett.* 91:214501

Chew GF, Goldberger ML, Low FE. 1956. *Proc. R. Soc. London Ser. A* 236:112–18

Chiang W-H, Bregman JN. 1988. *Ap. J.* 328: 427–39

Chiang W-H, Prendergast KH. 1985. *Ap. J.* 297:507–30

Cho J, Lazarian A. 2002a. *Ap. J.* 575:L63–66
Cho J, Lazarian A. 2002b. *Phys. Rev. Lett.* 88:245001
Cho J, Lazarian A, Vishniac ET. 2002a. *Ap. J.* 564:291–301
Cho J, Lazarian A, Vishniac ET. 2002b. *Ap. J.* 566:L49–52
Cho J, Lazarian A. 2003. *MNRAS* 345:325–39
Cho J, Lazarian A, Vishniac ET. 2003a. See Falgarone & Passot 2003, pp. 56–100
Cho J, Lazarian A, Vishniac ET. 2003b. *Ap. J.* 595:812–23
Christensson M, Hindmarsh M, Brandenburg A. 2001. *Phys. Rev. E* 64:056405
Connaughton C, Nazarenko S, Newell AC. 2003. *Physica D* 184:86–97
Court A. 1965. *Q. J. R. Meteor. Soc.* 91:234–35
Clark BG. 1965. *Ap. J.* 142:1398–422
Crovisier J, Dickey JM. 1983. *Astron. Astrophys.* 122:282–96
Crutcher RM. 1999. *Ap. J.* 520:706–13
Dame T, Elmegreen BG, Cohen R, Thaddeus P. 1986. *Ap. J.* 305:892–908
de Avillez MA. 2000. *MNRAS* 315:479–97
de Avillez MA, Berry DL. 2001. *MNRAS* 328:708–18
de Avillez MA, Breitschwerdt D. 2003. In *Star Formation through Time. ASP Conf. Ser. 297*, ed. E Perez, RM Gonzalez Delgado, G Tenorio-Tagle, pp. 55–60
de Avillez MA, Breitschwerdt D. 2004. *Astrophys. Space Sci.* 289:479–88
Deiss BM, Just A, Kegel WH. 1990. *Astron. Astrophys.* 240:123–36
Delgado-Donate EJ, Clarke CJ, Bate MR. 2004. *MNRAS* 347:759–70
Deshpande AA, Dwarakanath KS, Goss WM. 2000. *Ap. J.* 543:227–34
Dewan EM. 1985. *Radio Sci.* 20:1301–7
Dickey JM. 1985. In *The Milky Way Galaxy*, ed. H van Woerden, RJ Allen, WB Burton, pp. 311–17. Dordrecht: Reidel
Dickey JM, Lockman FJ. 1990. *ARAA* 28:215–61
Dickey JM, McClure-Griffiths NM, Stanimirovic S, Gaensler BM, Green AJ. 2001. *Ap. J.* 561:264–71
Dickey JM, Salpeter EE, Terzian Y. 1977. *Ap. J.* 211:L77–82
Dickman RL. 1985. See Black & Matthews 1985, pp. 150–74
Dmitruk P, Gómez DO, Matthaeus WH. 2003. *Phys. Plasmas* 10:3584–91
Domaradzki JA, Rogallo RS. 1990. *Phys. Fluids A* 2:413–26
Dopazo C. 1994. In *Turbulent Reacting Flows*, ed. PA Libby, FA Williams, pp. 375–473. New York: Academic
Dopazo C, Valino L, Fueyo N. 1997. *Intern. J. Mod. Phys. B* 11:2975–3014
Dubinski J, Narayan R, Phillips TG. 1995. *Ap. J.* 448:226–31
Dubrulle B. 1994. *Phys. Rev. Lett.* 73:959–62
Elmegreen BG. 1991. In *The Physics of Star Formation and Early Stellar Evolution*, ed. CJ Lada, ND Kylafis, pp. 35–60. Dordrecht: Kluwer
Elmegreen BG. 1993. *Ap. J.* 419:L29–32
Elmegreen BG. 1999. *Ap. J.* 527:266–84
Elmegreen BG. 2000. *Ap. J.* 530:277–81
Elmegreen BG, Elmegreen DM. 2001. *Astron. J.* 121:1507–11
Elmegreen BG, Elmegreen DM, Leitner SN. 2003. *Ap. J.* 590:271–83
Elmegreen BG, Kim S, Staveley-Smith L. 2001. *Ap. J.* 548:749–69
Elmegreen DM, Elmegreen BG, Eberwein KS. 2002. *Ap. J.* 564:234–43
Esquivel A, Lazarian A, Pogosyan D, Cho J. 2003. *MNRAS* 342:325–36
Falgarone E, Hily-Blant P, Levrier F. 2003. In *Magnetic Fields and Star Formation: Theory versus Observations*, ed. AI Gomez de Castro, et al. Dordrecht: Kluwer. (astro-ph/0307013)
Falgarone E, Lis DC, Phillips TG, Pouquet A, Porter DH, Woodward PR. 1994. *Ap. J.* 436:728–40
Falgarone E, Panis J-F, Heithausen A, Perault M, Stutzki J, et al. 1998. *Astron. Astrophys.* 331:669–96
Falgarone E, Passot T, eds. 2003. *Turbulence and Magnetic Fields in Astrophysics, Springer Lect. Notes Phys.*, 614

Falgarone E, Pety J, Phillips TG. 2001. *Ap. J.* 555:178–90
Falgarone E, Phillips TG. 1990. *Ap. J.* 359:344–54
Falgarone E, Phillips TG, Walker CK. 1991. *Ap. J.* 378:186–201
Falgarone E, Puget JL, Perault M. 1992. *Astron. Astrophys.* 257:715–30
Falgarone E, Verstraete L, Pineau des Forets G, Hily-Blant P. 2004. *Astron. Astrophys.* In press
Fatuzzo M, Adams FC. 2002. *Ap. J.* 570:210–21
Ferriere KM, Zweibel EG, Shull JM. 1988. *Ap. J.* 332:984–94
Field GB, Goldsmith DW, Habing HJ. 1969. *Ap. J.* 155:L149–54
Fisher RT. 2004. *Ap. J.* 600:769–80
Fleck RC Jr. 1981. *Ap. J.* 246:L151–54
Fosalba P, Lazarian A, Prunet S, Tauber JA. 2002. *Ap. J.* 564:762–72
Franco J, Carraminana A, eds. 1999. *Interstellar Turbulence*. Cambridge: Cambridge Univ. Press. 287 pp.
Frisch U. 1995. *Turbulence*. Cambridge: Cambridge Univ. Press. 296 pp.
Fuchs B, von Linden S. 1998. *MNRAS* 294:513–22
Fukunaga M, Tosa M. 1989. *PASJ* 41:241–62
Galtier S. 2003. *Phys. Rev. E* 68:015301
Galtier S, Nazarenko SV, Newell AC, Pouquet A. 2000. *J. Plasma Phys.* 63:447–88
Galtier S, Nazarenko SV, Newell AC, Pouquet A. 2002. *Ap. J.* 564:L49–52
Gammie CF. 2001. *Ap. J.* 553:174–83
Gammie CF, Lin Y-T, Stone JM, Ostriker EC. 2003. *Ap. J.* 592:203–16
Gammie CF, Ostriker JP, Jog CJ. 1991. *Ap. J.* 378:565–75
Gaustad JE, VanBuren D. 1993. *PASP* 105:1127–40
Gautier TN, Boulanger F, Perault M, Puget JL. 1992. *Astron. J.* 103:1313–24
Gazol A, Vázquez-Semadeni E, Sánchez-Salcedo FJ, Scalo J. 2001. *Ap. J.* 557:L121–24
Gazol-Patiño A, Passot T. 1999. *Ap. J.* 518:748–59
Gerola H, Kafatos M, McCray R. 1974. *Ap. J.* 189:55–66
Gill AG, Henriksen RN. 1990. *Ap. J.* 365:L27–30
Goldman I. 2000. *Ap. J.* 541:701–6
Goldreich P, Kwan J. 1974. *Ap. J.* 189:441–54
Goldreich P, Sridhar S. 1995. *Ap. J.* 438:763–75
Goldreich P, Sridhar S. 1997. *Ap. J.* 485:680–88
Goldsmith PF, Arquilla R. 1985. See Black & Matthews 1985, pp. 137–49
Goodman AA, Bastien P, Menard F, Myers PC. 1990. *Ap. J.* 359:363–77
Goodman AA, Benson PJ, Fuller GA, Myers PC. 1993. *Ap. J.* 406:528–47
Goodwin SP, Whitworth AP, Ward-Thompson D. 2004. *Astron. Astrophys.* 414:633–50
Gotoh T, Kraichnan RH. 1993. *Phys. Fluids A* 5:445–57
Grant HL, Stewart RW, Moillet A. 1962. *J. Fluid Mech.* 12:241–68
Green DA. 1993. *MNRAS* 262:327–42
Hall AN. 1980. *MNRAS* 190:353–69
Hartmann L, Ballesteros-Paredes J, Bergin EA. 2001. *Ap. J.* 562:852–68
Hasegawa A. 1985. *Adv. Phys.* 34:1–42
Hatakeyama N, Kambe T. 1997. *Phys. Rev. Lett.* 79:1257–60
Haugen NEL, Brandenburg A, Dobler W. 2003. *Ap. J.* 597:L141–44
Heiles C. 1970. *Ap. J.* 160:51–58
Heiles C. 2001. *Ap. J.* 551:L105–8
Heiles C, Goodman AA, McKee CF, Zweibel EG. 1993. See Levy & Lunine 1993, pp. 279–326
Heithausen A. 1996. *Astron. Astrophys.* 314: 251–57
Heitsch F, Mac Low M-M, Klessen RS. 2001. *Ap. J.* 547:280–91
Heitsch F, Zweibel EG, Slyz AD, Devriendt JEG. 2004. *Ap. J.* 603:165–79
Hetem A Jr, Lepine JRD. 1993. *Astron. Astrophys.* 270:451–61
Heyer MH, Brunt C, Snell RL, Howe JE, Schloerb FP, Carpenter JM. 1998. *Ap. J. Suppl.* 115:241–58
Heyer MH, Carpenter JM, Snell RL. 2001. *Ap. J.* 551:852–66

Heyer MH, Schloerb FP. 1997. *Ap. J.* 475:173–87
Higdon JC. 1986. *Ap. J.* 309:342–61
Hinze JO. 1975. *Turbulence*. New York: McGraw-Hill. 790 pp. 2nd ed.
Hobbs LM. 1974. *Ap. J.* 191:395–99
Hobson MP. 1992. *MNRAS* 256:457–76
Houde M, Bastien P, Dotson JL, Dowell CD, Hildebrand RH, et al. 2002. *Ap. J.* 569:803–14
Houlahan P, Scalo J. 1992. *Ap. J.* 393:172–87
Huber D, Pfenniger D. 2001. *Astron. Astrophys.* 374:465–93
Huber D, Pfenniger D. 2002. *Astron. Astrophys.* 386:359–78
Hunter JH Jr, Sandford MT II, Whitaker RW, Klein RI. 1986. *Ap. J.* 305:309–32
Ikeuchi S, Spitzer L Jr. 1984. *Ap. J.* 283:825–32
Ingalls JG, Bania TM, Lane AP, Rumitz M, Stark AA. 2000. *Ap. J.* 535:211–26
Iroshnikov PS. 1964. *Sov. Astron.* 7:566–71
Jackson T, Werner M, Gautier TN III. 2003. *Ap. J. Suppl.* 149:365–73
Jayesh, Warhaft Z. 1991. *Phys. Rev. Lett.* 67: 3503–6
Jenkins EB, Meloy DA. 1974. *Ap. J.* 193:L121–25
Jenkins JB. 2004. *Astrophys. Space Sci.* 289: 215–23
Jessop NE, Ward-Thompson D. 2001. *MNRAS* 323:1025–34
Jijina J, Myers PC, Adams FC. 1999. *Ap. J. Suppl.* 125:161–236
Kaneda Y, Ishihara T, Yokokawa M, Itakura K, Uno A. 2003. *Phys. Fluids* 15:L21–24
Kanekar N, Subrahmanyan R, Chengalur JN, Safouris V. 2003. *MNRAS* 346:L57–61
Kaplan SA. 1958. In *Electromagnetic Phenomena in Cosmical Physics. Proc. IAU Symp. 6th,* ed. B Lehnert, pp. 504–12. Cambridge: Cambridge Univ. Press
Kawamura A, Onishi T, Yonekura Y, Dobashi K, Mizuno A, et al. 1998. *Ap. J. Suppl.* 117: 387–425
Kegel WH. 1989. *Astron. Astrophys.* 225:517–20
Kida S, Murakami Y. 1989. *Fluid Dyn. Res.* 4:347–70
Kim J, Balsara D, Mac Low M-M. 2001. *J. Korean Astron. Soc.* 34:333–35
Kim S, Staveley-Smith L, Dopita MA, Freeman KC, Sault RJ, et al. 1998. *Ap. J.* 503:674–88
Kim S, Staveley-Smith L, Dopita MA, Sault RJ, Freeman KC, et al. 2003. *Ap. J. Suppl.* 148:473–86
Kim W-T, Ostriker E, Stone J. 2003. *Ap. J.* 599:1157–72
Kinney RM, McWilliams JC. 1998. *Phys. Rev. E* 57:7111–21
Kitamura Y, Sunada K, Hayashi M, Hasegawa T. 1993. *Ap. J.* 413:221–36
Klein RI, Fisher RT, Krumholz MR, McKee CF. 2003. In *Winds, Bubbles Explosions: A Conference to Honour John Dyson*, ed. SJ Arthur, WJ Henney, *Rev. Mex. Astron. Astrophys.* 15:92–96
Klein RI, Woods DT. 1998. *Ap. J.* 497:777–99
Kleiner SC, Dickman RL. 1985. *Ap. J.* 295: 466–78
Kleiner SC, Dickman RL. 1987. *Ap. J.* 312: 837–47
Klessen RS. 2000. *Ap. J.* 535:869–86
Klessen RS. 2001. *Ap. J.* 556:837–46
Klessen RS, Burkert A. 2000. *Ap. J. Suppl.* 128:287–319
Klessen RS, Burkert A. 2001. *Ap. J.* 549:386–401
Klessen RS, Burkert A, Bate MR. 1998. *Ap. J.* 501:L205–8
Klessen RS, Heitsch F, Mac Low M-M. 2000. *Ap. J.* 535:887–906
Kolesnik I, Ogul'Chanskii II. 1990. In *Physical Processes in Fragmentation and Star Formation,* ed. R Capuzzo-Dolcetta, C Chiosi, A di Fazio, pp. 81–86. Dordrecht: Kluwer
Kolmogorov AN. 1941. *Proc. R. Soc. London Ser. A* 434:9–13. Reprinted in 1991
Kornreich P, Scalo J. 2000. *Ap. J.* 531:366–83
Korpi MJ, Brandenburg A, Shukurov A, Tuominen I. 1999a. *Astron. Astrophys.* 350:230–39
Korpi MJ, Brandenburg A, Shukurov A, Tuominen I, Nordlund A. 1999b. *Ap. J.* 514:L99–102

Kraichnan RH. 1965. *Phys. Fluids* 8:1385–87
Kraichnan RH. 1967. *Phys. Fluids* 10:1417–23
Kritsuk AG, Norman ML. 2002a. *Ap. J.* 580: L51–55
Kritsuk AG, Norman ML. 2002b. *Ap. J.* 569: L127–31
Kritsuk AG, Norman ML. 2004. *Ap. J.* 601: L55–58
Kudoh T, Basu S. 2003. *Ap. J.* 595:842–57
Kulkarni SR, Heiles C. 1988. In *Galactic and Extragalactic Radio Astronomy*, ed. GL Verschuur, KI Kellerman, pp. 95–153. New York: Springer-Verlag
Kulsrud RM. 1983. In *Basic Plasma Physics*, ed. AA Galeev, RN Sudan, 1:115–45. Amsterdam: North-Holland
Kurien S, Taylor MA, Matsumoto T. 2003. Cascade time-scales for energy and helicity in homogeneous isotropic turbulence. (ADS arxiv.org nlin.CD/0312034)
Langer WD, Velusamy T, Kuiper TBH, Levin S, Olsen E, Migenes V. 1995. *Ap. J.* 453:293–307
Langer WD, Wilson RW, Anderson CH. 1993. *Ap. J.* 408:L45–48
Larson RB. 1981. *MNRAS* 194:809–26
Laveder D, Passot T, Sulem PL. 2001. *Physica D* 152–153:694–704
Laveder D, Passot T, Sulem PL. 2002. *Phys. Plasmas* 9:293–304
Lazarian A. 1999. See Ostrowski & Schlickeiser 1999, pp. 28–47
Lazarian A, Esquivel A. 2003. *Ap. J.* 592:L37–40
Lazarian A, Pogosyan D. 2000. *Ap. J.* 537:720–48
Lazarian A, Pogosyan D, Vázquez-Semadeni E, Pichardo B. 2001. *Ap. J.* 555:130–38
Lazarian A, Vishniac ET, Cho J. 2004. *Ap. J.* 603:180–97
Lee H, Ryu D, Kim J, Jones TW, Balsara D. 2003. *Ap. J.* 594:627–36
Lele SK. 1994. *Annu. Rev. Fluid Mech.* 26:211–54
Lelong M-P, Riley JJ. 1991. *J. Fluid Mech.* 232:1–19
Leorat J, Passot T, Pouquet A. 1990. *MNRAS* 243:293–311
Lesieur M. 1990. *Turbulence in Fluids: Stochastic and Numerical Modeling.* Dordrecht: Kluwer. 412 pp.
Leslie DC. 1973. *Developments in the Theory of Turbulence.* Oxford: Clarendon. 368 pp.
Levy EH, Lunine JI, eds. 1993. *Protostars and Planets III.* Tucson: Univ. Ariz.
Li PS, Norman ML, Mac Low M-M, Heitsch F. 2004. *Ap. J.* 605:800–18
Li Y, Klessen RS, Mac Low M-M. 2003. *Ap. J.* 592:975–85
Lis DC, Keene J, Li Y, Phillips TG, Pety J. 1998. *Ap. J.* 504:889–99
Lis DC, Pety J, Phillips TG, Falgarone E. 1996. *Ap. J.* 463:623–29
Liszt HS, Wilson RW, Penzias AA, Jefferts KB, Wannier PG, Solomon PM. 1974. *Ap. J.* 190:557–64
Lithwick Y, Goldreich P. 2001. *Ap. J.* 562: 279–96
Lithwick Y, Goldreich P. 2003. *Ap. J.* 582: 1220–40
Little LT, Matheson DN. 1973. *MNRAS* 162: 329–38
Liu L, She Z-S. 2003. *Fluid Dyn. Res.* 33:261–86
Loren RB. 1989. *Ap. J.* 338:902–24
Low FJ, Young E, Beintema DA, Gautier TN, Beichman CA, et al. 1984. *Ap. J.* 278:L19–22
Lundgren TS. 1982. *Phys. Fluids* 25:2193–203
L'vov VS, L'vov YuV, Pomyalov A. 2000. *Phys. Rev. E* 61:2586–94
Mac Low M-M. 1999. *Ap. J.* 524:169–78
Mac Low M-M. 2003. In *Simulations of Magnetohydrodynamic Turbulence in Astrophysics*, ed. T Passot, E Falgarone, *Springer Lect. Notes Phys.* pp. 182–212
Mac Low M-M, Klessen RS. 2004. *Rev. Mod. Phys.* 76:125–94
Mac Low M-M, Klessen RS, Burkert A, Smith MD. 1998. *Phys. Rev. Lett.* 80:2754–57
Mac Low M-M, Norman ML. 1993. *Ap. J.* 407:207–18
Mac Low M-M, Norman ML, Konigl A, Wardle M. 1995. *Ap. J.* 442:726–35
Maron J, Goldreich P. 2001. *Ap. J.* 554:1175–96
Martos MA, Cox DP. 1998. *Ap. J.* 509:703–16

Mathieu J, Scott J. 2000. *An introduction to Turbulent Flow.* Cambridge: Cambridge Univ. Press. 374 pp.
Matthaeus WH, Bieber JW, Zank GP. 1995. *Rev. Geophys. Suppl.* 33:609–14
Matthaeus WH, Oughton S, Ghosh S, Hossain M. 1998. *Phys. Rev. Lett.* 81:2056–59
McComb WD. 1990. *Physics of Fluid Turbulence*. Oxford: Oxford Univ. Press. 572 pp.
McCray R, Snow TP Jr. 1979. *Annu. Rev. Astron. Astrophys.* 17:213–40
McGee RX, Milton JA, Wolfe W. 1966. *Aust. J. Phys. Suppl.* 1:3–39
McKee CF, Ostriker JP. 1977. *Ap. J.* 218:148–69
McKee CF, Zweibel EG. 1992. *Ap. J.* 399:551–62
Mebold U, Hachenberg O, Laury-Micoulaut CA. 1974. *Astron. Astrophys.* 30:329–38
Miesch MS, Bally J. 1994. *Ap. J.* 429:645–71
Miesch MS, Scalo JM. 1995. *Ap. J.* 450:L27–30
Miesch MS, Scalo J, Bally J. 1999. *Ap. J.* 524:895–922
Miesch MS, Zweibel EG. 1994. *Ap. J.* 432:622–40
Minkowski R. 1955. In *Gas Dynamics of Cosmic Clouds*, ed. JM Burgers, HC van de Hulst, pp. 3–12. Amsterdam: North Holland
Miville-Deschênes M-A, Joncas G, Falgarone E. 1999. See Franco & Carraminana 1999, pp. 169–73
Miville-Deschênes M-A, Levrier F, Falgarone E. 2003. *Ap. J.* 593:831–47
Moisy F, Tabeling P, Willaime H. 1999. *Phys. Rev. Lett.* 82:3994–97
Monin AS, Yaglom AM. 1975. *Statistical Fluid Mechanics: Mechanics of Turbulence*, Vols. 1 and 2, ed. J Lumley. Cambridge, MA: MIT Press. 769 pp. 874 pp.
Montgomery D, Matthaeus WH. 1995. *Ap. J.* 447:706–7
Mouri H, Takaoka M, Hori A, Kawashima Y. 2003. *Phys. Rev. E* 68:036311
Mouschovias TC. 1991. *Ap. J.* 373:169–86
Mouschovias TC, Paleologou EV. 1979. *Ap. J.* 230:204–22
Müller W-C, Biskamp D. 2000. *Phys. Rev. Lett.* 84:475–78
Müller W-C, Biskamp D. 2003. See Falgarone & Passot 2003, pp. 3–27
Müller W-C, Biskamp D, Grappin R. 2003. *Phys. Rev. E* 67:066302
Myers PC. 1983. *Ap. J.* 270:105–18
Myers PC, Fuller GA, Goodman AA, Benson PJ. 1991. *Ap. J.* 376:561–72
Nakayama K. 2002. *PASJ* 54:1065–78
Ng CS, Bhattacharjee A. 1996. *Ap. J.* 465:845–54
Ng CS, Bhattacharjee A. 1997. *Phys. Plasmas* 4:605–10
Nordlund A, Padoan P. 1999. In *Interstellar Turbulence, Proc. 2nd Guillermo Haro Conf.*, ed. J Franco, A Carraminana, pp. 218–22. Cambridge: Cambridge Univ. Press
Nordlund A, Padoan P. 2003. In *Simulations of Magnetohydrodynamic Turbulence in Astrophysics: Recent Achievements and Perspectives*, ed. E Falgarone, T Passot, *Lect. Notes Phys.*, 614:271–98
Norman CA, Ferrara A. 1996. *Ap. J.* 467:280–91
Noullez A, Wallace G, Lempert W, Miles RB, Frisch U. 1997. *J. Fluid Mech.* 339:287–307
Oey MS, Clarke CJ. 1997. *MNRAS* 289:570–88
Oort JH, Spitzer L Jr. 1955. *Ap. J.* 121:6–23
Ossenkopf V. 2002. *Astron. Astrophys.* 391: 295–315
Ossenkopf V, Klessen RS, Heitsch F. 2001. *Astron. Astrophys.* 379:1005–16
Ossenkopf V, Mac Low M-M. 2002. *Astron. Astrophys.* 390:307–26
Ostriker EC. 2003. In *Simulations of Magnetohydrodynamic Turbulence in Astrophysics*, ed. T Passot, E Falgarone, *Springer Lect. Notes Phys*., pp. 252–70
Ostriker EC, Gammie CF, Stone JM. 1999. *Ap. J.* 513:259–74
Ostriker EC, Stone JM, Gammie CF. 2001. *Ap. J.* 546:980–1005
Ostrowski M, Schlickeiser R, eds. 1999. *Plasma Turbulence and Energetic Particles in Astrophysics.* Kraków: Obs. Astron. Univ. Jagiell.
Ottino JM. 1989. *The Kinematics of Mixing: Stretching, Chaos and Transport.* Cambridge: Cambridge Univ. Press. 364 pp.

Padoan P, Bally J, Billawala Y, Juvela M, Nordlund A. 1999. *Ap. J.* 525:318–29
Padoan P, Boldyrev S, Langer W, Nordlund A. 2003a. *Ap. J.* 583:308–13
Padoan P, Cambrésy L, Langer W. 2002. *Ap. J.* 580:L57–60
Padoan P, Goodman AA, Juvela M. 2003. *Ap. J.* 588:881–93
Padoan P, Jimenez R, Nordlund A, Boldyrev S. 2004. *Phys. Rev. Lett.* 92:191102
Padoan P, Jones BJT, Nordlund A. 1997. *Ap. J.* 474:730–34
Padoan P, Juvela M, Bally J, Nordlund A. 1998. *Ap. J.* 504:300–13
Padoan P, Juvela M, Bally J, Nordlund A. 2000. *Ap. J.* 529:259–67
Padoan P, Juvela M, Goodman AA, Nordlund A. 2001b. *Ap. J.* 553:227–34
Padoan P, Kim S, Goodman A, Staveley-Smith L. 2001c. *Ap. J.* 555:L33–36
Padoan P, Nordlund A. 1999. *Ap. J.* 526:279–94
Padoan P, Zweibel EG, Nordlund A. 2000. *Ap. J.* 540:332–41
Park Y-S, Hong SS, Minh YC. 1996. *Astron. Astrophys.* 312:981–88
Parravano A, Hollenbach DJ, McKee CF. 2003. *Ap. J.* 584:797–817
Passot T, Pouquet A, Woodward P. 1988. *Astron. Astrophys.* 197:228–34
Passot T, Sulem PL. 2003a. *Phys. Plasmas* 10:3887–905
Passot T, Sulem PL. 2003b. *Phys. Plasmas* 10:3914–21
Passot T, Vázquez-Semadeni E. 1998. *Phys. Rev.* 58:4501–10
Passot T, Vázquez-Semadeni E. 2003. *Astron. Astrophys.* 398:845–55
Passot T, Vázquez-Semadeni E, Pouquet A. 1995. *Ap. J.* 455:536–55
Pavlovski G, Smith MD, Mac Low M-M, Rosen A. 2002. *MNRAS* 337:477–87
Peng R, Langer WD, Velusamy T, Kuiper TBH, Levin S. 1998. *Ap. J.* 497:842–49
Pérault M, Falgarone E, Puget JL. 1986. *Astron. Astrophys.* 157:139–47
Pety J, Falgarone E. 2000. *Astron. Astrophys.* 356:279–86
Pety J, Falgarone E. 2003. *Astron. Astrophys.* 412:417–30
Pichardo B, Vázquez-Semadeni E, Gazol A, Passot T, Ballesteros-Paredes J. 2000. *Ap. J.* 532:353–60
Piehler G, Kegel WH. 1995. *Astron. Astrophys.* 297:841–53
Piontek RA, Ostriker EC. 2004. *Ap. J.* 601:905–20
Plume R, Bensch F, Howe JE, Ashby MLN, Bergin EA, et al. 2000. *Ap. J.* 539:L133–36
Plume R, Jaffe DT, Evans NJ, Martin-Pintado J, Gomez-Gonzalez J. 1997. *Ap. J.* 476:730–49
Politano H, Pouquet A. 1995. *Phys. Rev. E* 52: 636–41
Politano H, Pouquet A, Carbone V. 1998. *Europhys. Lett.* 43:516–21
Pope SB. 2000. *Turbulent Flows.* Cambridge: Cambridge Univ. Press. 771 pp.
Porter D, Pouquet A, Sytine I, Woodward P. 1999. *Physica A* 263:263–70
Porter D, Pouquet A, Woodward P. 2002. *Phys. Rev. E* 66:026301
Porter D, Woodward P, Pouquet A. 1998. *Phys. Fluids* 10:237–45
Pouquet A, Frisch U, Léorat J. 1976. *J. Fluid Mech.* 77:321–54
Pouquet A, Rosenberg D, Clyne J. 2003. *Statistical Theories and Computational Approaches to Turbulence*, ed. Y Kaneda, T Gotoh, pp. 3–14. New York: Springer-Verlag. 409 pp.
Pullin DI, Saffman PG. 1998. *Annu. Rev. Fluid Mech.* 30:31–51
Pumir A. 1996. *Phys. Fluids* 8:3112–27
Pushkarev A, Resio D, Zakharov V. 2003. *Physica D* 184:29–63
Radjai F, Roux S. 2002. *Phys. Rev. Lett.* 89: 064302
Rickett BJ. 1970. *MNRAS* 150:67–91
Ricotti M, Ferrara A. 2002. *MNRAS* 334:684–92
Roberts WW. 1969. *Ap. J.* 158:123–43
Rosen A, Bregman JN, Norman ML. 1993. *Ap. J.* 413:137–49
Rosolowsky EW, Goodman AA, Wilner DJ, Williams JP. 1999. *Ap. J.* 524:887–94

Rotman D. 1991. *Phys. Fluids A* 3:1792–806
Ryden BS. 1996. *Ap. J.* 471:822–31
Saffman PG. 1971. *Stud. Appl. Math.* 50:377–83
Sakamoto S, Sunada K. 2003. *Ap. J.* 594:340–46
Salpeter EE. 1969. *Nature* 221:31–33
Sánchez-Salcedo FJ, Vázquez-Semadeni E, Gazol A. 2002. *Ap. J.* 577:768–88
Sarson GR, Shukurov A, Nordlund A, Gudiksen B, Brandenburg A. 2003. In *Magnetic Fields and Star Formation: Theory versus Observations*, ed. AI Gomez de Castro, et al. Dordrecht: Kluwer. (astro-ph/0307013)
Sasao T. 1973. *PASJ* 25:1–33
Scalo J. 1990. In *Physical Processes in Fragmentation and Star Formation*, ed. R Capuzzo-Dolcetta, C Chiosi, A DiFazio, pp. 151–76. Dordrecht: Kluwer
Scalo J, Vázquez-Semadeni E, Chappell D, Passot T. 1998. *Ap. J.* 504:835–53
Scalo JM. 1977. *Ap. J.* 213:705–11
Scalo JM. 1984. *Ap. J.* 277:556–61
Scalo JM. 1987. In *Interstellar Processes*, ed. DJ Hollenbach, HA Thronson Jr, pp. 349–92. Dordrecht: Reidel
Scheffler H. 1967. *Z. Ap.* 65:60–83
Schekochihin AA, Maron JL, Cowley SC, McWilliams JC. 2002. *Ap. J.* 576:806–13
Schlegel DJ, Finkbeiner DP, Davis M. 1998. *Ap. J.* 500:525–53
Schlichting H, Gersten K. 2000. *Boundary Layer Theory*, Chap. 16.5.4. Berlin: Springer-Verlag. 799 pp. 8th ed.
Schneider S, Elmegreen BG. 1979. *Ap. J. Suppl.* 41:87–95
Sellwood JA, Balbus SA. 1999. *Ap. J.* 511:660–65
Semelin B, de Vega HJ, Sanchez N, Combes F. 1999. *Phys. Rev. D* 59:125021–40
Seto N, Yokoyama J. 1998. *Ap. J.* 496:L59–62
She Z-S. 1991. *Fluid Dyn. Res.* 8:1
She Z-S, Chen S, Doolen G, Kraichnan RH, Orszag SA. 1993. *Phys. Rev. Lett.* 70:3251–54
She Z-S, Leveque E. 1994. *Phys. Rev. Lett.* 72:336–39
Shebalin JV, Matthaeus WH, Montgomery D. 1983. *J. Plasma Phys.* 29:525–47
Shivamoggi BK. 1997. *Europhys. Lett.* 38:657–62
Shukurov A, Sarson GR, Nordlund A, Gudiksen B, Brandenburg A. 2004. *Astrophys. Space Sci.* 289:319–22
Simon R, Jackson JM, Clemens DP, Bania TM, Heyer MH. 2001. *Ap. J.* 551:747–63
Smith MD, Mac Low M-M, Heitsch F. 2000. *Astron. Astrophys.* 362:333–41
Smith MD, Mac Low M-M, Zuev JM. 2000. *Astron. Astrophys.* 356:287–300
Snyder PB, Hammett GW, Dorland W. 1997. *Phys. Plasmas* 4:3974–85
Solomon PM, Rivolo AR, Barrett J, Yahil A. 1987. *Ap. J.* 319:730–41
Spitzer L Jr. 1968. *Diffuse Matter in Space*. New York: Interscience. 170 pp.
Sreenivasan KR. 1991. *Annu. Rev. Fluid Mech.* 23:539–604
Sreenivasan KR, Antonia RA. 1997. *Annu. Rev. Fluid Mech.* 29:435–72
Sreenivasan KR, Dhruva B. 1998. *Prog. Theor. Phys. Suppl.* 130:103–20
Stanimirovic S, Lazarian A. 2001. *Ap. J.* 551: L53–56
Stanimirovic S, Staveley-Smith L, Dickey JM, Sault RJ, Snowden SL. 1999. *MNRAS* 302:417–36
Stanimirovic S, Staveley-Smith L, van der Hulst JM, Bontekoe TJR, Kester DJM, Jones PA. 2000. *MNRAS* 315:791–807
Stenholm LG. 1984. *Astron. Astrophys.* 137: 133–37
Stone JM, Ostriker EC, Gammie CF. 1998. *Ap. J.* 508:L99–102
Stützki J, Bensch F, Heithausen A, Ossenkopf V, Zielinsky M. 1998. *Astron. Astrophys.* 336:697–20
Tabeling P. 2002. *Phys. Rep.* 362:1–62
Tabeling P, Willaime H. 2002. *Phys. Rev. E* 65:066301
Tachihara K, Onishi T, Mizuno A, Fukui Y. 2002. *Astron. Astrophys.* 385:909–20
Tagger M, Falgarone E, Shukurov A. 1995. *Astron. Astrophys.* 299:940–46

Takaoka M. 1995. *Phys. Rev. E* 52:3827–34
Tauber JA, Goldsmith PF, Dickman RL. 1991. *Ap. J.* 375:635–41
Tennekes H, Lumley JL. 1972. *A First Course in Turbulence.* Cambridge, MA: MIT Press. 300 pp.
Thomasson M, Donner KJ, Elmegreen BG. 1991. *Astron. Astrophys.* 250:316–23
Troland TH, Heiles C. 1986. *Ap. J.* 301:339–45
Truelove JK, Klein RI, McKee CF, Holliman JH II, Howell LH, Greenough JA. 1997. *Ap. J.* 489:L179–83
Tsinober A. 2001. *An Informal Introduction to Turbulence*. Dordrecht: Kluwer. 324 pp.
Tsytovich VN. 1972. *An Introduction to the Theory of Plasma Turbulence.* Oxford: Pergamon Press. vii. 135 pp.
Vainshtein SI. 2003. Most singular vortex structures in fully developed turbulence. (arXiv:physics/0310008)
van Buren D. 1985. *Ap. J.* 294:567–77
Vázquez-Semadeni E. 1994. *Ap. J.* 423:681–92
Vázquez-Semadeni E. 1999. *Millimeter-Wave Astronomy: Molecular Chemistry and Physics in Space*, ed. WF Wall, A Carraminana, L Carrasco, pp. 171–94. New York: Kluwer Acad.
Vázquez-Semadeni E, Ballesteros-Paredes J, Rodriguez LF. 1997. *Ap. J.* 474:292–307
Vázquez-Semadeni E, Canto J, Lizano S. 1998. *Ap. J.* 492:596–602
Vázquez-Semadeni E, García N. 2001. *Ap. J.* 557:727–35
Vázquez-Semadeni E, Gazol A. 1995. *Astron. Astrophys.* 303:204–10
Vázquez-Semadeni E, Gazol A, Scalo J. 2000. *Ap. J.* 540:271–85
Vázquez-Semadeni E, Ostriker EC, Passot T, Gammie CF, Stone JM. 2000. In *Protostars and Planets IV*, ed. V Mannings, AP Boss, SS Russell, pp. 3–28. Tucson: Univ. Ariz.
Vázquez-Semadeni E, Passot T, Pouquet A. 1995. *Ap. J.* 441:702–25
Vázquez-Semadeni E, Passot T, Pouquet A. 1996. *Ap. J.* 473:881–93
Vestuto JG, Ostriker EC, Stone JM. 2003. *Ap. J.* 590:858–73
Vishniac ET. 1994. *Ap. J.* 428:186–208
Vogelaar MGR, Wakker BP. 1994. *Astron. Astrophys.* 291:557–68
Vollmer B, Beckert T. 2002. *Astron. Astrophys.* 382:872–87
Vollmer B, Beckert T. 2003. *Astron. Astrophys.* 404:21–34
von Hoerner S. 1951. *Z. Astrophys.* 30:17–64
von Weizsäcker CF. 1951. *Ap. J.* 114:165–86
Wada K, Meurer G, Norman CA. 2002. *Ap. J.* 577:197–205
Wada K, Norman CA. 1999. *Ap. J.* 516:L13–16
Wada K, Norman CA. 2001. *Ap. J.* 547:172–86
Wada K, Spaans M, Kim S. 2000. *Ap. J.* 540: 797–807
Wakker BP. 1990. *Interstellar neutral hydrogen at high velocities*. PhD thesis, Rijks Univ., Groningen, Germany. 179 pp.
Walder R, Folini D. 1998. *Astron. Astrophys.* 330:L21–24
Waleffe F. 1992. *Phys. Fluids A* 4:350–63
Wentzel DG. 1968a. *Ap. J.* 152:987–96
Wentzel DG. 1969b. *Ap. J.* 156:L91–95
Westpfahl DJ, Coleman PH, Alexander J, Tongue T. 1999. *Astron. J.* 117:868–80
Wilson OC, Minich G, Flather E, Coffeen MF. 1959. *Ap. J. Suppl.* 4:199–256
Wilson RW, Jefferts KB, Penzias AA. 1970. *Ap. J.* 161:L43–44
Xie T. 1997. *Ap. J.* 475:L139–42
Xu J, Stone JM. 1995. *Ap. J.* 454:172–81
Yeung PK, Brasseur JG. 1991. *Phys. Fluids* 3:884–97
Yeung PK, Brasseur JG, Wang Q. 1995. *J. Fluid Mech.* 283:43–95
Yue ZY, Zhang R, Winnewisser G, Stutzki J. 1993. *Ann. Phys.* 2:9–25
Zakharov V, L'vov V, Falkovich G. 1992. *Kolmogorov Spectra of Turbulence.* Berlin: Springer-Verlag. 254 pp.

Zank GP, Matthaeus WH. 1993. *Phys. Fluids A* 5:257–73
Zhang X, Lee Y, Bolatto A, Stark AA. 2001. *Ap. J.* 553:274–87
Zhou Y. 1993. *Phys. Fluids A* 5:1092–94
Zhou Y, Yeung PK, Brasseur JG. 1996. *Phys. Rev. E* 53:1261–64
Zielinsky M, Stützki J. 1999. *Astron. Astrophys.* 347:630–33
Zuckerman B, Evans NJ II. 1974. *Ap. J.* 192: L149–52
Zuckerman B, Palmer P. 1974. *Annu. Rev. Astron. Astrophys.* 12:279–313
Zweibel EG. 2002. *Ap. J.* 567:962–70
Zweibel EG, Brandenburg A. 1997. *Ap. J.* 478:563–68
Zweibel EG, McKee CF. 1995. *Ap. J.* 439:779–92

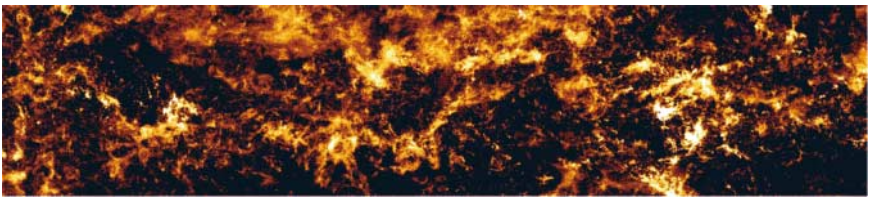

**Figure 1** $^{12}$CO emission from the outer Galaxy spanning a range of Galactic longitude from 102.5° to 141.5° and latitude from −3° to 5.4°, sampled every 50″ with a 45″ beam. The emission is integrated between −110 km s$^{-1}$ and 20 km s$^{-1}$. The high latitude emission is mostly from local gas at low velocity, consisting of small structures that tend to be nonself-gravitating. The low latitude emission is a combination of local gas plus gas in the Perseus arm at higher velocity. The Perseus arm gas includes the giant self-gravitating clouds that formed the OB associations that excite W3, W4, and W5 (*left*) and NGC 7538 (*right*). Most structures are hierarchical and self-similar on different scales, so the distant massive clouds look about the same on this map as the local low-mass clouds. This image was kindly provided by M. Heyer using data from Heyer et al. (1998).

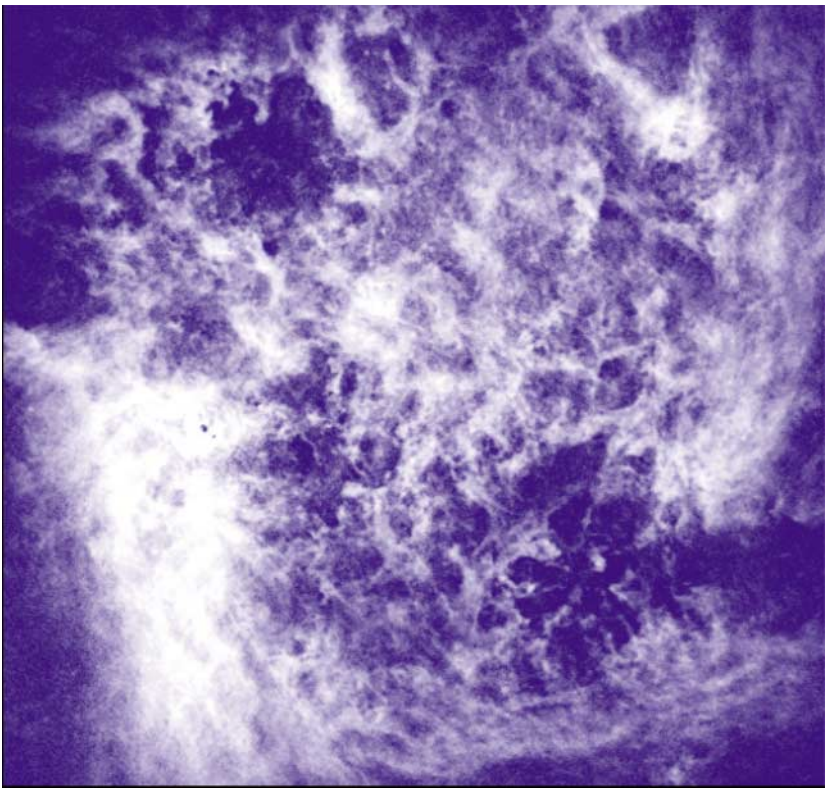

**Figure 2** Integrated *H I* emission from the LMC showing shells and filaments covering a wide range of scales. The 2D power spectrum of this emission is a power law from 20 pc to 1 kpc with a slope of ~–3.2. Data from Elmegreen, Kim & Staveley-Smith (2001). Illustration used with permission from Mercury Magazine and the Astronomical Society of the Pacific.

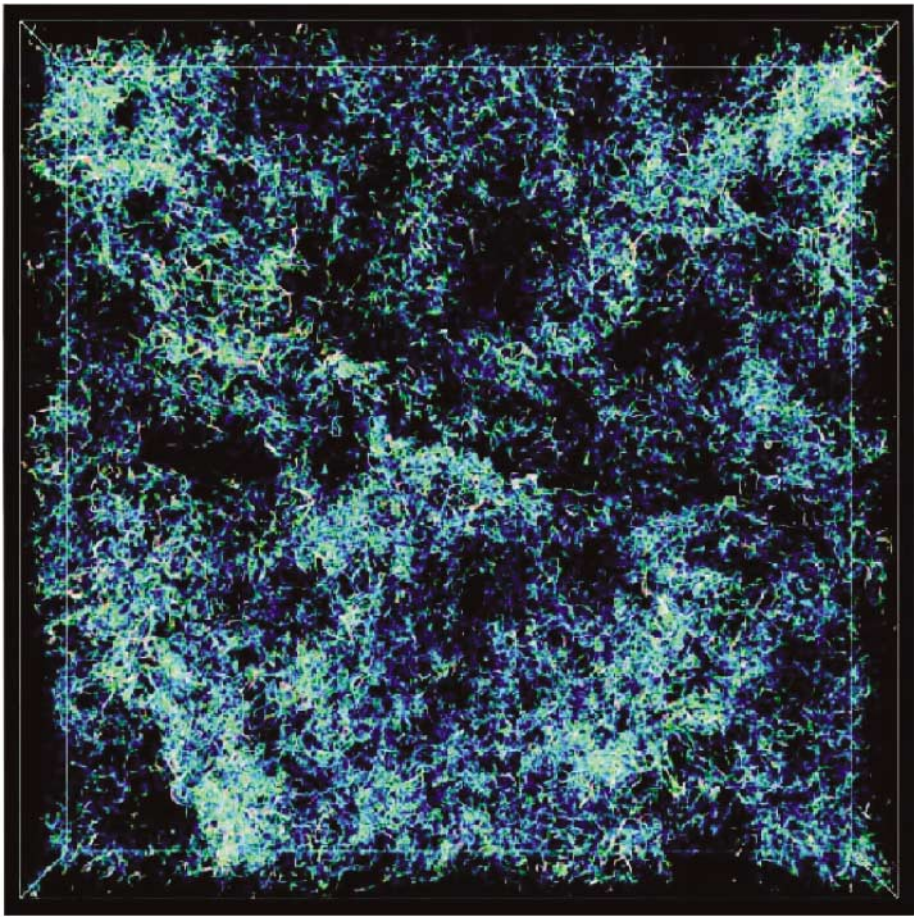

**Figure 3** Vorticity structures in a $1024 \times 1024 \times 128$ section of a $1024^3$ simulation of compressible decaying nonmagnetic turbulence with initial rms Mach number of unity. Reprinted with permission from Porter, Woodward & Pouquet (1998), *Physics of Fluids*, Vol. 10, pp. 237–45. 

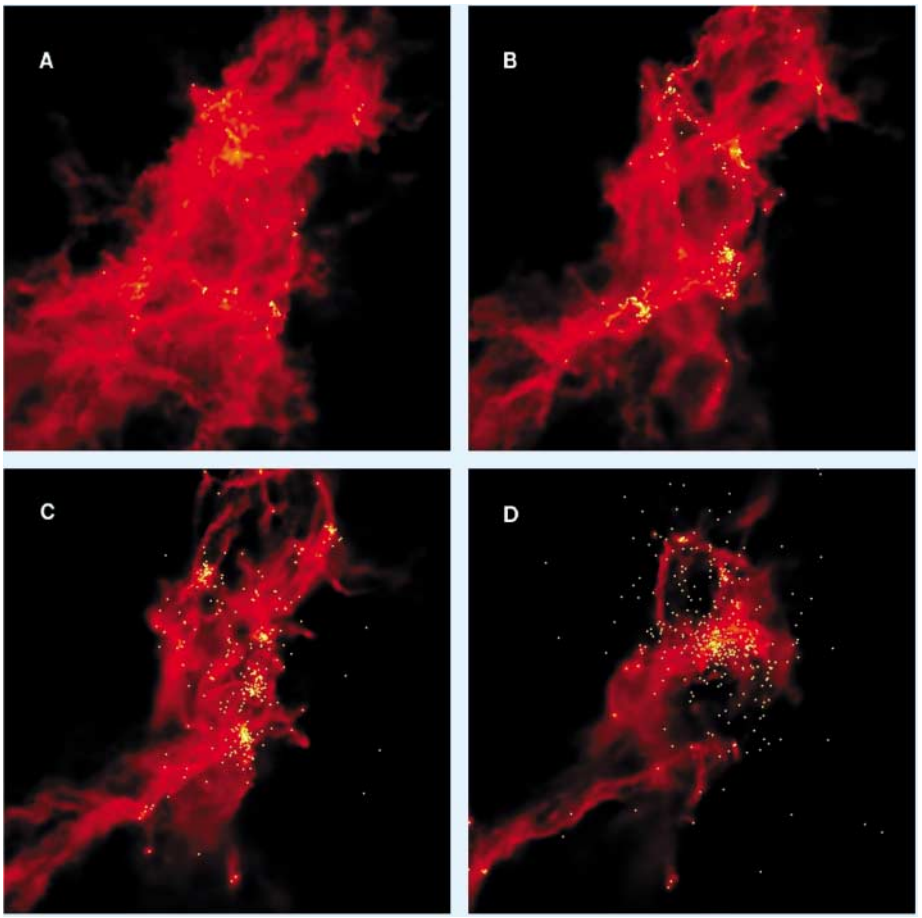


**Figure 5** Four time steps in an SPH hydrodynamic simulation with self-gravity and $5 \times 10^5$ fluid particles. Collapsing cores that represent stars are replaced by sink particles in the simulation and are shown here by white dots. Most stars form in a very dense gaseous core and then get ejected into the general cluster field by two-body interactions. Objects ranging in mass from brown dwarfs to ~30 $M_\odot$ stars are made (from Bonnell et al. 2003, "The hierarchical formation of a stellar cluster," Monthly Notices of the Royal Astronomical Society, Vol. 343, p. 413, Blackwell Publishing, Ltd.).